IS-T-537

EXPERIMENTAL EQUATIONS OF STATE FOR SOLID NEON, ARGON, KRYPTON, AND XENON

M.S. Thesis Submitted to Iowa State University,
August, 1972

M. S. Anderson

Ames Laboratory, USAEC
Iowa State University
Ames, Iowa 50010

Date of Manuscript: August, 1972

PREPARED FOR THE U. S. ATOMIC ENERGY COMMISSION
DIVISION OF RESEARCH UNDER CONTRACT NO. W-7405-eng-82

DISCLAIMER

Available from: National Technical Information Service
Department A
Springfield, VA 22151

Price: Microfiche $0.95

Experimental equations of state for solid neon, argon, krypton, and xenon

by

Marvin Sydney Anderson

A Thesis Submitted to the
Graduate Faculty in Partial Fulfillment of
The Requirements for the Degree of
MASTER OF SCIENCE

Department: Physics

Major: Solid State Physics

Approved:

C. A. Swenson
In Charge of Major Work

For the Major Department

For the Graduate College

Iowa State University
Ames, Iowa

1972

TABLE OF CONTENTS

Experimental equations of state for solid neon, argon, krypton, and xenon

Marvin Sydney Anderson

Under the supervision of C. A. Swenson
From the Department of Physics
Iowa State University of Science and Technology

The experimental pressure-volume-temperature relationships have been determined for solid neon, argon, krypton, and xenon, using the piston displacement technique for pressures to 20 kbar and temperatures from 4.2 K to near the triple point. A 4.2 K equation of state is presented for each solid. A reduced equation of state is found to be valid for these solids at 4.2 K, except at low pressures where systematic deviations appear. Temperature dependent contributions to the equation of state, $P^{*}(T,V)$, are calculated for each solid, and are found to be slightly volume dependent at constant temperature. High temperature Grüneisen parameters calculated for argon, krypton, and xenon from these data are in agreement with direct experimental values. Comparison with recent theories which include three-body interactions are made.

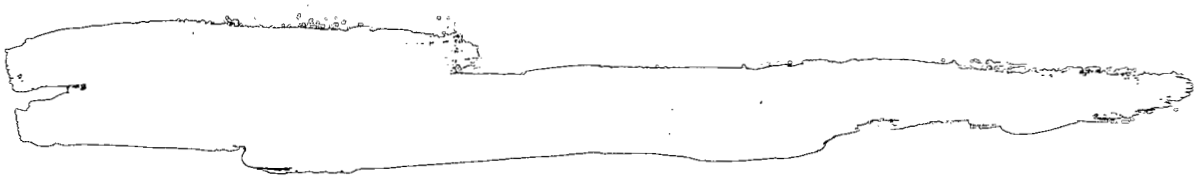

CHAPTER 1. INTRODUCTION

The rare gas solids, neon, argon, krypton, and xenon, are perhaps the most elementary examples of the class of molecular solids. These solids are characterized as weakly bound insulators with filled electronic shells and spherically symmetric charge distributions. They solidify into the cubic close-packed (face-centered cubic) structure and have low melting points. Table 1 lists some relative properties for these solids.

The weak binding energies for these solids are due primarily to the small interactions between the closed electronic shells (the ϵ in Table 1), and the cohesive energies are reduced even more due to the relatively large values of the zero point energy (i.e., the kinetic energy of the

Table 1. Some properties of the rare gas solids at T=0 K.

Solid	Nearest Neighbor Distance a_o (Å)	Triple Point (K)	Cohesive Energy (eV/atom)	Zero Point Energy (eV/atom)	Parameters Lennard-Jones Potential[a] σ (Å)	ϵ (eV)
neon	3.13	24.6	0.026	0.008	3.13	0.0032
argon	3.76	83.8	0.108	0.010	3.82	0.0103
krypton	4.01	116.1	0.155	0.008	4.08	0.0142
xenon	4.35	161.3	0.223	0.007	4.45	0.0199

[a]These parameters are for the 6-12 case and all neighbor interactions (Reference 1).

atomic vibrations at 0 K) (2). Thus, the properties of these solids reflect the relative importance of the zero point energy to the cohesive energy since the ratio of these quantities varies from 30% in neon to 3% for xenon (Table 1). The zero point energy also increases the T=0 K equilibrium volume of these solids to a value which is considerably greater than would be expected for a classical solid. The relative importance of the zero point energy should decrease with increasing pressure, since the zero point energy is a slowly varying function of volume (roughly V^{-2}), while the static lattice energy (repulsive term) varies as V^{-4} (2).

The basic description for a solid is given by the Helmholtz free energy, which can be written as

$$F(T,V) = U_o(V) + F^*(T,V) \qquad (I-1)$$

where $U_o(V)$ is the cohesive energy at 0 K and $F^*(T,V) = U^*(T,V) - TS(T,V)$ is a temperature-dependent term with S, the entropy, and U^*, the thermal energy, being associated with the lattice vibrations for the rare gas solids. All quantities indicated by an asterisk (*) in this and following equations represent quantities which are temperature-dependent and approach zero as the temperature approaches 0 K. In writing Equation I-1 and the following equations in this form, the assumption is made that the ground state and temperature-dependent contributions are independent and additive.

The equation of state or P-V-T (pressure-volume-temperature) relationship follows directly from Equation I-1 as

$$P(T,V) = -\left(\frac{\partial F}{\partial V}\right)_T = P_o(V) + P^*(T,V) \ , \qquad (I\text{-}2)$$

with the isothermal bulk modulus being given by

$$B(T,V) = -V\left(\frac{\partial P}{\partial V}\right)_T = V\left(\frac{\partial^2 F}{\partial V^2}\right)_T$$

$$= B_o(V) + B_T{}^*(T,V) \ . \qquad (I\text{-}3)$$

The entropy and the internal energy also can be calculated from the free energy as

$$S(T,V) = -\left(\frac{\partial F}{\partial T}\right)_V = -\left(\frac{\partial F^*}{\partial T}\right)_V \qquad (I\text{-}4)$$

and

$$U(T,V) = -T^2 \left(\frac{\partial \left(\frac{F}{T}\right)}{\partial T}\right)_V = U_o(V) + U^*(T,V) \ . \qquad (I\text{-}5)$$

The equation of state at 0 K, which is given by $P_o(V)$ (Equation I-2), reflects directly the volume dependence of the cohesive energy, so it is important that reliable experimental P-V data be obtained close to 0 K. Stewart has used the piston displacement technique to obtain P-V-T data for solid neon to 19.6 kbar at 4 K (3). Other measurements by Stewart for neon, argon, and krypton (4) have been taken for higher temperature isotherms and have been extrapolated to obtain a 0 K relation. A detailed piston displacement equation of state for solid xenon was reported by Packard and Swenson (5). Their values for the 0 K equation of state were obtained by extrapolation from their lowest temperature isotherm at 20 K.

The thermal contributions to the equation of state are contained in the second term of Equation I-2, $P^*(T,V)$. This term, called the thermal pressure, is the pressure that is necessary to hold the volume of the solid constant as the temperature is raised. If $P^*(T,V)$ is known precisely, the following equations can be used to obtain information about the vibrational properties of the lattice

$$B^*(T,V) = -V\left(\frac{\partial P^*}{\partial V}\right)_T , \qquad (I-6)$$

$$\left(\frac{\partial S}{\partial V}\right)_T = \left(\frac{\partial P}{\partial T}\right)_V = \left(\frac{\partial P^*}{\partial T}\right)_V , \qquad (I-7)$$

and

$$\left(\frac{\partial U^*}{\partial V}\right)_T = T\left(\frac{\partial P^*}{\partial T}\right)_V - P^* . \qquad (I-8)$$

The P-V-T data of Packard and Swenson (5) for xenon covered a sufficiently wide range of temperatures and pressures to determine $P^*(T,V)$ with some precision. Stewart's measurements for argon and krypton were for two isotherms each, while he measured only one isotherm for neon (4). Recently, a capacitance strain gauge technique was used to obtain an isochoric (constant volume) equation of state for solid argon in the 0 to 5 kbar region (6). A P-V-T relation for solid neon was obtained from recent direct determinations of the constant volume heat capacity in the 0 to 2.5 kbar region (7).

Simmons and co-workers have used the x-ray technique to measure the change in the lattice constant with pressure (0 to 20 bar) for neon (8), argon (9,10), and krypton (10,11). From these measurements the P=0 value

for the isothermal compressibility, $\chi_T=1/B_T$, can be calculated. χ_T for krypton at low pressures also has been obtained from interferometric measurements (12).

Adiabatic elastic constant determinations have been made using ultrasonic techniques for polycrystalline neon (13,14), and krypton and xenon (15), while single crystals were used for argon (16). The value of the elastic constants for solid xenon have been measured at P=0 and 156 K using a Brillouin scattering technique (17). P=0 values for the bulk modulus can be obtained from both of these techniques.

The foregoing discussion illustrates that very limited equation of state data exist for the rare gas solids. The investigation of xenon by Packard and Swenson (5) is the most extensive in both range of temperature and pressure. This discussion has suggested the importance of obtaining a 0 K equation of state, and of investigating the temperature-dependent contributions to the equation of state over as wide a temperature and pressure range as possible.

Historically, the Lennard-Jones two-body potential has been used to calculate the properties of the rare gas solids. This potential is given by

$$V(r) = \frac{m6\epsilon}{m-6}\left[\frac{1}{m}\left(\frac{\sigma}{r}\right)^m - \frac{1}{6}\left(\frac{\sigma}{r}\right)^6\right] \qquad (1\text{-}9)$$

where ϵ is the depth of the potential well, σ is the potential minimum, m is a measure of the repulsive energy (usually m=12), and the second term is the van der Waals attraction. σ and ϵ (Table 1) usually are calculated from the 0 K lattice constant and sublimation energy respectively. A review article by Horton (1) gives several other two-body potentials which

were used by early theories for calculating the thermodynamic properties for the inert gas solids. Hansen (18) has used a Lennard-Jones 6-12 potential with a Monte Carlo determination of the zero point energy to calculate an equation of state for solid neon at 0 K.

Barker and his co-workers recently have developed true two-body potentials for argon (19,20,21) and krypton (22) from a correlation of gas, liquid, and solid properties. They find that three-body terms must be included for the correct calculation of the properties for the solid and liquid. The calculations for the solids, especially at high temperature, must take into account the highly anharmonic nature of the lattice vibrations using the theory of self-consistent phonons. Klein, et al. have used this potential, plus three-body interactions and the improved self-consistent phonon theory to calculate the P=0 temperature-dependence of the bulk modulus for solid argon (23). They also have calculated the P=0 bulk modulus at T=0 K for solid krypton (22). No direct equation of state calculations have been reported using these theories.

The objectives for the present work are to obtain detailed P-V-T data for each of the rare gas solids, neon, argon, krypton, and xenon for pressures in the 0 to 20 kbar region and for temperatures from 4.2 K to close to the triple point for each solid. These data hopefully will provide reliable $P_o(V)$ relations and some information about the temperature-dependent equation of state for these solids.

CHAPTER II. EXPERIMENTAL APPARATUS

Method

The piston-displacement technique which is used in this experiment to determine the pressure-volume-temperature relationships for the rare gas solids, neon, argon, krypton, and xenon is similar to that used by Beecroft and Swenson (24) and Packard and Swenson (5). A sample with low yield stress (length $\approx$ diameter) is placed in a thick-walled cylindrical sintered tungsten carbide (Kennametal) sample holder which has closely fitting pistons on each end. The sample holder is placed in a ten-ton hydraulic press, Figure 1A, and a dial gauge is connected as shown in Figure 1B to read the relative movement of the two pistons. A dead weight gauge, not shown, is used to generate the oil pressure in the hydraulic ram. By adding or removing weights to the dead weight gauge, the pressure in the ram and hence the force on the sample can be varied incrementally. Three different diameter sample holders, 0.500 in. for pressures to 7 kbar, 0.354 in. for pressures to 14 kbar, and 0.250 in. for pressures to 20 kbar, are used to detect possible systematic discrepancies. The temperature of the sample holder is controlled automatically above 40 K, while manual control must be used for lower temperatures. In each mode the flow of refrigerant into the heat exchanger, Figure 1A, is continuously adjusted so that the heat of vaporization and vapor enthalpy of the gas just balance the heat leak down the press. The sample holder temperature in either case can be controlled to 0.2 K for long periods of time in the 4.2 to 473 K region (5). Compression data are taken for each of the different diameter sample holders at approximately the same

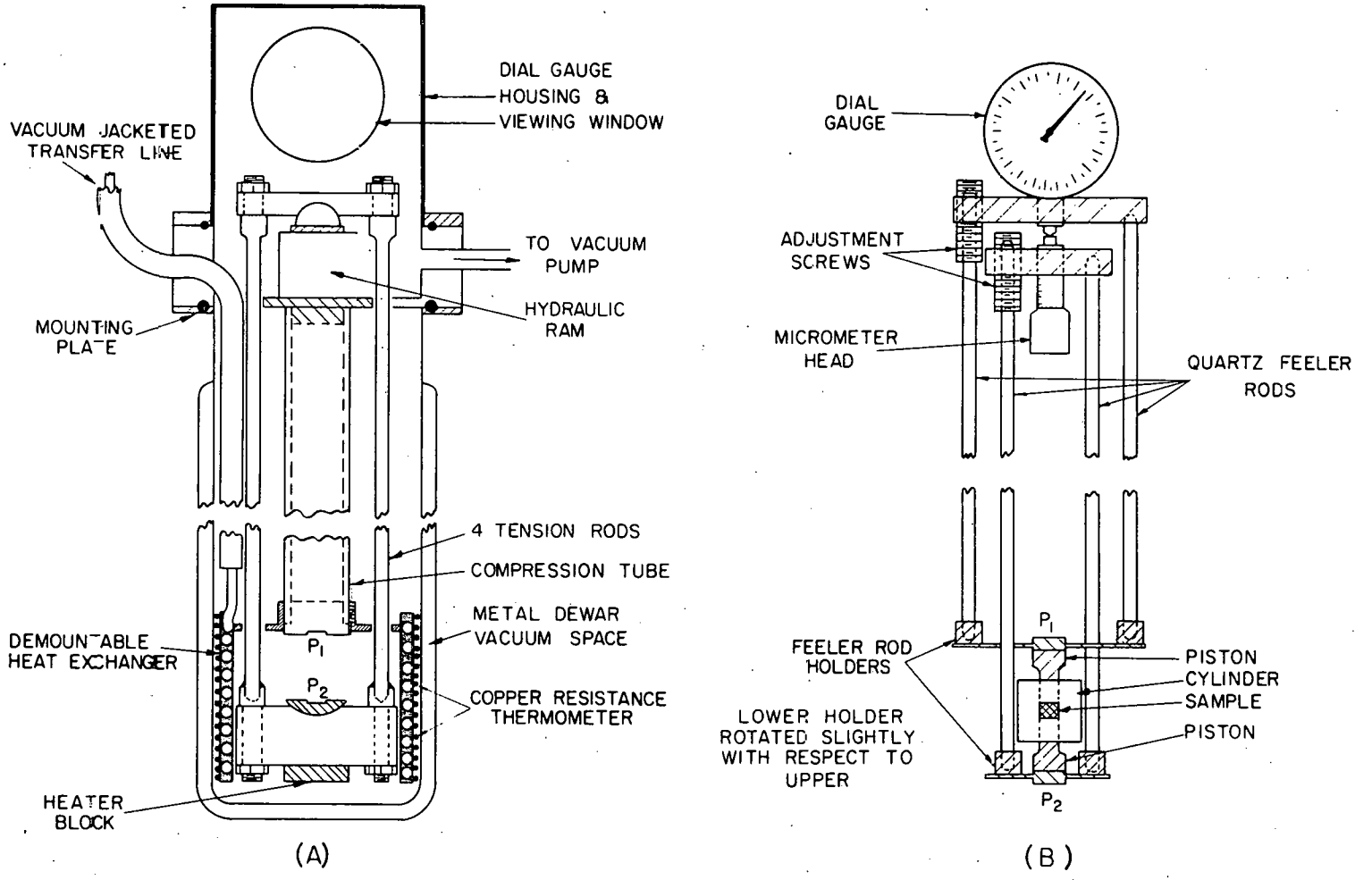

Figure 1. The press, (A), and the compression measuring system, (B) (Reference 24). A second dewar (not shown) surrounds the metal dewar in (A) when working below 77 K.

temperature so that comparisons described later can be made.

Press

The press as shown in Figure 1A and as described in the literature cited above was not modified for these measurements. However, the vacuum jacket on the refrigerant supply dewar end of the transfer tube, not shown, was lengthened to accommodate a 50 liter liquid helium dewar, and the temperature range was extended to 4.2 K.

Compression Measuring System

Two different Starrett dial gauges are used for this work; the first (model No. 655-441, local No. 12) has a 1.000 in. range with 0.001 in. graduations, while the second (model No. 655-611, local No. 6) has a range of 0.2100 in. and graduations of 0.0001 in. The gauge with the 1 in. range is used in the initial compression run and to determine the sample length. The second gauge is used to measure the relative motion of the pistons (with a precision of 2×10^{-5} in.) during a compression run.

A flexible mechanical coupling is used to keep both components of the dial gauge holder, Figure 1B, in physical contact at all times (25). Careful adjustment of the dial gauge holder and micrometer screw distributes the weight equally between each pair of quartz feeler rods. This is necessary so that the movement of the pistons will be reflected directly in the dial gauge reading.

Sample Holder

Figure 2 is a sketch of the sample holder which is used for the 0.250 in. and 0.354 in. cylinders. The Kennametal (K-92) cylinder is jacketed

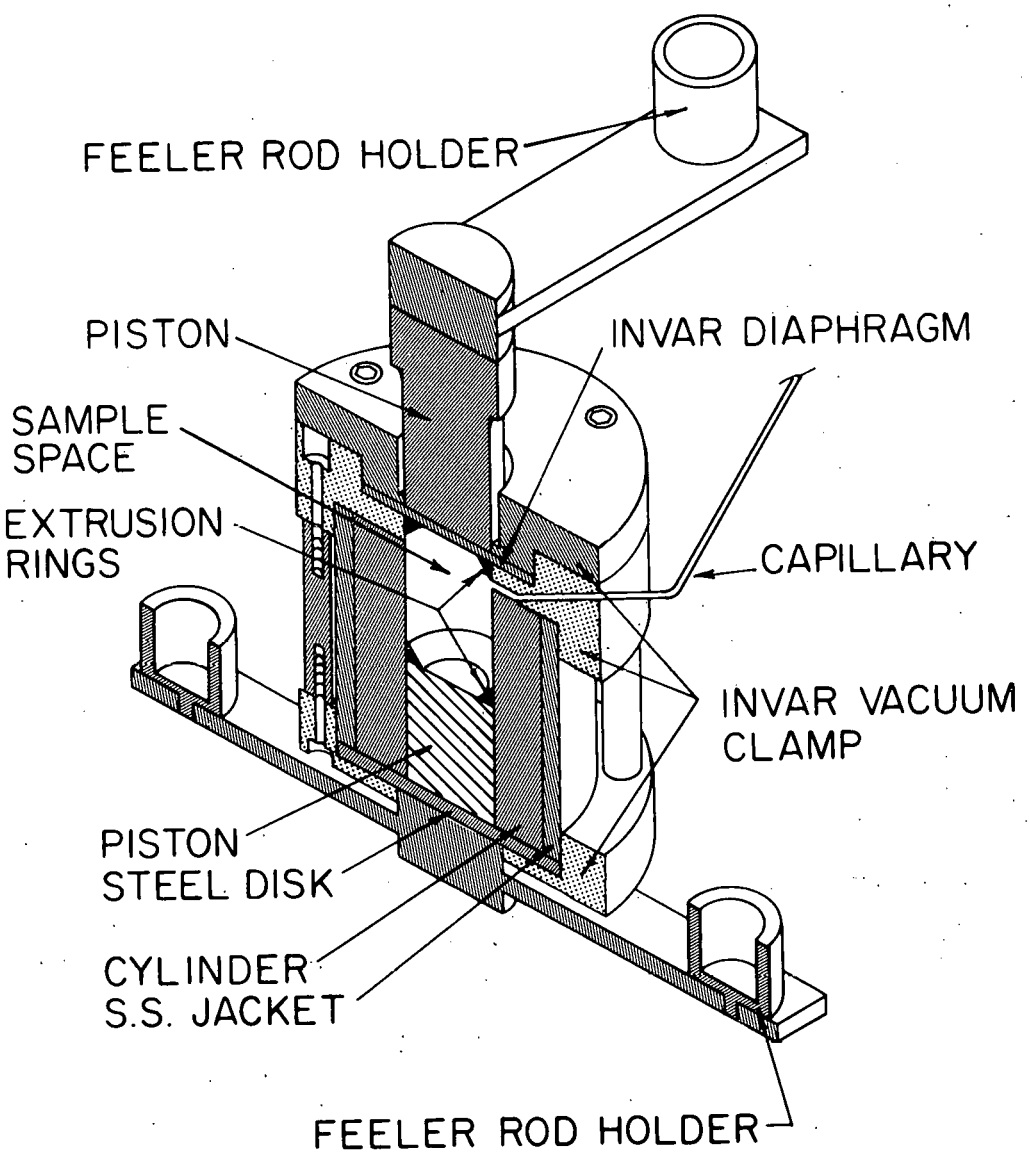

Figure 2. Sample holder details.

with a stainless steel cylinder to prevent a catastrophic loss if the cylinder should fail while at high pressure. The top piston and blind (dead) piston used to apply force to the sample are made from Kennametal (K-96). The three piece Invar vacuum clamp is used to obtain a vacuum-tight sample space. The triangular extrusion rings (brass for the 0.500 in. and 0.354 in. and cold rolled steel for the 0.250 in. diameter sample holders) are used to prevent the sample from leaking past the pistons. The maraging steel disk, which is used to support the blind piston and to form the bottom vacuum seal, is greased lightly (Dow Corning High Vacuum grease) and placed on the bottom of the cylinder. The top of the cylinder is greased lightly and the middle and bottom pieces of the Invar clamp are put in place and the screws are tightened. Care must be taken to insure that the grease used to make the vacuum seal does not creep into the sample space since this would give a false length and compression measurement. The bore must line up perfectly with the middle piece of the clamp to prevent the top piston from hitting the top edge of the cylinder after puncturing the diaphragm. The resulting chipping of the piston leads to piston failure at high pressures. The diaphragm (0.010 in. Invar) is greased lightly and is clamped tightly between the top and middle pieces of the Invar clamp. The copper capillary in the middle piece of the clamp connects to the gas handling system which is described below. A thin Invar disk (0.010 in.) is placed between the extrusion ring and the blind piston in the 0.250 in. sample holder to prevent breakage of the blind piston from sample motion at high pressure. The diaphragm serves the same purpose for the top piston.

The brass vacuum clamp used by Packard and Swenson (5) was used for preliminary compression data on argon, but it was impossible to make the sample space consistently vacuum tight. The problem is believed to be due to the large differential thermal expansion between the brass clamp and the Kennametal cylinder. The vacuum clamp for the present experiment is made of Invar because the thermal expansion of this metal is very close to that of the Kennametal. Little difficulty is experienced making the sample space vacuum tight with the Invar clamp.

The 0.500 in. sample holder and vacuum clamp are made from maraging steel, while the pistons are made from drill rod. These metals can be used since the 7 kbar maximum pressure is less than the yield strength of these steels. The 0.500 in. sample holder has components similar to those discussed above and shown in Figure 2, although it is physically different.

The effectiveness of the sealing of the extrusion rings is increased by chamfering the 90^{o} corner. This also reduces the friction in the sample holder since the rings are kept from extruding between the piston and cylinder wall. On occasion, the gas (liquid) did not leak past the extrusion rings at temperatures above the triple point until several weights pressure (a few kbar) had been applied. This suggests that the extrusion rings in those experiments were well-seated to both the cylinder wall and piston face.

If the difference between the diameter of the piston and the diameter of the bore of the cylinder is equal to or greater than 0.001 in., the friction in the sample holder is reduced. The excess friction which is eliminated is believed to be due to the lateral expansion of the pistons as the pressure is increased.

Temperature Sensing and Cryogens

Temperatures are determined using a copper-constantan thermocouple which is referenced to the ice-point in conjunction with a Leeds and Northrup K-3 Universal potentiometer and a Honeywell 0-100 microvolt potentiometric recorder. The thermocouple is calibrated in the 4.2 to 20 K region using a germanium resistor (serial No. 638) as a standard. This resistance thermometer was used in the neon heat capacity experiments of Fugate and Swenson (26). A calibration table for our thermocouple is constructed using these data and an additional 77 K point in conjunction with the National Bureau of Standards thermocouple tables (27). Temperatures are believed to be accurate to 0.1 K from 13.5 to 20 K, and to 0.5 K above 20 K.

Liquid helium is used as the refrigerant in controlling temperature between 4.2 and 77 K, while liquid nitrogen is used for temperatures above 77 K. Approximately 25 liters of liquid helium are used over a 16 hour period while taking compression data for an average set of isotherms, 77 K, 40 K, 4.2 K, 20 K, 60 K, and 77 K.

Gas Handling and Samples

The sample gas is received from the manufacturer in a small high pressure cylinder which contains from 10 to 25 liters STP. The cylinder is connected with appropriate fittings to a one liter standard volume which is connected through a valve to the copper capillary leading to the sample holder. A vacuum pump is connected to the system also, and both a compound gauge and a mercury manometer are used to measure the pressure in the standard volume.

The gases used to make the samples were purchased commercially with a stated purity of greater than 99.99% in all cases. The manufacturer and designation for each gas are as follows; neon (Matheson, Research Grade gas), argon (Air Products, supplied from the Ames Laboratory stock with a guaranteed purity of 99.996%), krypton (Linde, Research Grade gas), and xenon (Cryogenic Rare Gas Laboratories, Research Grade gas).

CHAPTER III. EXPERIMENTAL PROCEDURE

Sample Solidification and the Taking of Data

The sample holder is assembled carefully with the minimum amount of grease required to ensure vacuum-tight seals. The vacuum seal is checked by thermally shocking the sample holder between room temperature and 77 K with the requirement that the sample space hold a good (10^{-2} torr) vacuum the whole time. The sample holder is inserted into the press and the copper capillary is connected to the standard volume. The quartz feeler rods are put in place with the 1 in. travel dial gauge installed. The vacuum insulated dewars are mounted in place. The sample space is evacuated and flushed several times with the sample gas, to prevent contamination by other gases, and a pressure of approximately 15 psig is left in the sample space. Liquid nitrogen is transferred and the sample holder is cooled to roughly 20 K above the triple point of the sample. The sample space is evacuated and if it remains vacuum tight, the sample holder is cooled to the triple point and as the pressurized standard volume is connected, a very rapid warming spike is noted on the temperature recorder. Rapid condensation is necessary to prevent capillary blocking. After condensing a predetermined amount of gas (as is indicated by the pressure drop in the standard volume), the valve between the sample holder and standard volume is closed.

It is very important that the extrusion rings be tightly seated against the cylinder wall to prevent sample leakage at high pressures. Since the solid sample has a relatively higher shear yield stress at low temperatures than near the triple point, the sample holder is cooled to a

temperature considerably below the triple point before the diaphragm is broken and the initial compression run is made.

After the temperature of the sample holder is stable, a dial gauge reading is taken which will be used later in determining the sample length, and the pressure is increased slowly until the diaphragm breaks. The jarring of the compression measuring system during this operation is believed to cause the major uncertainty in the sample length calculation. The sample then is "seasoned" by cycling to maximum pressure and back to minimum pressure several times until the dial gauge readings reproduce to less than 10^{-4} in.

The first set of compression data now is taken by recording the dial gauge reading as a function of the number of weights on the pan of the dead weight gauge as the pressure is increased and then decreased monotonically. The 1 in. travel dial gauge is replaced with the 0.21 in. travel gauge and the first compression run is repeated at exactly the same temperature to tie the scales of the two dial gauges together.

A typical set of compression data is shown in Figure 3 for two temperatures. The hysteresis loop exists because of the friction in the press, the sample, and sample holder components. The greater hysteresis for the lower temperature curve presumably is due to the increase in shear yield stress of the sample with decreasing temperature.

Data are taken for a number of isotherms for a given sample. The order in which the isotherms are taken is chosen so as to indicate systematic differences in the data (dial gauge readings) which could be caused by sample loss or by jarring of the apparatus, etc. In particular, one of

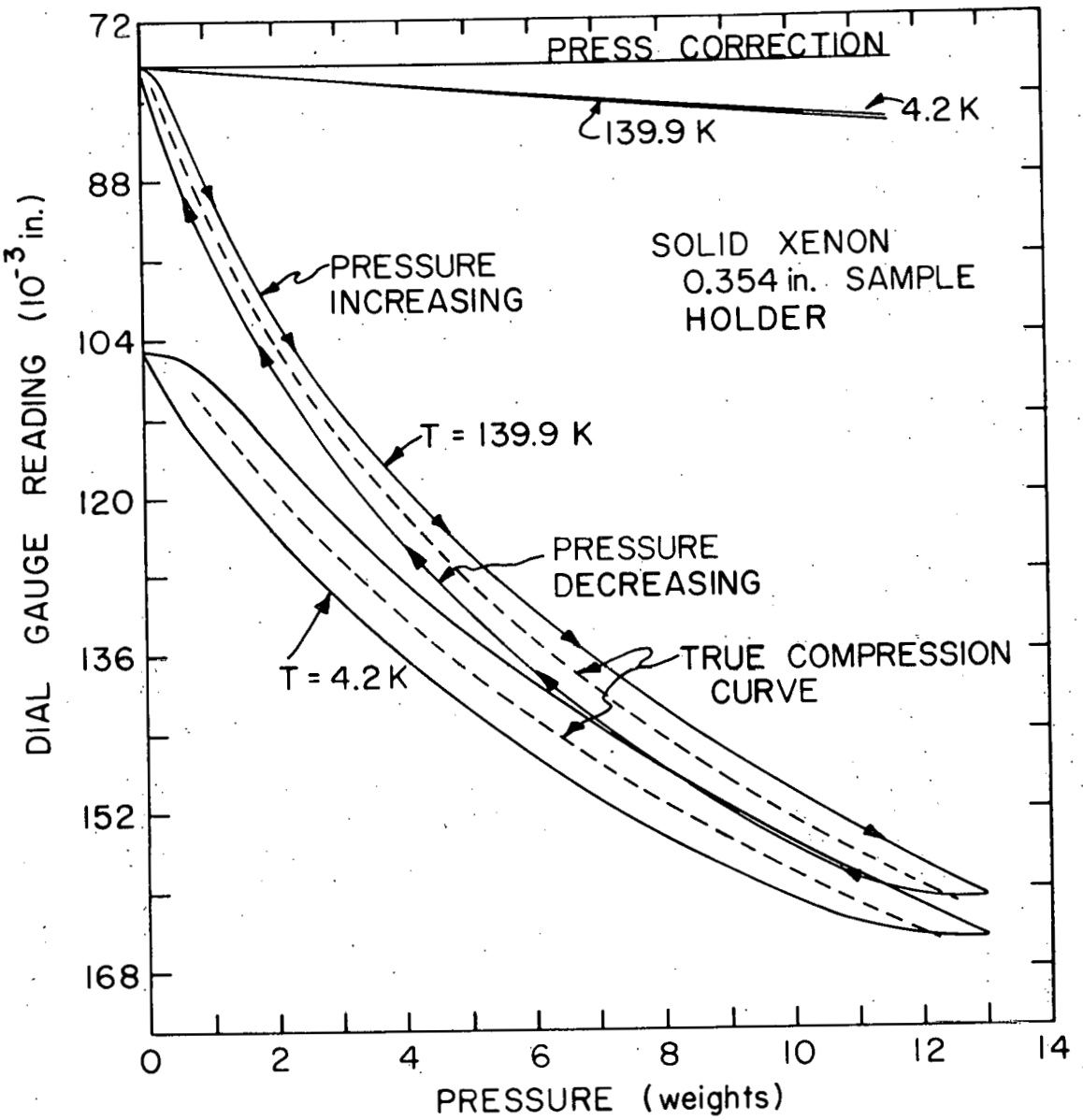

Figure 3. A typical raw data plot showing sample length change vs. increasing and decreasing pressure for two isotherms. The true compression curve is obtained by averaging the frictional force at constant displacement as is described in the text.

the isotherms, usually the initial one, is repeated at the end of a run to establish the internal consistency of the data.

Sample Length Determination

The experimental sample length is determined by two independent methods, one of which is used at the beginning and the other at the end of a run. The agreement of the two methods often is as good as $\pm$ 0.5%, although inconsistencies of up to 2% are found for the 0.250 in. diameter sample when results for it are compared with results for the 0.500 in. and 0.354 in. diameter samples.

The first method used to determine the experimental sample length is similar to that described by Packard and Swenson (5). Before assembling the sample holder, Figure 2, the distance from the bottom of the diaphragm to the bottom of the steel disk is measured carefully, and the thickness of the steel disk, the length of the blind piston, and the equivalent length of the extrusion rings all are subtracted from the measurement to obtain the total sample-space-available. The piston motion is determined by subtracting the dial gauge reading prior to breaking the diaphragm from a dial gauge reading on the true-compression curve of the first compression run. The sample length at a given temperature and pressure then is obtained by subtracting the piston motion from the total sample-space-available minus the small corrections which are discussed below.

The second method for experimental sample length determination is similar to that used by Stewart (3). This length determination is made after all compression data for a given sample are taken. A compression run is completed just below the triple point of the sample. The 0.21 in.

travel dial gauge is replaced with the 1 in. travel gauge and another set of compression data is recorded at the same temperature to tie the two dial gauge scales together. After the compression run is completed, the sample holder is warmed above the triple point of the sample, and the sample is allowed to leak past the extrusion rings. After the sample escapes, the top piston is driven down as close to the bottom piston as the extrusion rings will allow, a force of several weights is applied to ensure that the extrusion rings are together, and the dial gauge reading is recorded. The piston travel is calculated by subtracting the dial gauge reading at some pressure and temperature before the sample escapes from the dial gauge reading taken after driving the pistons together. The press now is warmed to room temperature and disassembled. The distance between the bottom of the steel disk and the top of the top piston is measured, and the lengths of all components between these two points are subtracted from this reading to obtain a small additional sample space not previously recorded on the dial gauge. This additional sample space is added to the piston travel recorded above to obtain the sample length as a function of temperature and pressure.

CHAPTER IV. DATA ANALYSIS

True Compression Curve

The friction-corrected (true piston motion) curve is obtained from the hysteresis loops shown in Figure 3 by assuming that for a given dial gauge reading the friction is identical in magnitude (but of opposite sign) for the pressure-increasing and pressure-decreasing curves. Thus, the true compression curve is found by averaging the pressures on the two curves at a given displacement.

The joining of these curves at both low and high pressures is caused by the reversal of the friction forces when the direction of the piston motion is reversed. In the low pressure region, the pressure-increasing and pressure-decreasing curves taper together smoothly, except at the very end. This tapered region is assumed to satisfy the condition stated above, and the true compression curve is determined by averaging the pressures. It is obvious from Figure 3 that this procedure cannot be carried out at the lowest pressures, nor can data be obtained at zero weights. In the high pressure region, the friction has approached a constant value by 6 weights, so the true compression curve is drawn parallel to the pressure-increasing curve by assuming that the friction remains constant to the highest pressure. The averaged pressure points are connected graphically with a smooth curve to obtain the true piston motion. The friction-corrected curve is determined for each isotherm and dial gauge readings corresponding to incremental pressures in kbar are recorded.

The conversion from pressure in weights (or force on the pistons),

to pressure in kilobars is given by

$$P = \frac{n + 0.151}{A} \qquad \text{(IV-1)}$$

where P is the pressure in kbar, n is the number of weights on the dead weight gauge (the pan is equivalent to 0.151 wts.) and A is a conversion factor which depends on the sample holder area. It is, respectively, 1.6821, 0.8413, and 0.4250 weights/kbar for the 0.500 in., 0.354 in., and 0.250 in. diameter sample holders which are used.

Corrections

The dial gauge readings reflect directly the compression of the sample and the linear and lateral distortion of the sample holder components. Similarly, temperature variations represent a combination of sample and sample holder effects. Hence, various corrections must be made to the dial gauge readings before the sample compression can be obtained.

The temperature and pressure dependence of the dial gauge reading, $R_{d.g.}$, is given by the relation

$$R_{d.g.}(T,P) = M + L_p(T,P) + \frac{V(T,P)}{A_{cyl}(T,P)} \qquad \text{(IV-2)}$$

where L_p is the length of the pistons, V/A_{cyl} is the sample length and M is a temperature- and pressure-independent constant which converts the dial gauge readings to true sample lengths. The stress dependence of $R_{d.g.}$ is obtained by differentiating Equation IV-2 with respect to force

$$\left(\frac{\partial R_{d.g.}}{\partial F}\right)_T = \left(\frac{\partial L_p}{\partial F}\right)_T - \frac{V}{A_{cyl}^2}\left(\frac{\partial A}{\partial F}\right)_T + \frac{1}{A_{cyl}}\left(\frac{\partial V}{\partial P}\right)_T \left(\frac{\partial P}{\partial F}\right)_T \qquad \text{(IV-3)}$$

where $(\partial L_p/\partial F)_T$, the piston compression, is slightly temperature dependent, the second term is a first order correction caused by the slight deformation of the cylinder bore with applied force, and the third term contains the quantity of interest, $(\partial V/\partial P)_T$ for the sample.

If the average area of the cylinder bore is given by $A_{cyl} = A_o(1 + \delta P)$, $(\partial A/\partial P)_T = A_o\delta = A_o(\partial A/\partial F)_T$. The area of the cylinder bore at the pistons, A'_{cyl}, which determines the sample pressure certainly is less than the average area defined above because the cylinder distortion will be barrel-shaped. If the area of the cylinder bore at each piston varies as $A'_{cyl} = A_o(1 + \epsilon P)$, with $\epsilon < \delta$, the force applied to the pistons is related to the pressure on the sample by $F = (A'_{cyl})P = A_o(1 + \epsilon P)P$, and $(\partial F/\partial P)_T = A_o(1 + 2\epsilon P)$. Equation IV-3 now becomes

$$\left(\frac{\partial V}{\partial P}\right)_T = A_o(1 + (\delta + 2\epsilon)P)\left[\left(\frac{\partial R_{d.g.}}{\partial P}\right)_T - B(L_s,T)\right] \qquad \text{(IV-4)}$$

where

$$B(L_s,T) = \left[\left(\frac{\partial L_p}{\partial P}\right)_T - L_s\delta\right] \qquad \text{(IV-5)}$$

and $L_s = V/A_{cyl}$. Since B is small compared with $(\partial R_{d.g.}/\partial P)_T$ (typically 10% for this experiment), the identity $A_o = A'_{cyl}$ has been assumed in its definition.

The "press correction," $B(L_s,T)$, is determined from compression data which are taken for several indium samples of different lengths at several temperatures in each of the sample holders used, using exactly the same press and sample holder configuration which is used for the solid gas compressions. An equation of state for indium is assumed for this

correction (28). When the indium compressions are subtracted from the friction-corrected data, the sample holder distortions are found to be linear to 10^{-4} in.; that is, B is independent of pressure. Experimentally, B is found to be temperature-independent also between 4.2 and 77 K (Figure 4), while it changes by roughly 10% in the 77 to 300 K region. B in effect reflects the temperature dependence of the elastic moduli of the piston and cylinder materials. The length-dependence of the "press correction" (Figure 5) is given by Equation IV-5 and is determined from the indium compression data using various length samples. The first order correction to the cylinder bore, δ, is estimated from Equation IV-5 and Figure 5 to be 4×10^{-4} kbar^{-1} for the Kennametal sample holders, and 1.33×10^{-3} kbar^{-1} for the maraging steel sample holder.

Equation IV-4 can be integrated to give

$$\Delta V = \Delta V_s + (\delta + 2\epsilon) \int_{V_1}^{V_2} P dV_s \qquad \text{(IV-6)}$$

where $\Delta V_s = \Delta L_s A_o = A_o[\Delta R_{d.g} - (B(L_s,T))\Delta P]$. The second term in Equation IV-6 represents a second order correction for δ, and a first order correction for ϵ. The magnitude of this correction must be evaluated to estimate the effect which it has on the data. For the neon isotherm at 19.9 K, which has the largest relative compression, the integral has approximate values of 7.5, 17.0, and 26.0 kbar cm^3/mole, respectively, for pressures from 0 to 7, 14, and 20 kbar which correspond to the pressure ranges for the various sample holders used. The correction can be evaluated for three typical values of ϵ; first, δ and ϵ are (unreasonably) assumed to be equal in magnitude, second, $\epsilon = \delta/2$, and last $\epsilon = 0$. The value of the

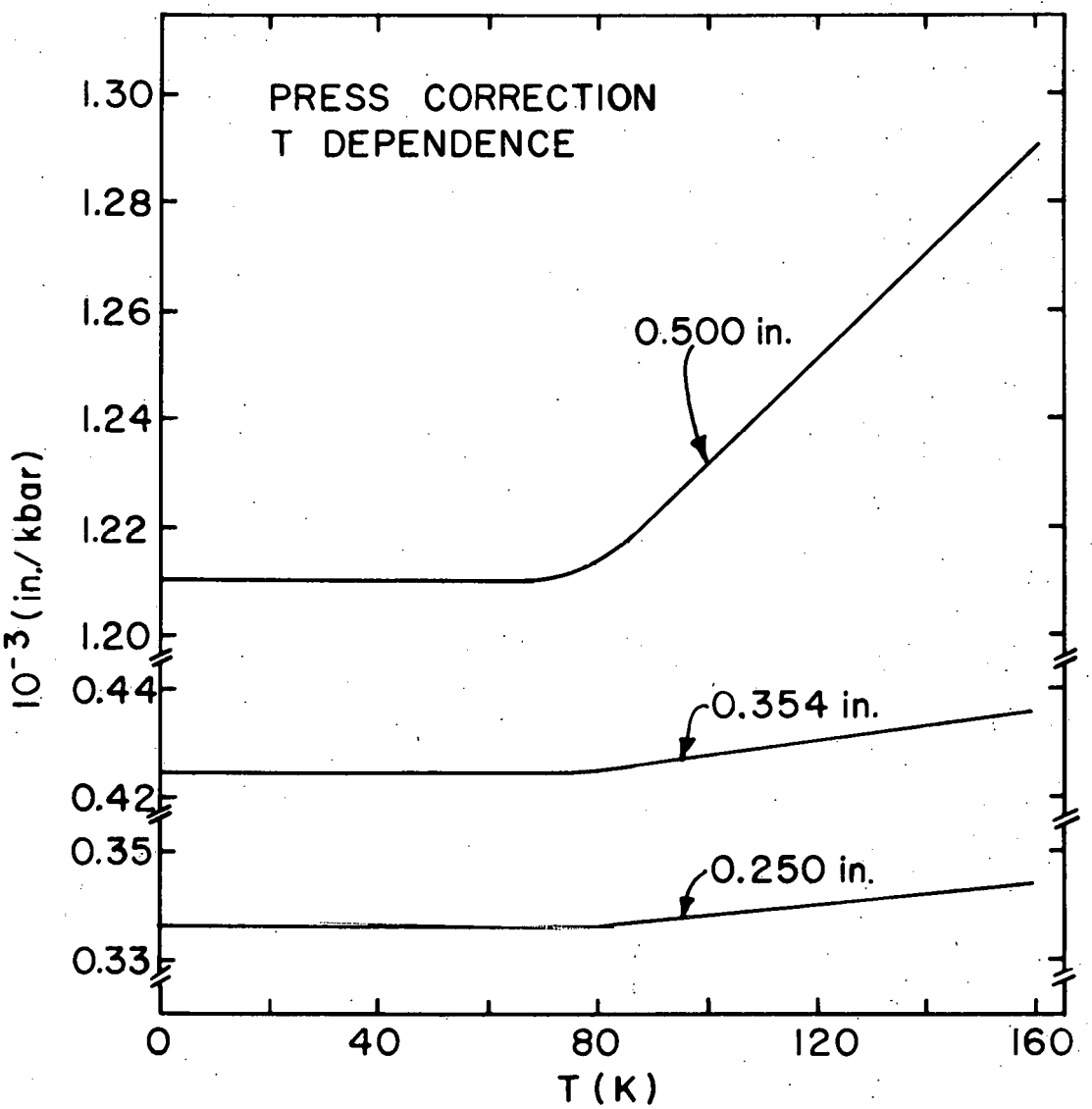

Figure 4. The temperature-dependence of the "press correction."

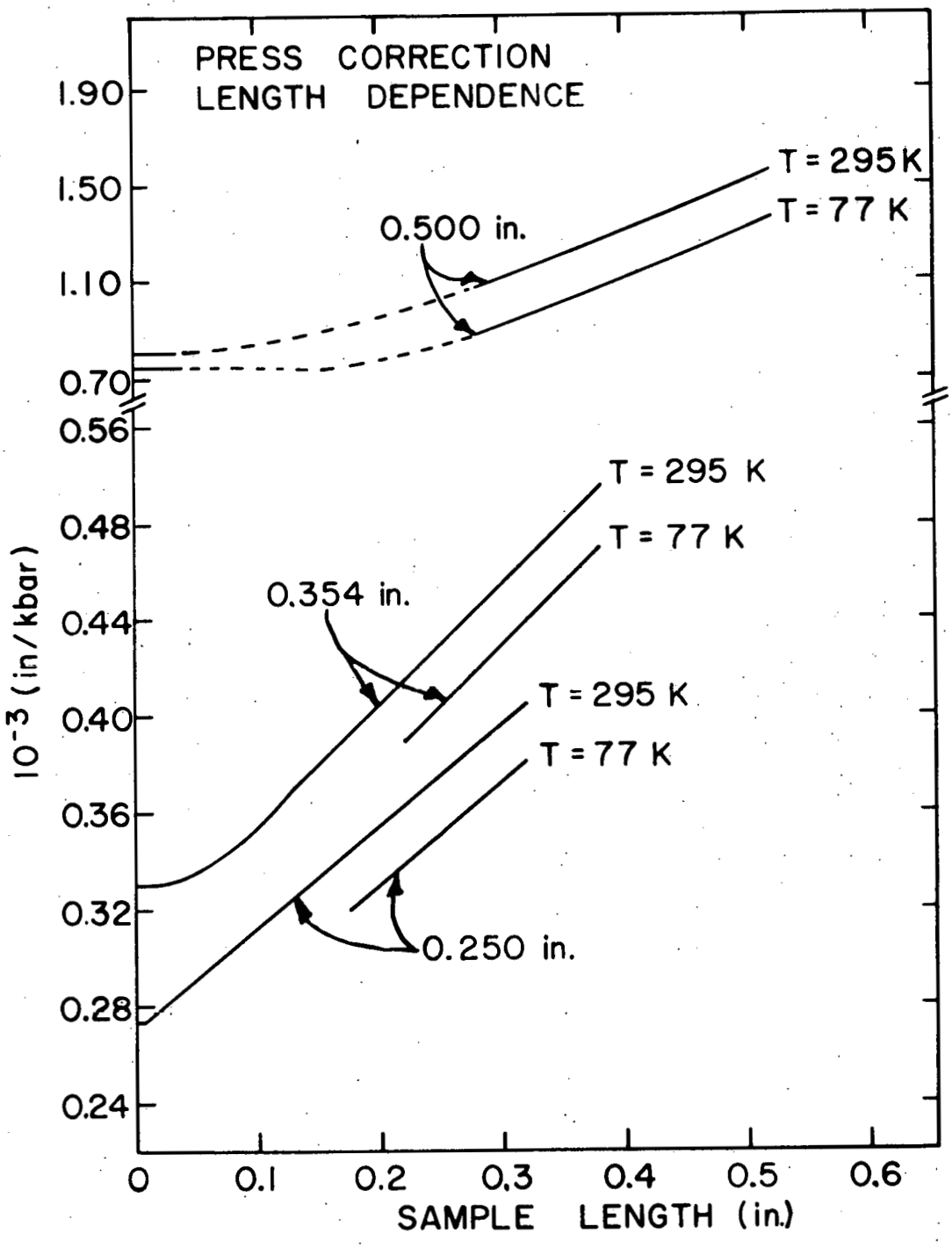

Figure 5. The sample length and temperature dependence of the "press correction."

correction for neon for each of these assumptions is given in Table 2. The $\epsilon = \delta/2$ value is believed to give approximately the right magnitude for the correction. Thus, the estimated correction is close to the estimated experimental precision in the high pressure limit ($0.2\%V_o$, or 2.8×10^{-2} cm^3/mole), and because it cannot be evaluated with any precision it is neglected in the data analysis. Neon is chosen as an example for these considerations, and represents an extreme case.

The area of the cylinder bore at the pistons is assumed to remain constant (i.e., $\epsilon = 0$) in the calculations of the pressure (force/area) on the sample. The error in the pressure due to this assumption is believed to be less than 0.5% (for $\epsilon = \delta/2$) at 20 kbar. Since the bulk moduli of all samples are approximately 150 kbar at these pressures, the equivalent

Table 2. The value of the relative correction, $\Delta V_c/V_o = (\delta + 2\epsilon) \int_{V_1}^{V_2} Pd(V_s/V_o)$, in percent, for values of $\epsilon = 0$, $\epsilon = \delta/2$, and $\epsilon = \delta$, as calculated for the 19.9 K neon isotherm for each of the sample holders.

Sample Holder Diameter (in.)	$\Delta V_c/V_o$ ($\epsilon = 0$) (%)	$\Delta V_c/V_o$ ($\epsilon = \delta/2$) (%)	$\Delta V_c/V_o$ ($\epsilon = \delta$) (%)
0.500	+0.07	+0.15	+0.22
0.354	+0.05	+0.10	+0.15
0.250	+0.07	+0.15	+0.22

uncertainty in the volume is less than 0.1%.

The solid gas sample compressions are quite large, so the total "press correction" or length change due to piston compression, etc., must be obtained by integration since B depends on the sample length. A suitable approximation to this procedure is given by choosing an average "press correction," $\overline{B}$, which gives the same total correction

$$\overline{B}P = \int_0^P B(L)\,dP \ . \qquad \text{(IV-7)}$$

As a general rule, $\overline{B}$ corresponds to sample lengths at pressures of 3, 6, and 7 kbar, respectively, for each of the sample holders used. The value of $\overline{B}$ varies with temperature as the sample length changes and, therefore, must be determined separately for each isotherm. The error introduced by this choice of an average value of B which corresponds to a sample length at a characteristic pressure is by actual calculation less than 0.1% of the volume.

The dial gauge readings are corrected for thermal expansion effects in the sample holder as follows. Equation IV-2 is differentiated with respect to temperature

$$\left(\frac{\partial R_{d.g.}}{\partial T}\right)_P = \left(\frac{\partial L_p}{\partial T}\right)_P - L_s \frac{1}{A_{cyl}} \left(\frac{\partial A_{cyl}}{\partial T}\right)_P + \frac{1}{A_{cyl}} \left(\frac{\partial V}{\partial T}\right)_P \qquad \text{(IV-8)}$$

where $(\partial L_p/\partial T)_P$ represents the thermal expansion of the piston material, the second term involves the area thermal expansion of the cylinder bore, and the third term contains the thermal expansion of the sample. The piston length and cylinder bore area can be written in terms of their

linear expansion coefficients, α_p and α_{cyl}, and after integrating Equation IV-8 with respect to temperature, the volume changes of the sample at constant pressure become

$$\Delta V = A_{cyl}[\Delta R_{d.g.} - L_p \int_{T=0}^{T} \alpha_p dT + 2L_s \int_{T=0}^{T} \alpha_{cyl} dT] \qquad (IV\text{-}9)$$

$$= A_{cyl}[\Delta R_{d.g} - C(L_s,T)] \qquad (IV\text{-}10)$$

where $C(L_s,T)$ is a pressure-independent thermal expansion correction. In general, the maximum variation in the cylinder bore area with temperature and pressure is less than 1%, while the volume changes at constant pressure are never greater than 11%, so A_{cyl} can be taken as equal to its zero pressure value.

Experimentally, it is found that C is temperature-independent between 4.2 and 77 K (Figure 6) although it decreases by from 1 to 2 x 10^{-3} in. from 77 to 300 K. The temperature dependence of C for the xenon samples is given in Figure 6.

Data Comparison and Computer Extrapolation

The corrected dial gauge readings give relative length changes, ΔL, as a function of temperature and pressure for each sample. In practice, the experimentally determined sample length (see the Experimental Procedure Section) is used to determine the constant M in Equation IV-2 so that actual sample lengths are obtained as a function of temperature and pressure, $L(T,P)$. While the absolute sample length only may be known to 0.5%

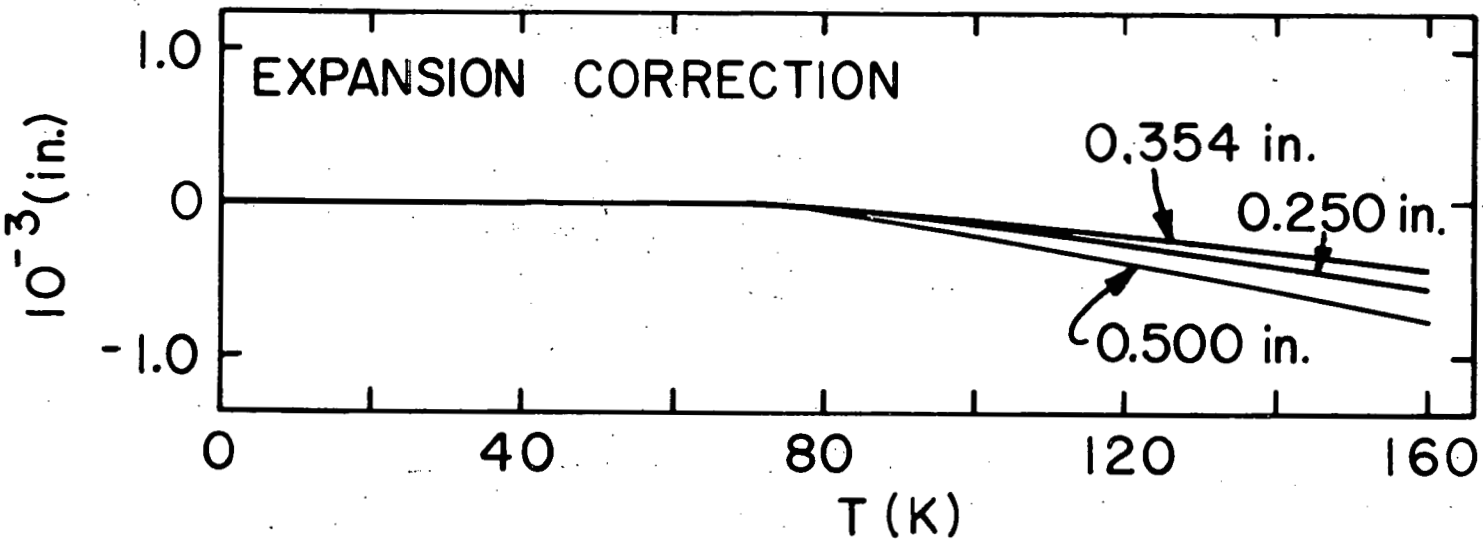

Figure 6. The thermal expansion corrections, C, which were used for the xenon samples.

(1 to 2 x 10^{-3} in.), relative length changes are known with a precision which is approximately an order of magnitude greater than this (0.1 to 0.2 x 10^{-3} in.).

The data for each of the sample holders are compared by forming the arbitrary ratio $L(T,P)/L_{o4}$, where $L_{o4} = L(4.2\ K,\ 4\ kbar)$. If the data are not taken at approximately the same temperature for the various sample holders, a graph of $L(T,P)/L_{o4}$ vs. temperature is made to normalize the data along the isotherms. A computer is used as described below to compare the data for the various sample holders. If systematic errors appear, the absolute sample length (or L_{o4}) is adjusted slightly for one of the samples to bring the data into better agreement.

Several empirical equations of state have been used successfully to fit P-V data (29). These relations give a sensitive method for comparing different sets of data, and also allow an extrapolation to be made to zero pressure for comparison with other experiments. In computer fitting equations to the data, the major uncertainty is in the determination of L (or V), so the quantity $\Sigma\Delta V_i^2 = \Sigma(V_i - V_{calc})^2 = \Sigma[(P_i - P_{calc})(V_i/B_T(V_i))]^2$ is minimized in the fitting routine for each of the equations discussed below, using an iterative procedure.

Earlier P-V data (5,30,31) were represented successfully by a relationship given by Birch (32), Anderson (33)

$$P(V,T) = P_o + \frac{3}{2} B_o (y^7 - y^5)[1 - \xi(y^2 - 1)] \qquad (IV\text{-}11)$$

where $y = (V_o/V)^{1/3}$ (or $(L_o/L)^{1/3}$), B_o and V_o (or L_o) are the bulk modulus and molar volume, respectively, at pressure P_o, and ξ is an adjustable

parameter which is related to $\eta = (\partial B_T/\partial P)_{T,P=0}$. Equation IV-11 can be rewritten in a generalized form as

$$P(V,T) = A_o + \frac{3}{2} y^5 \sum_{n=1}^{N} A_n (y^2 - 1)^n , \qquad (IV-12)$$

which is fit to the data using a least squares method with an IBM-360, model 65 computer. The value of V_o (or L_o) is adjusted by an iterative method until $A_o = P_o$ is zero.

The Lennard-Jones 6-12 potential has been widely used to describe the interatomic potential for the rare gas solids (1). A generalized equation of state based on a potential of this form is given by

$$P(V,T) = \sum_m A_m V^{-m} . \qquad (IV-13)$$

Several different forms of this equation were fit to the data using least squares techniques. First, even integer powers in V^{-m} were used, then odd integer powers, and finally all powers. The best results (see below) are obtained with $m \geq 3$ and odd. Thus, the equation used to fit the data is given by

$$P(V,T) = \sum_{n=0}^{N} A_n V^{-(2n + 3)} . \qquad (IV-14)$$

In addition to determining V_o and giving a smooth representation for the data, the computer programs calculate the isothermal bulk modulus, $B_T = -(\partial P/\partial \ln V)_T$, for each experimental pressure. The bulk modulus at zero pressure, B_o, is determined from the extrapolation to zero pressure.

The data for each of the three sample holders along each isotherm are

included in the computer fitting. Two different ranges of data are used to insure that the extrapolation to zero pressure is range-independent. The full-range fits include all data to maximum pressure, while the half-range fits include only volumes (or lengths) greater than $(V_o - \Delta V/2)$, where ΔV is the total compression.

Several different orders of Equations IV-12 and IV-14 are fit to the P-V data. The criteria used to determine the most satisfactory representation are first, that the root mean square deviation be equal to or less than 0.1% V_o and second, that the zero pressure thermal expansion obtained by extrapolation must agree with that obtained from direct P=0 experiments. This latter comparison can be made by noting that the extrapolated P=0 sample lengths and the P=0 molar volumes must be related by

$$\frac{L(T,P=0)}{L(4.2\ K,P=0)} = \frac{V(T,P=0)}{V(4.2\ K,\ P=0)} \quad . \qquad \text{(IV-15)}$$

The left hand side of this relation is obtained from the data, while the right hand side is obtained from the literature. In practice, L(4.2 K, P=0) is adjusted slightly to give the best agreement possible for Equation IV-15 at all temperatures. Then, the equation of state can be calculated as

$$V(T,P) = V(4.2\ K,P=0)\left[\frac{L(T,P)}{L(4.2\ K,P=0)}\right] \quad . \qquad \text{(IV-16)}$$

CHAPTER V. EXPERIMENTAL RESULTS

This chapter summarizes the experimental results for each of the solids. The actual data, after correction for sample holder thermal expansion, pressure distortion, and any sample loss or dial gauge shifts, are given in Appendix A where they are expressed in terms of molar volumes as a function of pressure for each isotherm. Appendix B gives the coefficients for the equation which best represents the data for each isotherm, and Appendix C presents plots of the differences between the data and the computer-calculated relations. The experimental values of the 4 kbar sample lengths at 4.2 K (L_{o4}) are given in Table 3 for the various samples. During the computer smoothing of the isotherm data for each solid, the values of L_{o4} for certain samples were adjusted to the values given in parentheses to make the final results internally consistent. The tabulations in Appendix A do not reflect this adjustment, but it is included in the fit coefficients of Appendix B and the "experimental data" of Appendix C. The experimental length change data for each sample first were expressed in terms of absolute lengths using the initial L_{o4} values of Table 3, then the molar volumes of Appendix A were calculated using the conversion factors which are listed in this Appendix.

The procedure which was used to analyze the data was identical for each solid. The Birch and Lennard-Jones relations (Equations IV-12 and IV-14) were fitted in turn first to the full-range (20 kbar) and then to the half-range (approximately 5 kbar) adjusted data. A satisfactory

Table 3. Experimental sample lengths at 4.2 K and 4 kbar for the various solid gas samples. The adjusted values used in the data analysis are given in parentheses.

Sample	Sample Holder Diameter		
	0.500 in. (in.)	0.354 in. (in.)	0.250 in. (in.)
neon	0.4079	0.3177	0.2557 (0.2570)
argon I	0.4394[a]	0.3079	0.2163 (0.2217)
II	0.4490	-	0.2769 (0.2804
krypton	0.4382 (0.4358)	0.2382	0.2198
xenon	0.4386 (0.4434)	0.3114	0.1969 (0.2008)

[a]The sample length is extrapolated to 4.2 K since the minimum temperature for this set of compression data is 20 K.

representation for each of these fits has a root mean square deviation of less than $10^{-3}V_o$ and shows no systematic deviations. The extrapolated P=0 values of the molar volume, V_o, and the bulk modulus, B_o, then are compared with direct P=0 measurements from other experiments and representations are chosen for each solid which reasonably reproduce these P=0 properties. In each case Lennard-Jones relations (Equation IV-14) were used to represent the data for all isotherms over

the entire pressure range while giving agreement with direct P=0 molar volume data. The P=0 bulk modulus data however, are not always in agreement.

Neon

Four compression runs were made on solid neon for each of the three sample holders in the 4.2 K to 20 K region. The low temperature brittleness of the sample reported by Stewart (4) did not appear to affect the results.

The isotherms for the 0.250 in. diameter sample were taken at slightly different temperatures from the other samples, so an isobaric plot (L/L_{o4} vs. temperature) was used to adjust these data to common temperatures. L_{o4} for the 0.250 in. diameter sample (Table 3) was lengthened by 0.5% to obtain better agreement with the data from the other sample holders.

Satisfactory representations of all the data for each isotherm are obtained for the Birch (Equation IV-12) and the Lennard-Jones (Equation IV-14) relations using the minimum values of N listed in Table 4. The resulting extrapolation to P=0 of the molar volume V_o for each of these representations is given in Figure 7 for comparison with the x-ray data of Batchelder et al. (8). Figure 8 gives the P=0 isothermal bulk modulus, B_o, for each representation along with those which are obtained from the ultrasonic results of Bezuglyi et al. (13). The dashed curve (Figure 8) also represents (within experimental accuracy) the x-ray measurements for the isothermal bulk moduli of Batchelder et al. (8) and the recent ultrasonic results above 18 K of Balzer et al. (14).

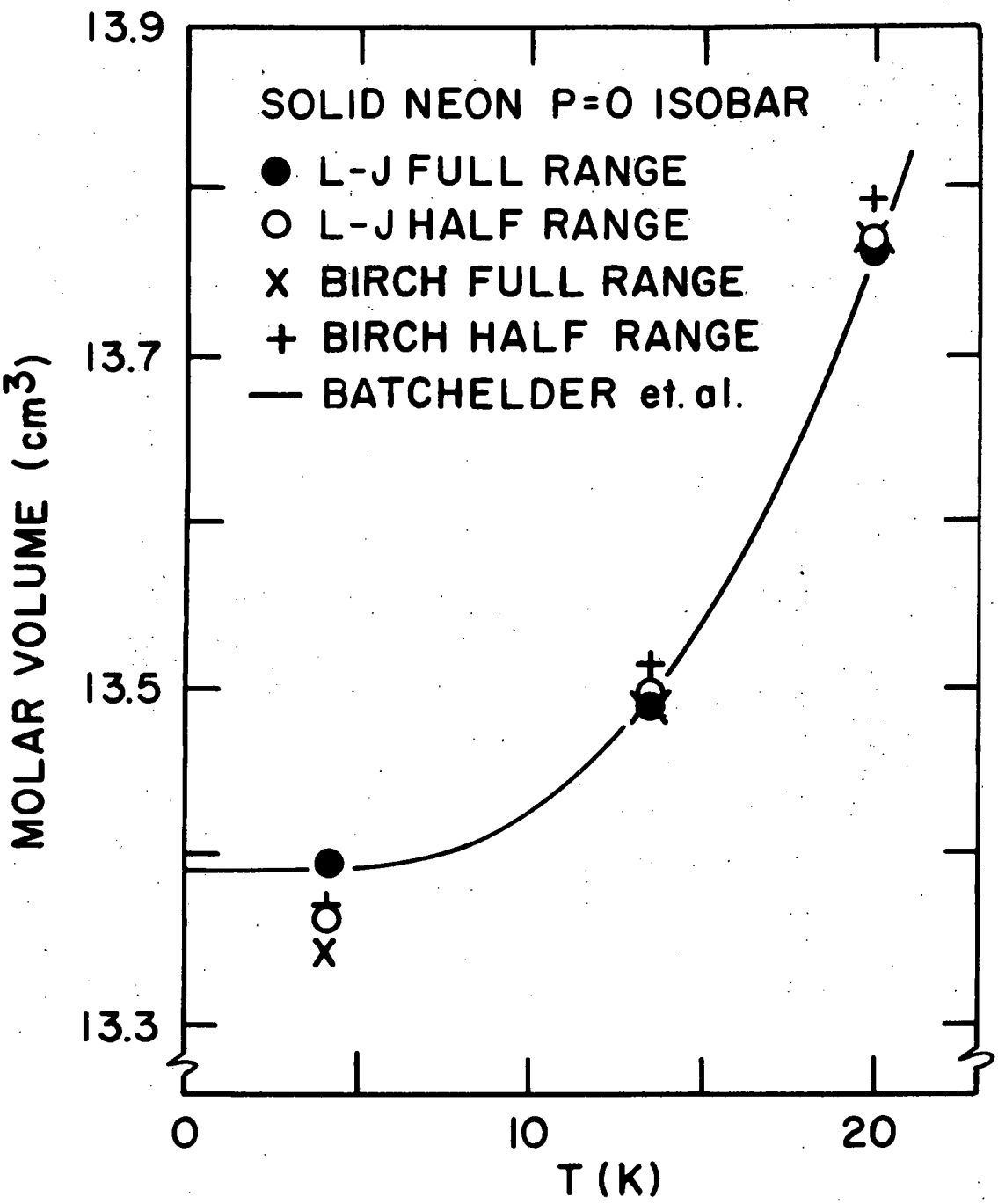

Figure 7. Various extrapolations of molar volumes to P=0 for solid neon for comparison with the x-ray measurements of Batchelder et al. (8).

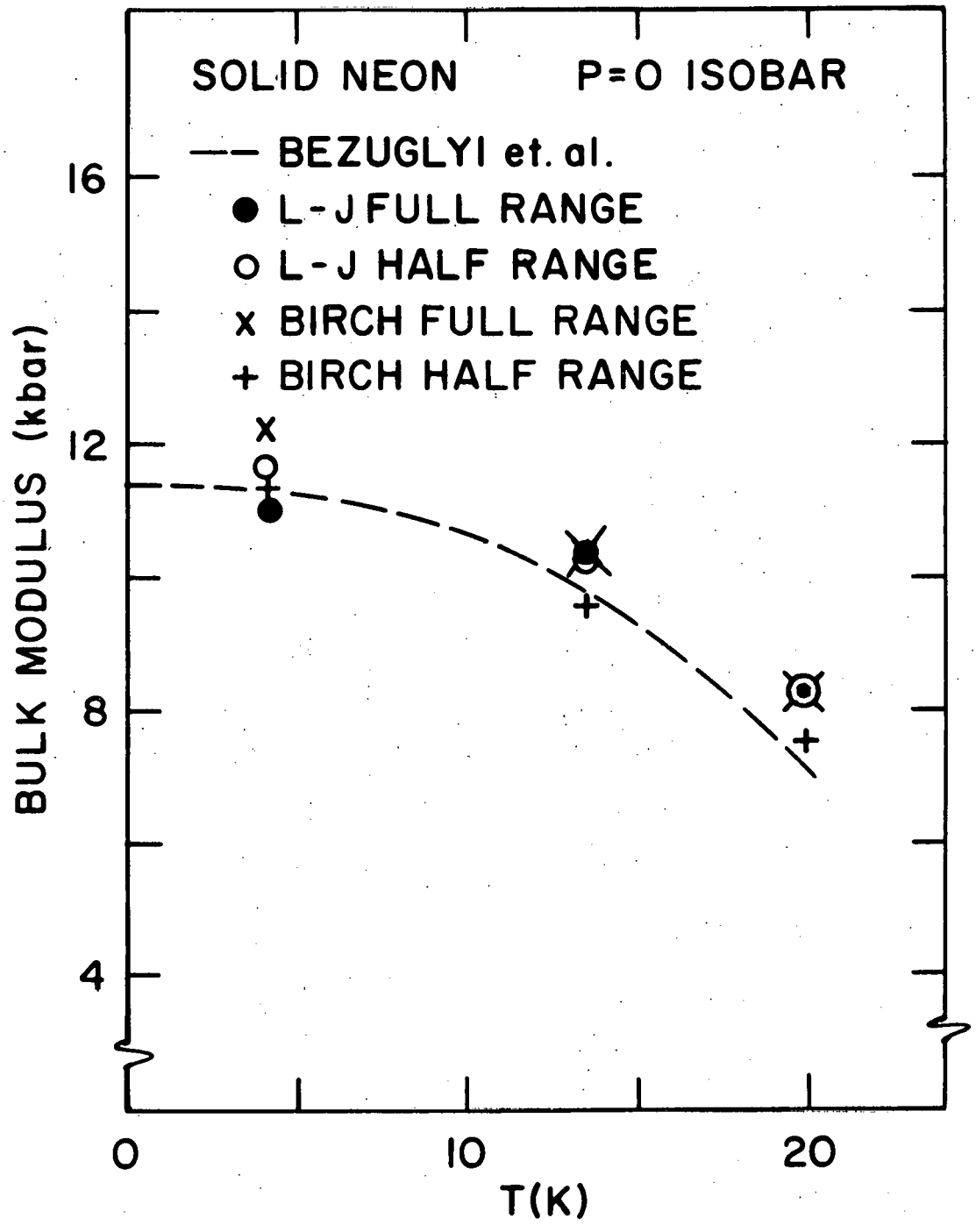

Figure 8. The zero pressure values of the isothermal bulk modulus, B_o, which are obtained for various extrapolations of the present data to P=0, and the smoothed ultrasonic results of Bezuglyi et al. (13).

Table 4. The minimum values of N for Equations IV-12 and IV-14 which give the best representations for the solid neon half- and full-range data.

	Temperature		
	4.2 K	13.5 K	19.9 K
Birch relation			
full-range	3	3	3
half-range	2	2	2
Lennard-Jones relation			
full-range	2	2	3
half-range	2	1	2

The full-range Lennard-Jones representations (Equations IV-14) were chosen to represent the isotherms because of the agreement with the other P=0 thermal expansion and isothermal bulk modulus data. The 14% discrepancy between the extrapolated and ultrasonic values of B_o at 19.9 K (Figure 8) may arise because Equation IV-14 is inadequate for the extrapolation of this isotherm. The conversion between reduced sample length and molar volume (Appendix A) is chosen to give a reasonable correspondence between the extrapolated values of V_o and the P=0 x-ray data at all three temperatures (Figure 7) for the chosen representation. The coefficients for Equation IV-14 which reproduce the data, along with the resulting values of V_o, B_o, and the root mean square deviation, are given in Appendix B. The deviations of the molar

volumes calculated using these equations from the experimental data are given as deviation plots in Appendix C. The excellent agreement between the data for the first and last isotherms in a series can be seen on the 4.2 K deviation plot (Appendix C). Systematic deviations from the fit equation, particularly at high pressure, could be meaningful, but they are well within the estimated high pressure precision of $2 \times 10^{-3} V$.

The smooth P-V relation for neon (Figure 9) shows that thermal effects are negligible for pressures greater than 6 kbar, with the insert giving the total compression in 20 kbar. While Stewart's earlier 4 K piston displacement results (3) are inconsistent with the present data, his measurements at 18 K (4) are in agreement within his experimental uncertainty. It is interesting however, that the present results do agree with Stewart's 4 K data (3) (within 3% of $\Delta V/V_o$) for pressures from 2043 to 20,000 kg/cm^2 (2.003 to 19.613 kbar), so the major difference occurs in the extrapolation to P=0. Figure 10 compares the present results with an equation of state which can be calculated from the high pressure heat capacity data of Fugate and Swenson (26). The agreement is excellent when a "reasonable" form of the Mie-Gruneisen equation of state is used (7).

Argon

Twenty four sets of compression data were taken from 4.2 to 77 K on five samples of solid argon. Extensive data which were taken on the first 0.500 in. diameter sample were limited to temperatures between 20 and 77 K since a dewar vacuum leak made it impossible to take

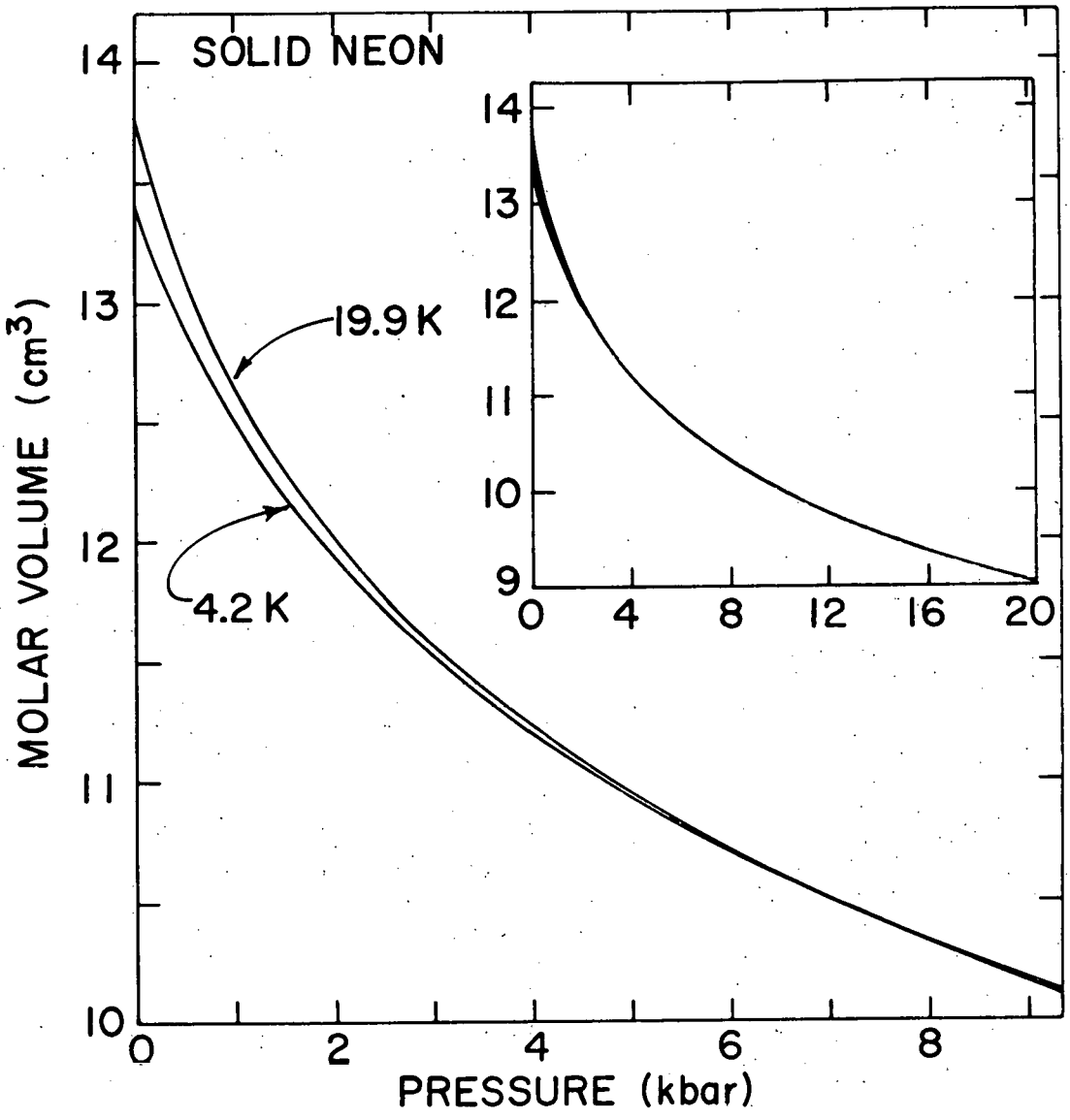

Figure 9. Smooth P-V relations for solid neon.

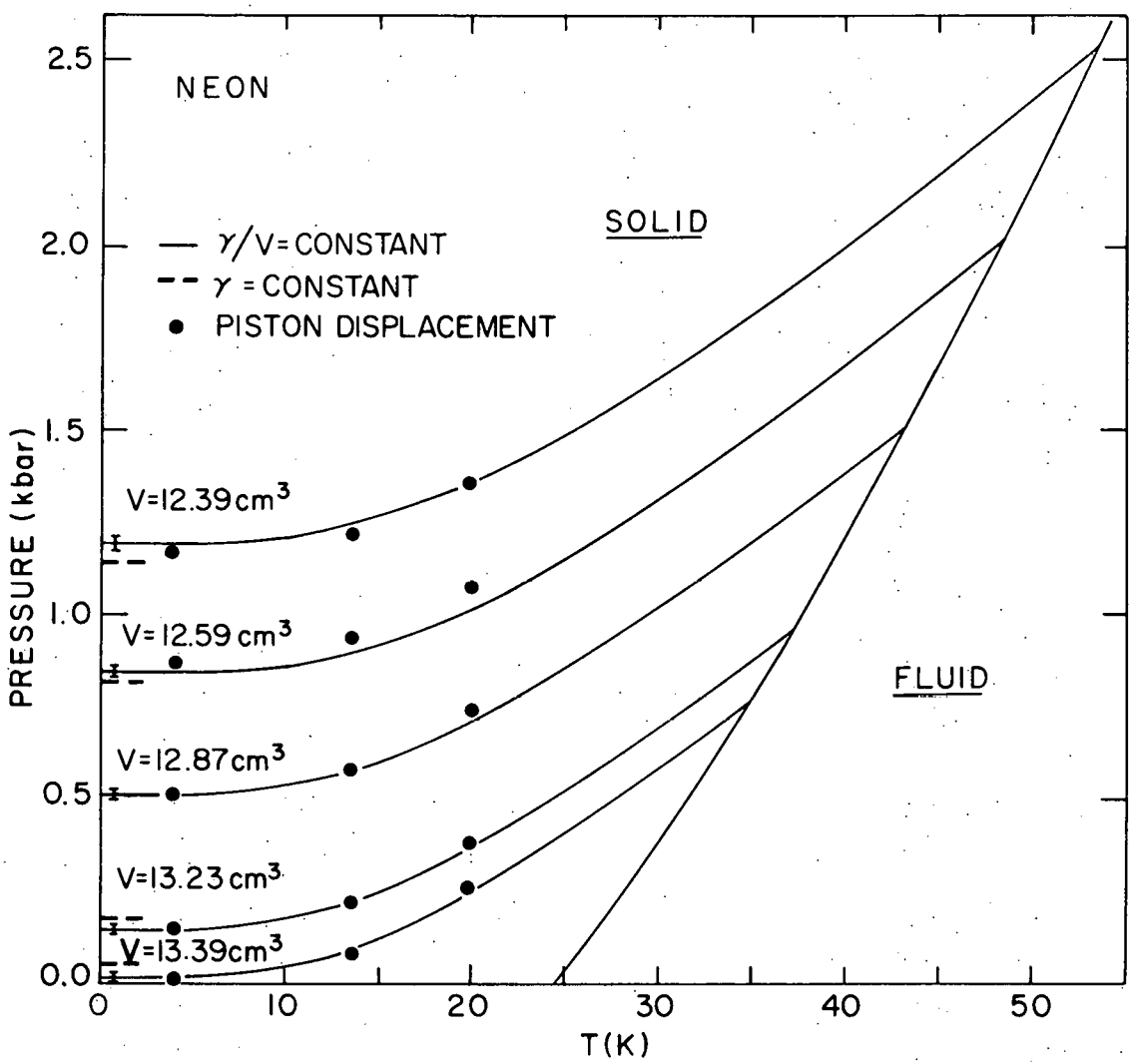

Figure 10. The present data (solid dots) compared with isochores calculated from heat capacity data (7). The error bars correspond to $\pm 10^{-3}$ V.

a 4.2 K point. Four compression runs on the second 0.500 in. diameter sample included a 4.2 K point. Two different samples also were run in the 0.250 in. sample holder, since the data for the first sample were not in good agreement with data from the other two sample holders. This disagreement later was found to be due to an error in the corrections which were used in the analysis of the first 0.250 in. diameter sample, and all data now are consistent. The corrected data before computer smoothing are given in Appendix A in terms of the molar volumes for each of the compression runs. The experimental sample lengths, L_{o4}, for the solid argon samples are given in Table 3 for each series of runs.

The minimum values of N for Equations IV-12 and IV-14 which are needed to represent the data for each isotherm satisfactorily are given in Table 5. The lengths of the two 0.250 in. diameter samples were

Table 5. The minimum values of N for Equations IV-12 and IV-14 which give the best representations for the solid argon half- and full-range data.

	Temperature	
	4.2 K to 60 K[a]	77 K
Birch relation		
full-range	2	3
half-range	2	2
Lennard-Jones relation		
full-range	2	3
half-range	1	2

[a]Including isotherms at 20 K and 40 K.

adjusted by +2.5% and +1.25% (Table 3) respectively, to obtain better agreement with the other data. The magnitudes of these corrections are outside the estimated precision of the sample length determination (0.5%) and are not understood. The extrapolation of the molar volume to P=0, V_o, is given in Figure 11 for each of the representations of Table 5 for comparison with the x-ray results of Peterson et al. (9). Figure 12 gives the P=0 isothermal bulk modulus, B_o, for each representation.

The Lennard-Jones representations (Equation IV-14) of the full-range data are chosen to represent the data because of the agreement with the P=0 thermal expansion data (Figure 11). The conversion factor for changing sample lengths into molar volumes (Appendix A) is chosen to obtain the best agreement between the extrapolated values of V_o and the P=0 x-ray data at all five temperatures (Figure 11) for this representation. The coefficients for Equation IV-14 which reproduce the data for each isotherm, along with the resulting values of V_o, B_o, and the root mean square deviation, are given in Appendix B. The deviations of the solid argon fit equations from the experimental data are given as deviation plots in Appendix C. The high pressure deviations appear to be systematic, although they lie within the estimated high pressure precision (2×10^{-3}V or 0.04 cm^3/mole). The 0.250 in. diameter data show internal inconsistencies at 60 K and 77 K at high pressure, and at 40 K at low pressure. Only the 40 K deviations appear to be outside the estimated experimental accuracy.

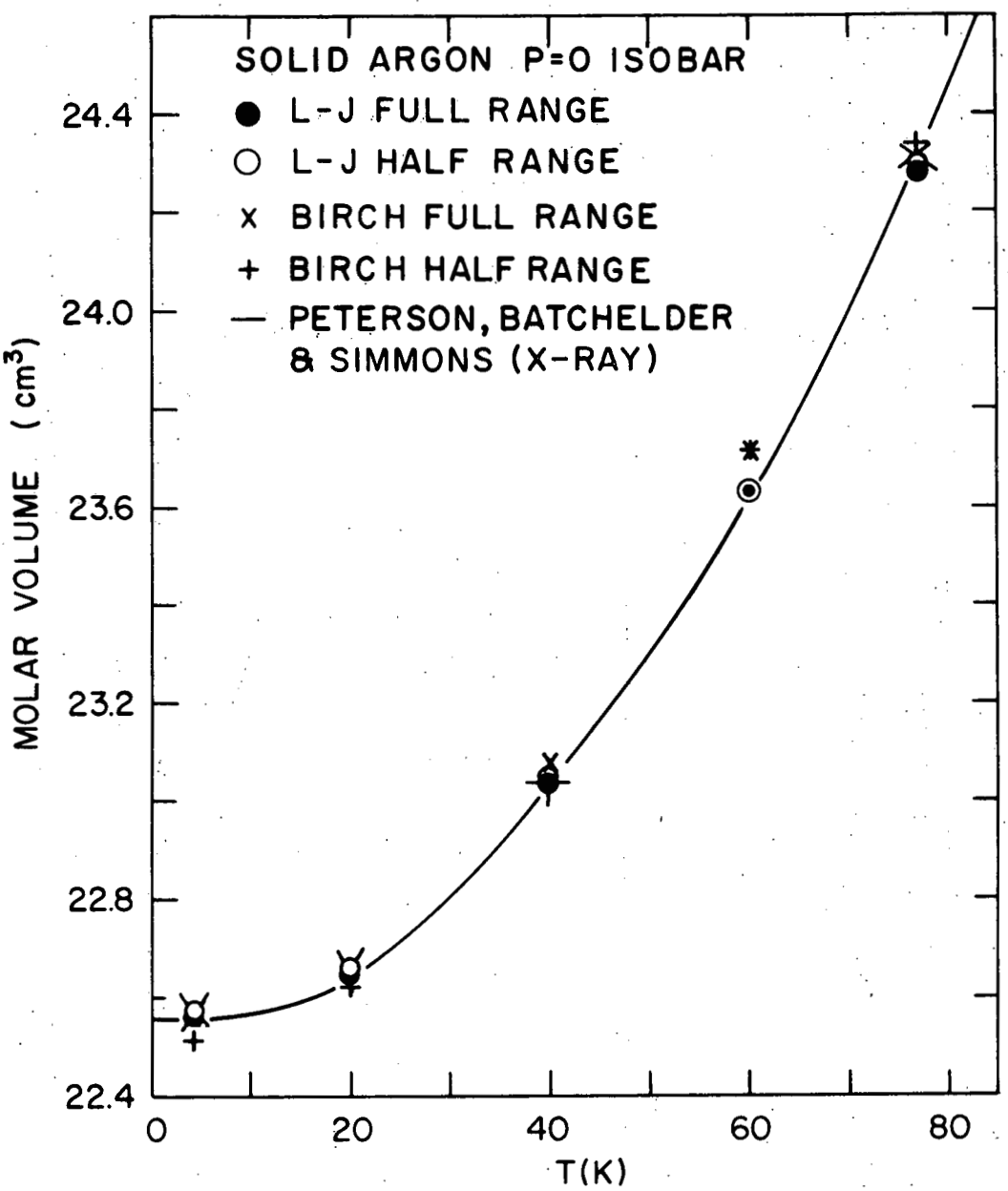

Figure 11. A comparison of x-ray measurements (9) for solid argon with molar volumes which are obtained from the extrapolation to P=0 of the present data using various representations.

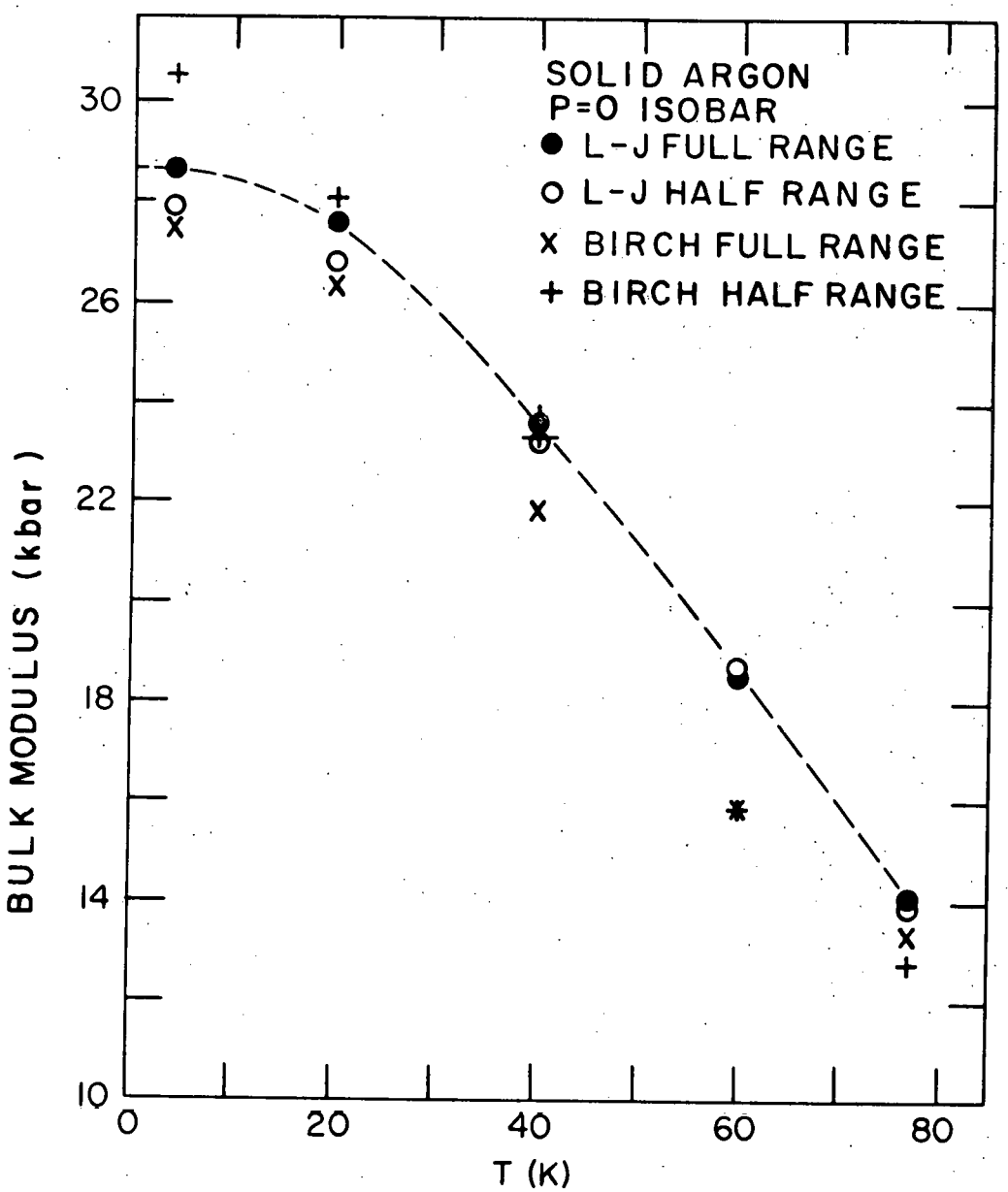

Figure 12. The zero pressure values of the isothermal bulk modulus, B_o, as obtained for various extrapolations of the present data to P=0.

The P=0 values of B_T ($B_o(T)$) can be obtained by extrapolation in two ways. First, the computer fits to the data (Appendix B) give B_o directly (broken line Figures 12 and 13). Second, since B_T has only a slight temperature dependence at constant volume, values of B_T which are obtained using actual isothermal data (solid dots in Figure 13) can be extrapolated at constant volume to the temperature at which P=0 for that volume. The slope of these curves, $(\partial B_T/\partial T)_V$, appears to be both volume and temperature independent, as is illustrated by the 22.00 cm^3/mole isochore in Figure 13. In principle, data obtained for any volume can be extrapolated to P=0 along an isochore, although in Figure 13 the P=0 volumes which correspond to the temperatures of the isotherms (Figure 11) are used. These two independent extrapolation methods for obtaining B_o (Figure 13) are in excellent agreement.

The adiabatic bulk modulus data of Keeler and Batchelder (16), were corrected to obtain the isothermal moduli which are given in Figure 13 for comparison with the present results. Figure 13 also gives the P=0 x-ray results for B_o of Peterson *et al.* (9) at 4.2 K and Urvas *et al.* (10) at 77.7 K, and the theoretical values of Klein *et al.* (23) for comparison with the present data.

The systematic deviation between the present results and other experimental data (Figure 13) for solid argon is surprising. The P=0 x-ray results (9,10) for B_o are believed to be unreliable due to an irreversible effect on the observed lattice spacing caused by the helium pressure medium (20). This low pressure hysteresis effect was relatively unimportant in similar measurements on the other gas

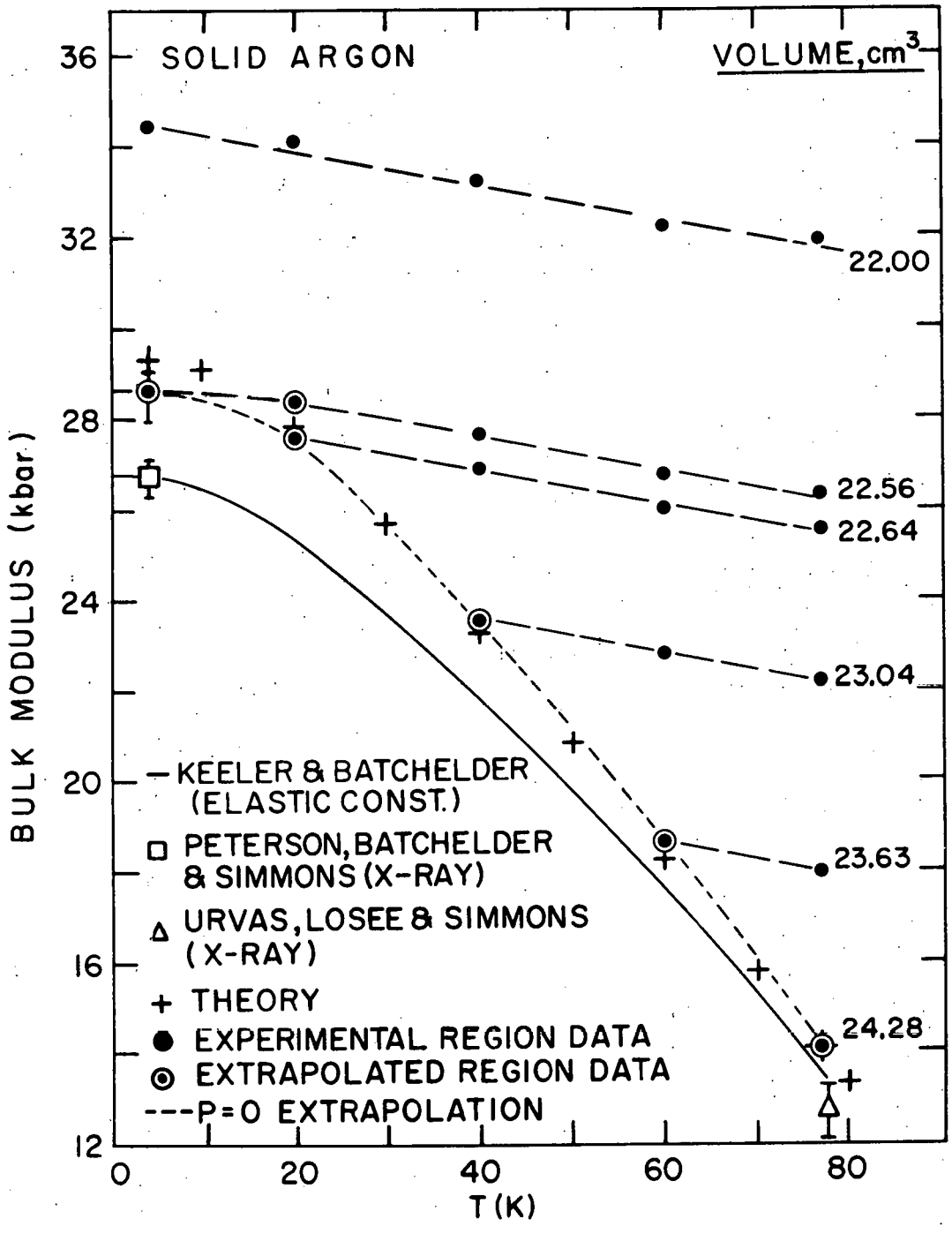

Figure 13. The temperature and volume dependence of B_T as calculated from the coefficients in Appendix B (solid and circled dots). The dashed lines correspond to isochoric extrapolations to P=0 (broken line, Figure 12) for molar volumes greater than 22.00 cm^3/mole. The P=0 x-ray (9,10) and ultrasonic (16) results, and theoretical values (23) also are given.

solids (10). The ultrasonic results of Keeler and Batchelder (16) also are believed to be unreliable, possibly due to strains since their quartz transducer was imbedded in the crystal (34). The present data are in very good agreement with the theoretical calculations of Klein et al. (23) (Figure 13), and a recent Monte Carlo calculation for solid argon by Fisher and Watts (35) (not shown).

The smooth P-V representations for solid argon are given in Figure 14. These data are in good agreement (better than 3% in $\Delta V/V_o$) with Stewart's piston displacement results at 38 and 77 K (4).

Benson (6) has made an independent determination of the equation of state for solid argon using a constant volume capacitance strain gauge technique, These data, for four isochores, are compared with the present results in Figure 15. The open circles (diameter approximately equal to $2 \times 10^{-3} V$) are calculated for the molar volumes of the isochores using the coefficients for argon in Appendix B. The agreement between these two very different sets of data is excellent.

Krypton

Twenty eight sets of compression data were taken from 4.2 K to 110 K on three samples of solid krypton. A small amount of the 0.500 in. diameter sample was lost at maximum pressure while on an initial compression at 110 K, and due to inconsistencies which appeared in the analysis, the data taken after the sample loss were discarded. No loss of sample was detected for either the 0.354 in. or 0.250 in. diameter sample holders at 110 K and the highest pressures. The data from the

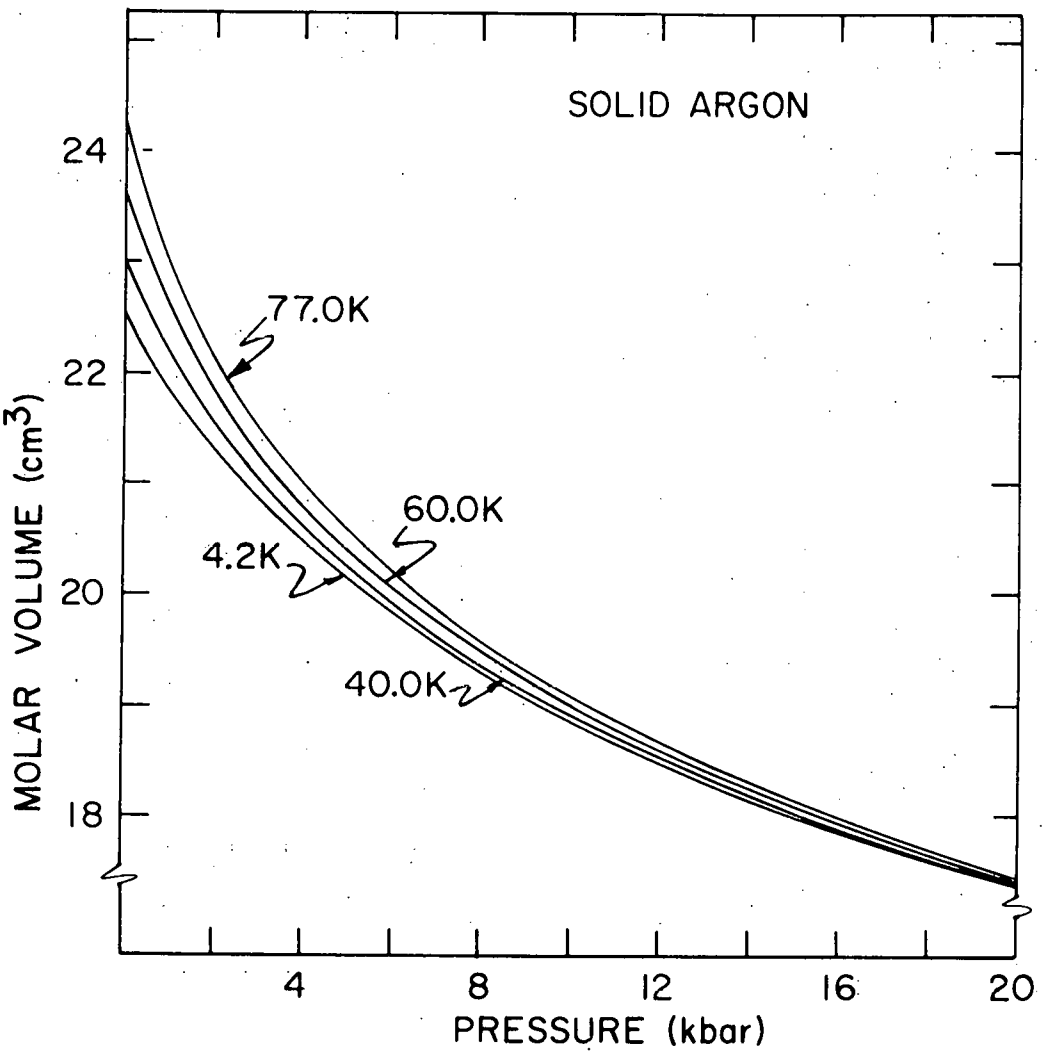

Figure 14. Smooth P-V relations for solid argon.

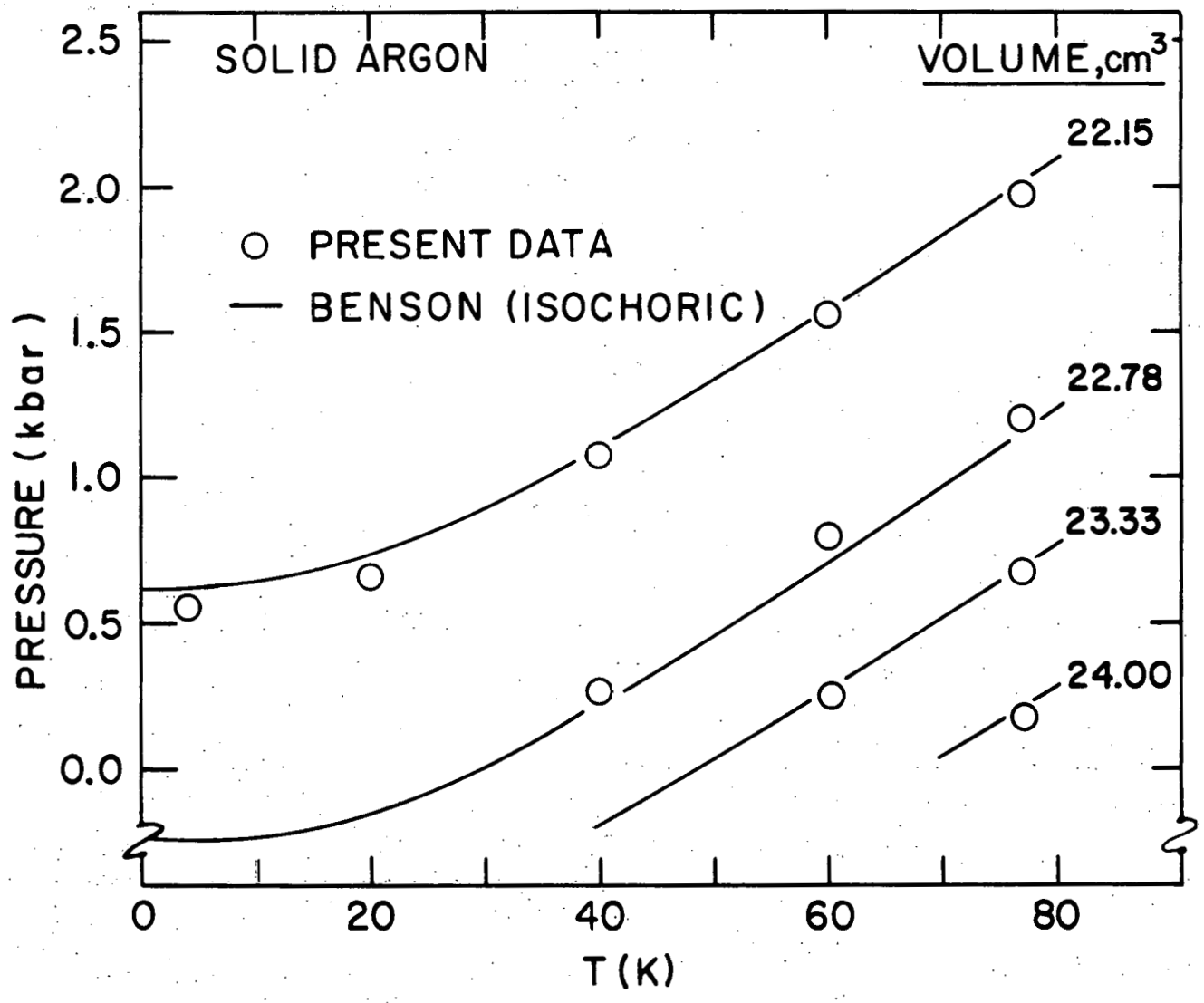

Figure 15. A comparison of Benson's isochoric data (6) with the present results (diameter of circles approximately equal to 2×10^{-3}V).

compression runs, corrected for pressure and thermal expansion effects, but not computer smoothed, are given in Appendix A in terms of molar volumes. The experimental sample lengths, L_{o4}, for each of the solid krypton samples are given in Table 3.

Some of the isotherms for the various samples of solid krypton (Appendix A) were taken at slightly different temperatures, so an isobaric plot (L/L_{o4} vs. temperature) was used to adjust these data to common temperatures. L_{o4} for the 0.500 in. diameter sample (Table 3) was shortened by 0.5% to obtain better agreement with the data from the other sample holders.

The minimum values of N for Equations IV-12 and IV-14 which are needed to represent the data for each isotherm satisfactorily are given in Table 6. The resulting extrapolation of the molar volume to P=0, V_o,

Table 6. The minimum values of N for Equation IV-12 and IV-14 which are necessary to represent satisfactorily the solid krypton half- and full-range data.

	Temperature		
	4.2 K to 70 K[a]	77 K to 100 K[b]	110 K
Birch relation			
full-range	3	3	3
half-range	2	2	2
Lennard-Jones relation			
full-range	3	1	2
half-range	2	1	1

[a] Including isotherms at 20 K, 40 K, and 60 K.
[b] Including the isotherm at 80 K.

and the P=0 isothermal bulk modulus, B_o, are given in Figures 16 and 17 respectively, for each of these representations. The basic comparison in these figures is with the x-ray measurements of Losee and Simmons (11).

The full-range Lennard-Jones representations (Equation IV-14) were chosen to represent the data because of the agreement with the P=0 thermal expansion data (Figure 16). The conversion factor for changing sample lengths into molar volumes (Appendix A) is chosen to obtain the best agreement between the extrapolated values of V_o for this representation and the P=0 x-ray measurements at all nine temperatures (Figure 16). The coefficients for Equation IV-14 which reproduce the data, along with the resulting values of V_o, B_o, and the root mean square deviation, are given in Appendix B. The deviations of the molar volumes which are calculated using these equations from the solid krypton data are given as deviation plots in Appendix C. The 0.500 in. data at 60 K and the 0.250 in. data at 77 K show systematic deviations which appear to be outside the estimated low pressure experimental accuracy (1×10^{-3}V or 0.028 cm^3/mole). The 0.354 in. diameter data show internal inconsistencies at 80 K and 100 K at low pressure. This possibly is caused by over-correction for a dial gauge shift between the two sets of 80 K data, the lower set (open triangles, Appendix C) being taken first. These low pressure deviations at 80 K and 100 K appear to be outside the estimated experimental accuracy.

The two independent methods of obtaining B_o (discussed under argon above) are given in Figure 18 for comparison with the x-ray data of

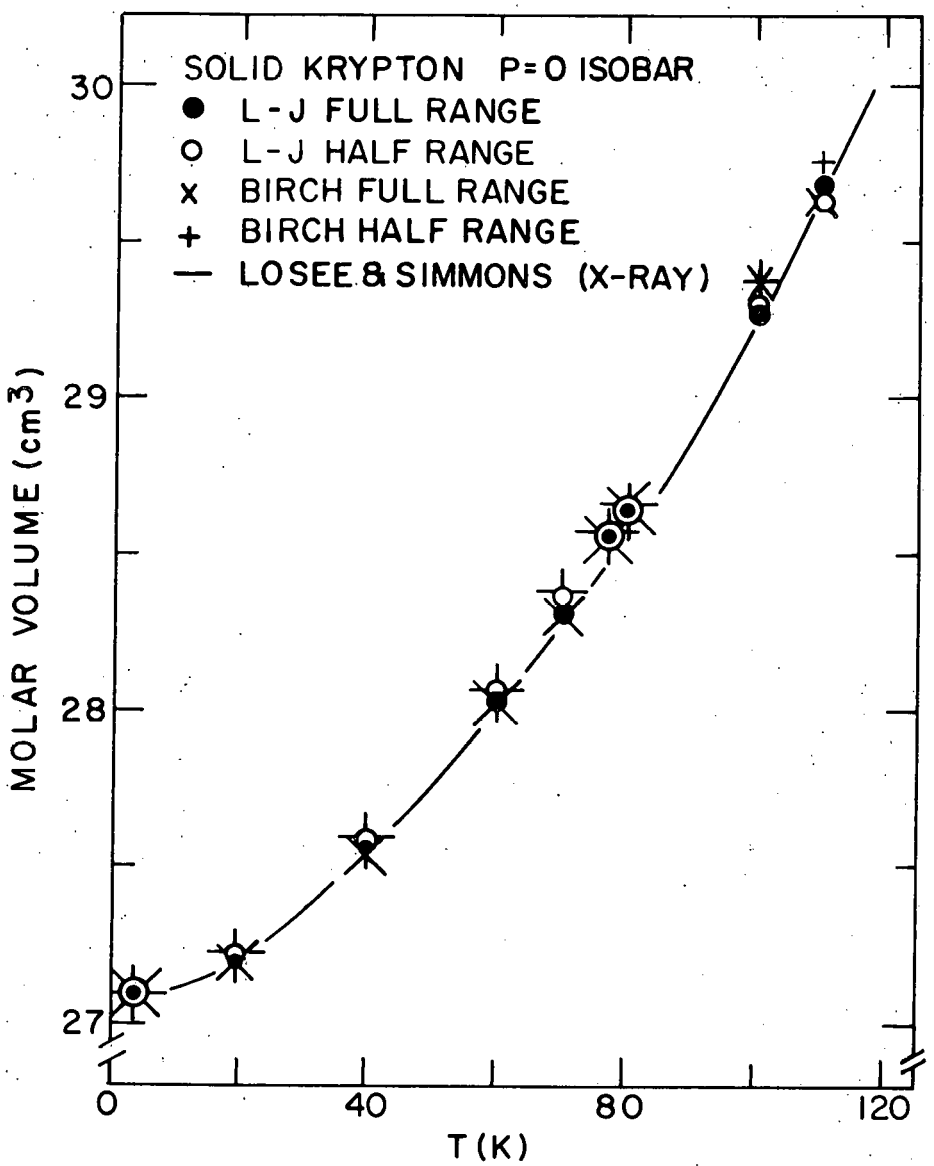

Figure 16. Various extrapolations of molar volumes to P=0 for solid krypton and the x-ray results of Losee and Simmons (11).

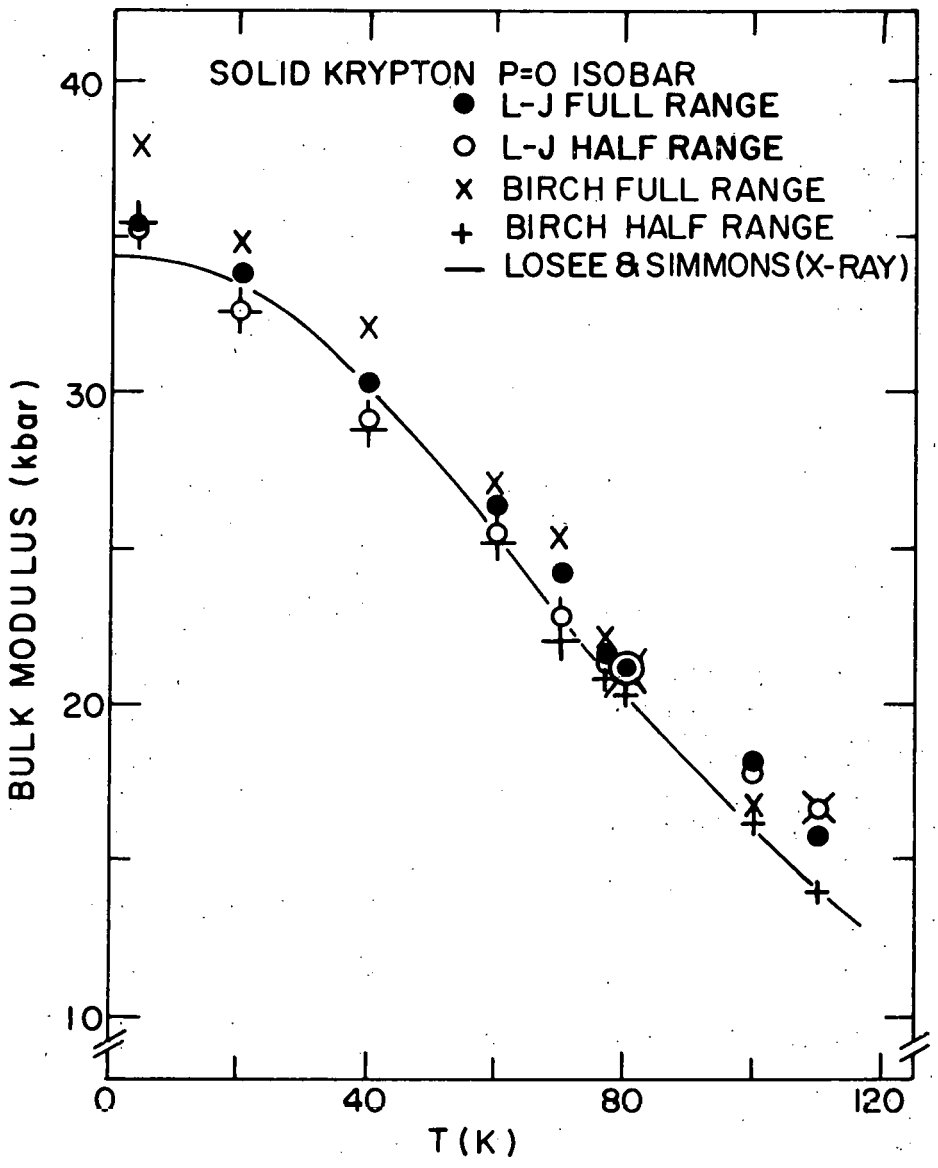

Figure 17. The zero pressure value of the isothermal bulk modulus, B_o, as is obtained for various extrapolations of the present data to P=0. The solid line represents the x-ray measurements of Losee and Simmons (11).

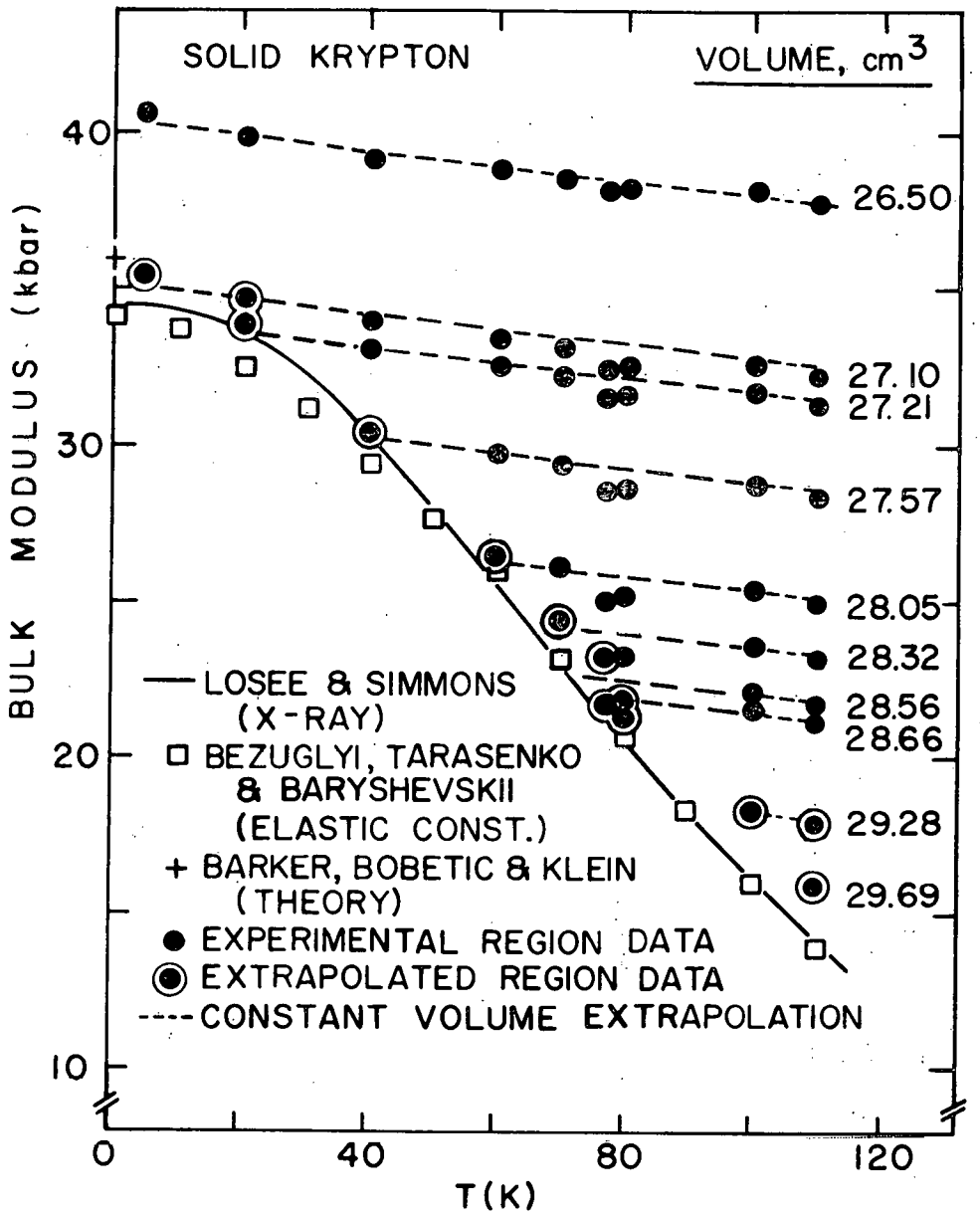

Figure 18. The temperature and volume dependence of B_T as calculated from the coefficients in Appendix B (solid and circled dots). The dashed lines are isochoric extrapolations to P=0 for molar volumes greater than 26.50 cm^3/mole. The P=0 x-ray (11) and ultrasonic (15) results, and a theoretical value (22) also are given.

Losee and Simmons (11) which agree with similar data by Urvas et al. (10)), the ultrasonic results of Bezuglyi et al. (15), and the theoretical value of Barker et al. (22). The molar volumes chosen for the isochoric extrapolation (Figure 18) correspond to the P=0 values for the temperatures of the isotherms (Figure 16). The agreement between the different experiments is satisfactory below 100 K, including interferometric data by Coufal et al. (12,36). The differences at temperatures above 100 K (Figure 18) may arise because Equation IV-14 is inadequate for extrapolating these isotherms.

The smooth P-V representations for solid krypton are given in Figure 19. These data are in good agreement (better than 3% in $\Delta V/V_o$) with Stewart's piston displacement results at 81 K and for pressures from 0 to 20 kbar (4).

Xenon

Fifty five sets of compression data were taken on three samples of solid xenon from 4.2 to 158.8 K. Inconsistencies in the initial series of data (e.g. larger than normal friction, small dial gauge shifts, etc.) caused the first few isotherms for each sample to be discarded. The data for each sample are more consistent after completing a compression run near the triple point temperature. The corrected data before computer smoothing are given in Appendix A in terms of the molar volumes. The experimental sample lengths, L_{o4}, for each of the solid xenon samples are given in Table 3.

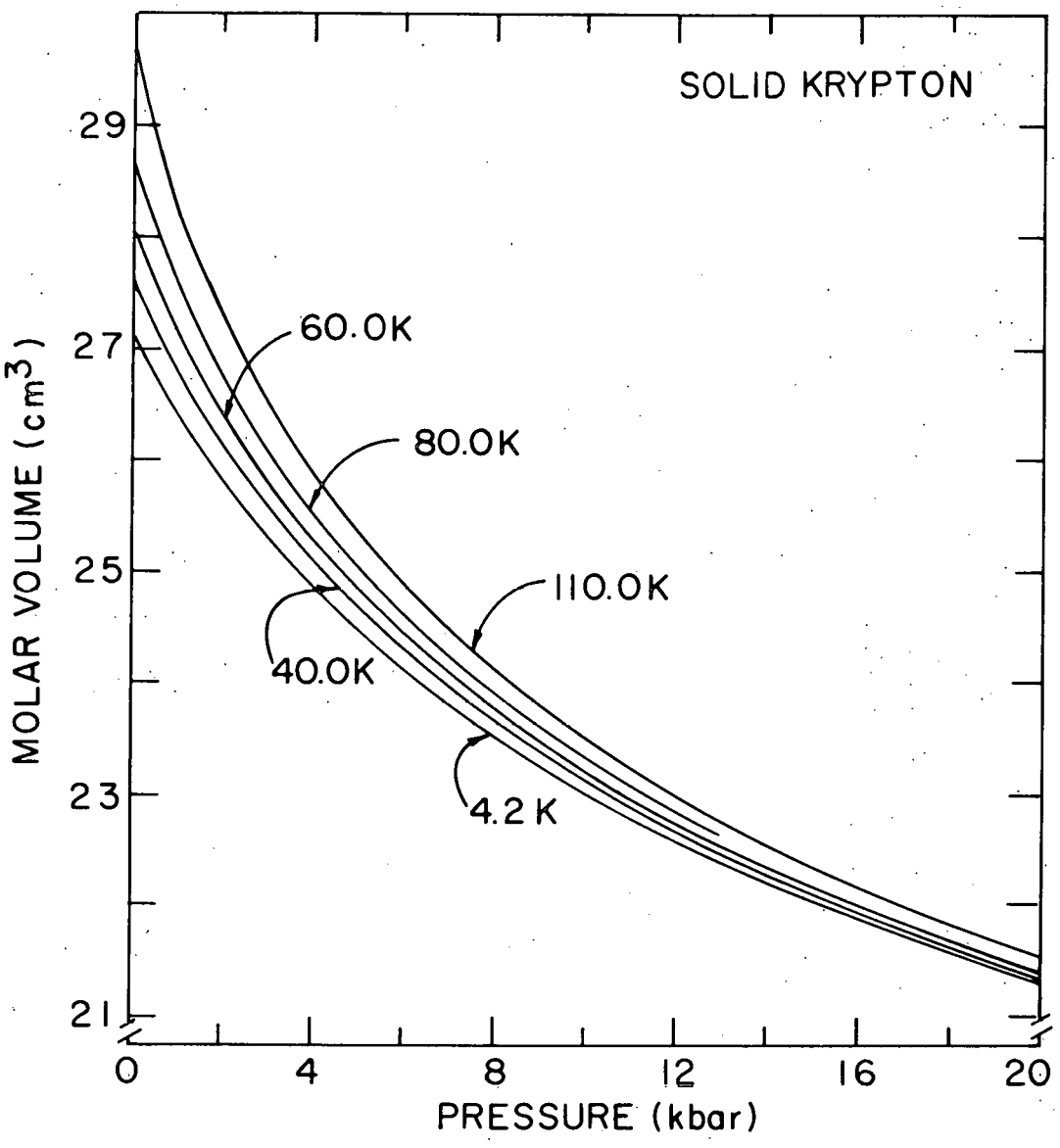

Figure 19. Smooth P-V relations for solid krypton.

The minimum values of N for Equations IV-12 and IV-14 which satisfactorily represent the data along each isotherm are given in Table 7.

Table 7. The minimum values of N (Equations IV-12 and IV-14) which are necessary to represent satisfactorily the solid xenon half- and full-range data.

	Temperature				
	4.2 K[a]	77 K[b]	100 K	140 K	158.8 K
Birch relation					
full-range	2	2	3	3	2
half-range	2	2	2	2	2
Lennard-Jones relation					
full-range	2	1	1	2	3
half-range	1	1	1	2	2

[a]Including isotherms at 20 K, 40 K, and 60 K.

[b]Including isotherms at 80 K and 120 K.

The lengths (L_{o4}) of the 0.500 in. and 0.250 in. diameter samples were adjusted by +1.1% and +2.0%, respectively (Table 3), to obtain better agreement with the 0.354 in. diameter sample. The reason for the large adjustment in the length of the 0.250 in. diameter sample is not understood, since it is definitely outside the estimated experimental precision (0.5%). The 0.354 in. diameter sample data were chosen as "correct" since the two length determinations agreed very well for

this sample. The resulting extrapolations of the molar volume to P=0, V_o, are given in Figure 20 for each of the representations in Table 7 for comparison with the capacitance dilatometer data of Tilford and Swenson (37) which agree with the quartz dilatometer results of Manzhelii et al. (38) (solid line from 1 to 105 K). The curves above 105 K are as obtained from the pycnometric results of Gavrilko and Manzhelii (39) (dashed line) and as quoted by Manzhelii et al. (38) (solid line). The P=0 isothermal bulk modulus, B_o, is given in Figure 21 for each representation, along with the ultrasonic results of Bezuglyi et al. (15) and the single Brillouin scattering result of Gornall and Stoicheff at 156 K (17).

The Lennard-Jones representations (Equations IV-14) of the full-range data were chosen to represent the data because of the agreement with the P=0 dilatometer results (Figure 20). The conversion factor used to convert sample lengths to molar volumes (Appendix A) was chosen to obtain the best agreement between the extrapolated P=0 values of V_o and the dilatometer data at all ten temperatures (Figure 20). The coefficients which reproduce the data (Equation IV-14), along with the resulting values of V_o, B_o, and the root mean square deviation, are given in Appendix B. The deviations of the molar volumes calculated using Equation IV-14 from the experimental data are given as deviation plots in Appendix C. The high pressure deviations at 4.2 K, 20 K, and 40 K appear to be systematic, although they lie within the estimated high pressure accuracy (2×10^{-3}V or 0.054 cm^3/mole). The 0.250 in.

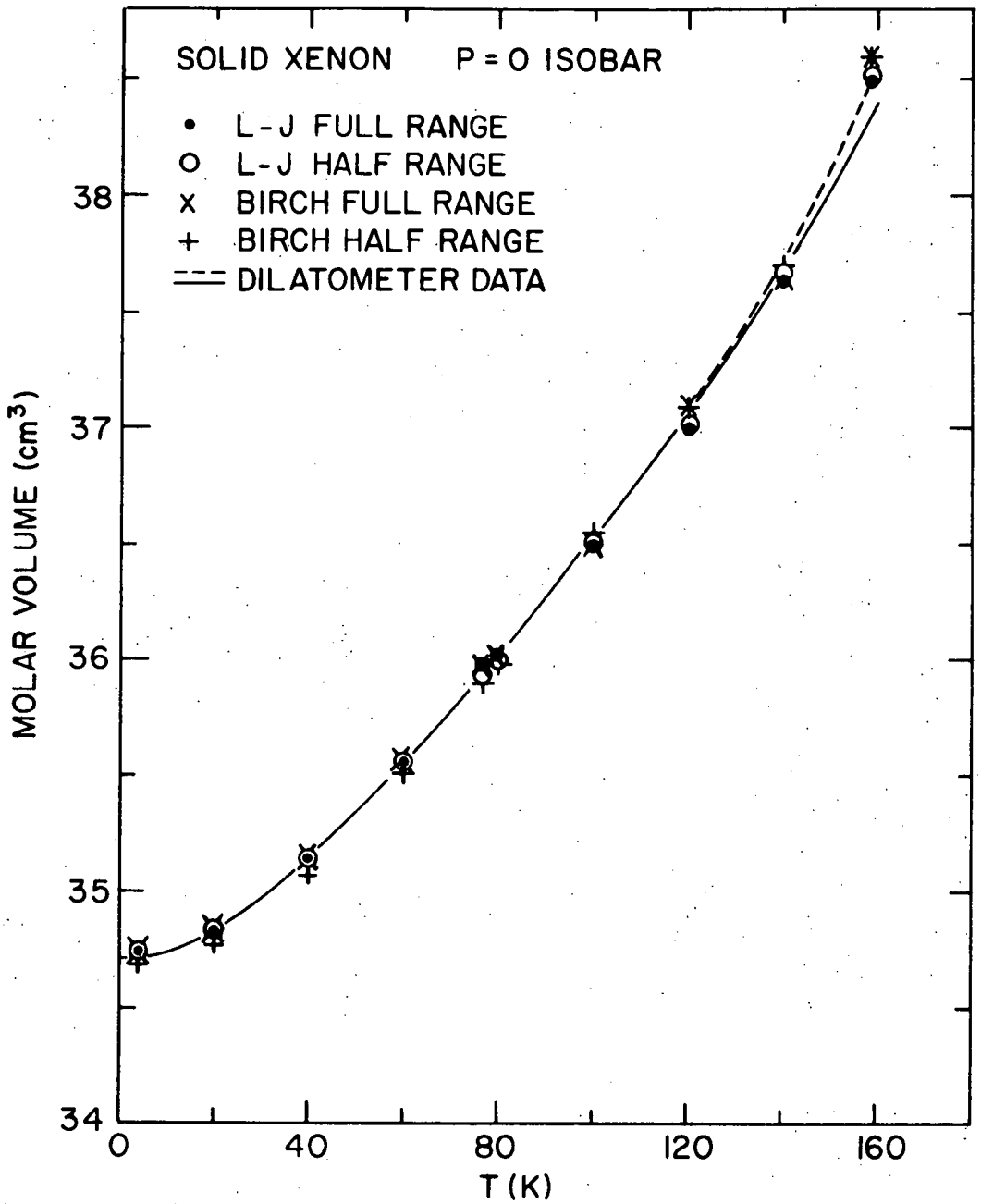

Figure 20. Various extrapolations of molar volumes to P=0 for solid xenon for comparison with the dilatometric data of Tilford and Swenson (37) (solid line to 105 K), and Manzhelii *et al.* (38) (solid line above 105 K), and the pycnometer results of Gavrilko and Manzhelii (39) (dashed line).

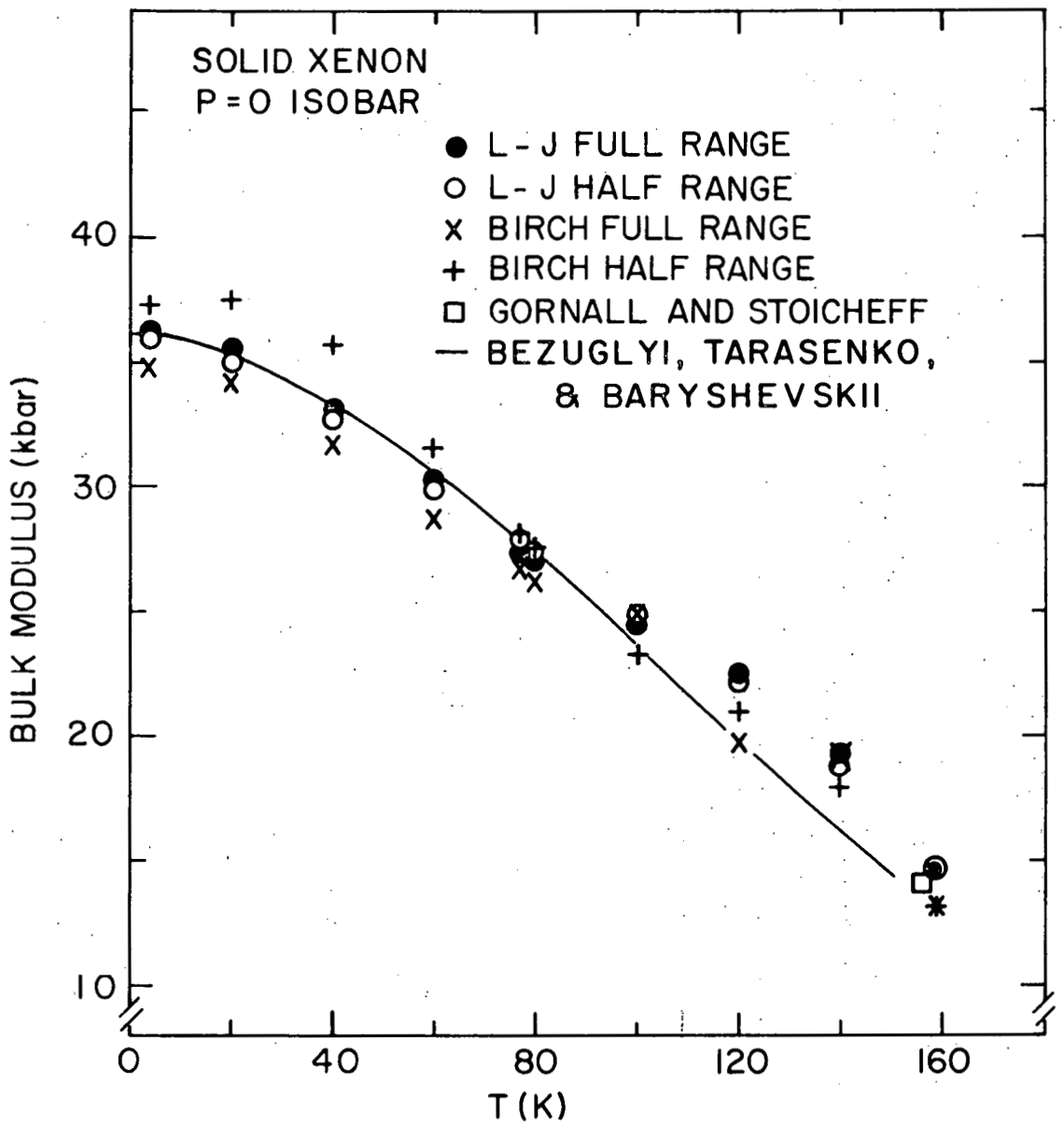

Figure 21. The P=0 value of the isothermal bulk modulus, B_o, obtained for various extrapolations compared with the ultrasonic results of Bezuglyi *et al.* (15) and the single Brillouin scattering result of Gornall and Stoicheff (17).

diameter sample shows large deviations at low pressure at 80 K and 100 K which appear to be outside the estimated low pressure accuracy (1×10^{-3}V or 0.035 cm^3/mole).

The two independent methods of obtaining B_o (discussed under argon above) are given in Figure 22 for comparison with ultrasonic results of Bezuglyi et al. (15), which is in good agreement with values obtained from a Monte Carlo calculation by Klein and Hoover (40,41) at 120 K and 160 K (not shown), and the single Brillouin scattering result at 156 K of Gornall and Stoicheff (17). The molar volumes chosen for the isochoric extrapolations (dashed line Figure 22) are identical with the volumes at P=0 for the temperatures of the isotherms (Figure 20).

The smooth P-V representations for solid xenon are given in Figure 23. The present results agree to better than 5% in $\Delta V/V_o$ with the previous piston displacement results of Packard and Swenson (5).

Sources of Error

The estimated errors in the final P(T,V) relations are quite difficult to assess, and will be discussed below in terms of volume uncertainties. The major sources of uncertainty appear to lie in two areas; first, the absolute sample length determination, and second, the dilation of the sample holder under pressure.

The precision of the absolute sample length determination should be close to $\pm 0.5\%$ for the three different sample holders used. However, the 0.250 in. diameter sample lengths for argon and xenon appeared to be in error by at least 1.5% due to the large adjustments that were

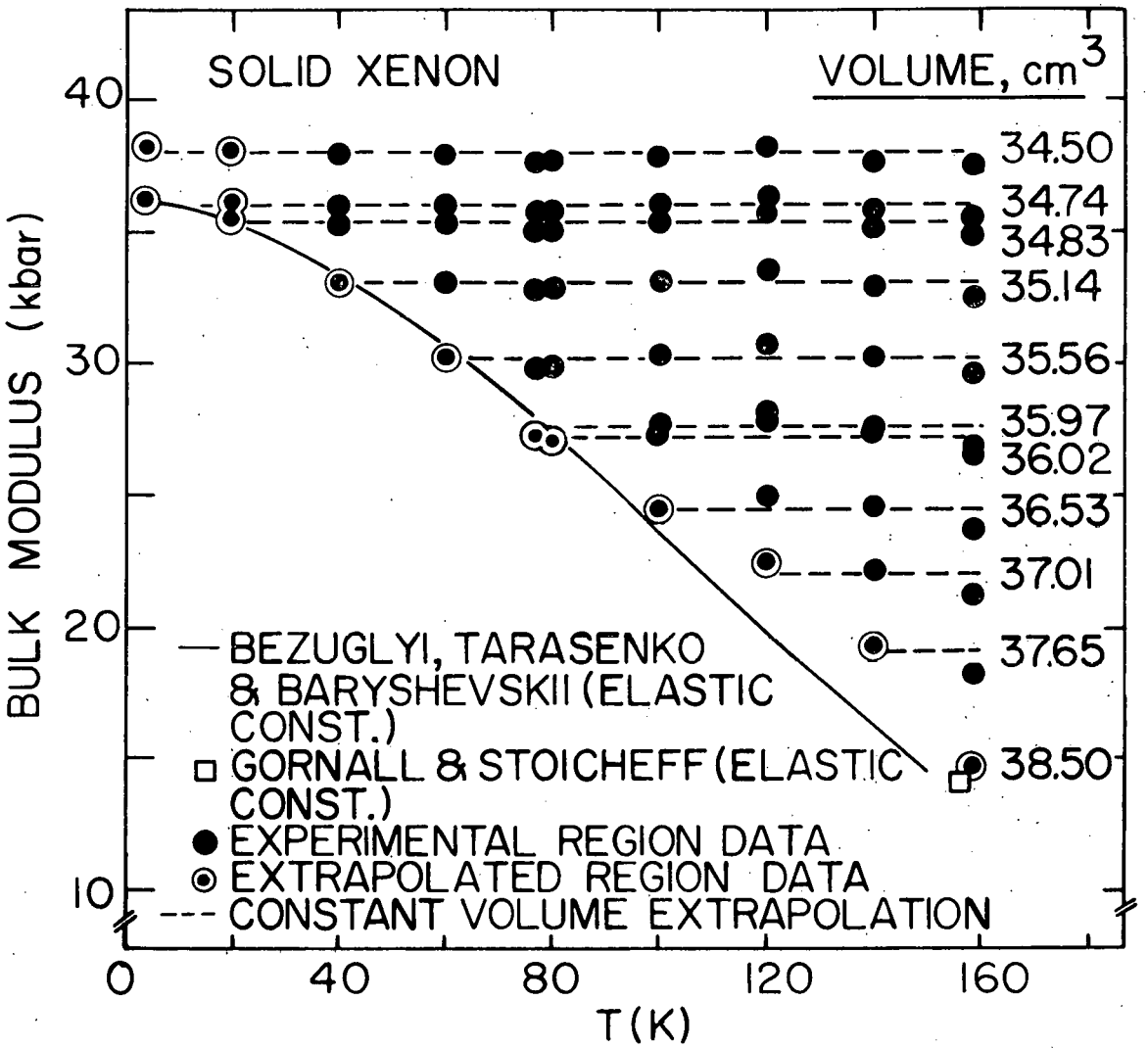

Figure 22. The temperature and volume dependence of B_T as calculated from the coefficients in Appendix B (solid and circled dots). The dashed lines correspond to isochoric extrapolations to P=0 for molar volumes greater than 34.50 cm^3/mole. The P=0 ultrasonic results of Bezuglyi et al. (15), and the single Brillouin scattering result of Gornall and Stoicheff (17) also are given.

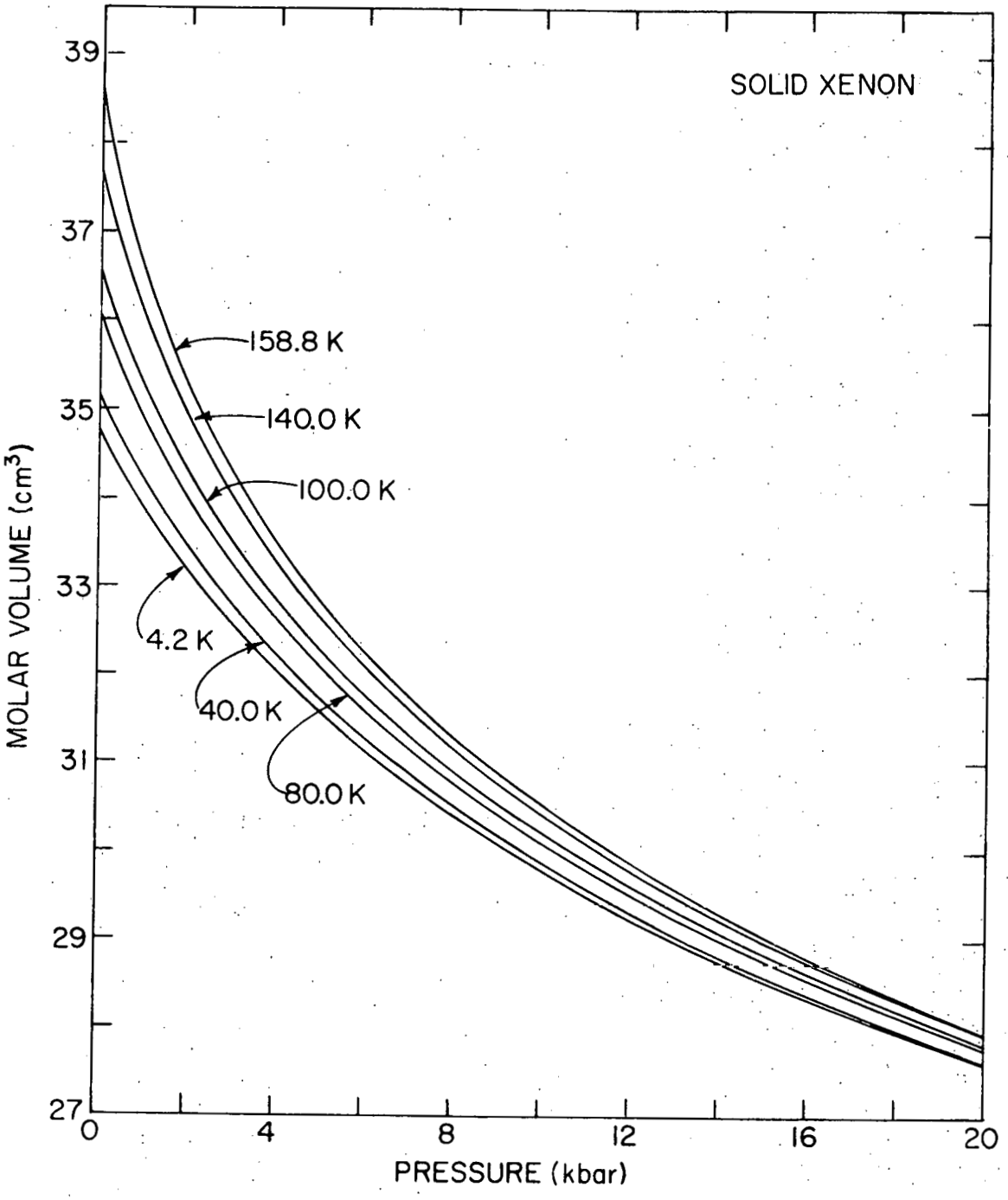

Figure 23. Smooth P-V relations for solid xenon.

necessary to obtain better agreement with the data for the other two sample holders. The reason for this discrepancy is not understood.

The sample holder dilation error discussed in conjunction with Equation IV-6 is due to second order effects. This error could be as large as $+2 \times 10^{-3} V_o$ (Table 2) for the highest pressures. However, since this error cannot be evaluated directly, the data analysis has not included a correction for it. The pressure on the sample also can be affected by this dilation with an estimated equivalent uncertainty in the volume of less than +0.1%. Thus, the dilation errors add and hence, could introduce systematic errors at the highest pressures. The overlap regions, as seen on the deviation plots (Appendix C) for the various sample holders, do not suggest the presence of these errors however.

The major contributions to the experimental uncertainties which can be evaluated are those due to the least count and reproducibility of the displacement readings (estimated as 0.2×10^{-3} in.), which are important at low pressures, and the uncertainties in the absolute sample length determination (estimated as 0.5%) which becomes important at high pressures. The net effects on the reported volumes for a given pressure have been estimated for the 19.9 K neon isotherm (which is typical) as 0.1% for pressures below 8 kbar, rising to 0.2% for pressures above 14 kbar. These estimates suggest that the total compressions in 20 kbar should be uncertain by roughly $\pm$ 0.5%. The internal consistency of the data as taken for the same temperature with different sample holders is well within these estimates. In addition, the behavior of

of the equation of state at the highest pressures (where the corrections of Table 2, and in fact all corrections, should be a function of temperature for xenon, for instance) is sufficiently "regular" that systematic errors do not appear to be important.

CHAPTER VI. DISCUSSION

The Equation of State at 0 K

The equation of state at absolute zero is obtained by neglecting the temperature-dependent term, $P^*(T,V)$, in Equation I-2 giving

$$P(0,V) = P_o(V) = -dU_o/dV \qquad (VI-1)$$

where $U_o(V)$ is the absolute zero cohesive energy, which includes zero point effects (2). The 4.2 K isotherms which are given in Figures 9, 14, 19, and 23, respectively, for solid neon, argon, krypton, and xenon are identical with the 0 K isotherm for all practical purposes. Smoothed 4.2 K values of the pressure and bulk modulus as calculated for selected molar volumes using the coefficients in Appendix B are given for each solid in Appendix D. The reason for including negative values for the pressure in these tables is discussed later.

A Monte Carlo calculation of $P_o(V)$ for solid neon by Hansen (18), which assumes a Lennard-Jones 6-12 potential, can be compared directly with the present 4.2 K isotherm. Figure 24 shows that the predicted molar volume at 20 kbar agrees with the experimental value to better than 0.2%. The deviation at 8 kbar (approximately 0.7%) is seven times larger than the estimated experimental accuracy in this region (0.1%), and may be an indication that the Lennard-Jones 6-12 potential is not correct.

Figure 25 gives the pressure dependence of the bulk modulus, $B_o(V)$, at 4.2 K for neon, argon, krypton (solid line), and xenon as is calculated using the coefficients in Appendix B. The krypton results appear to be

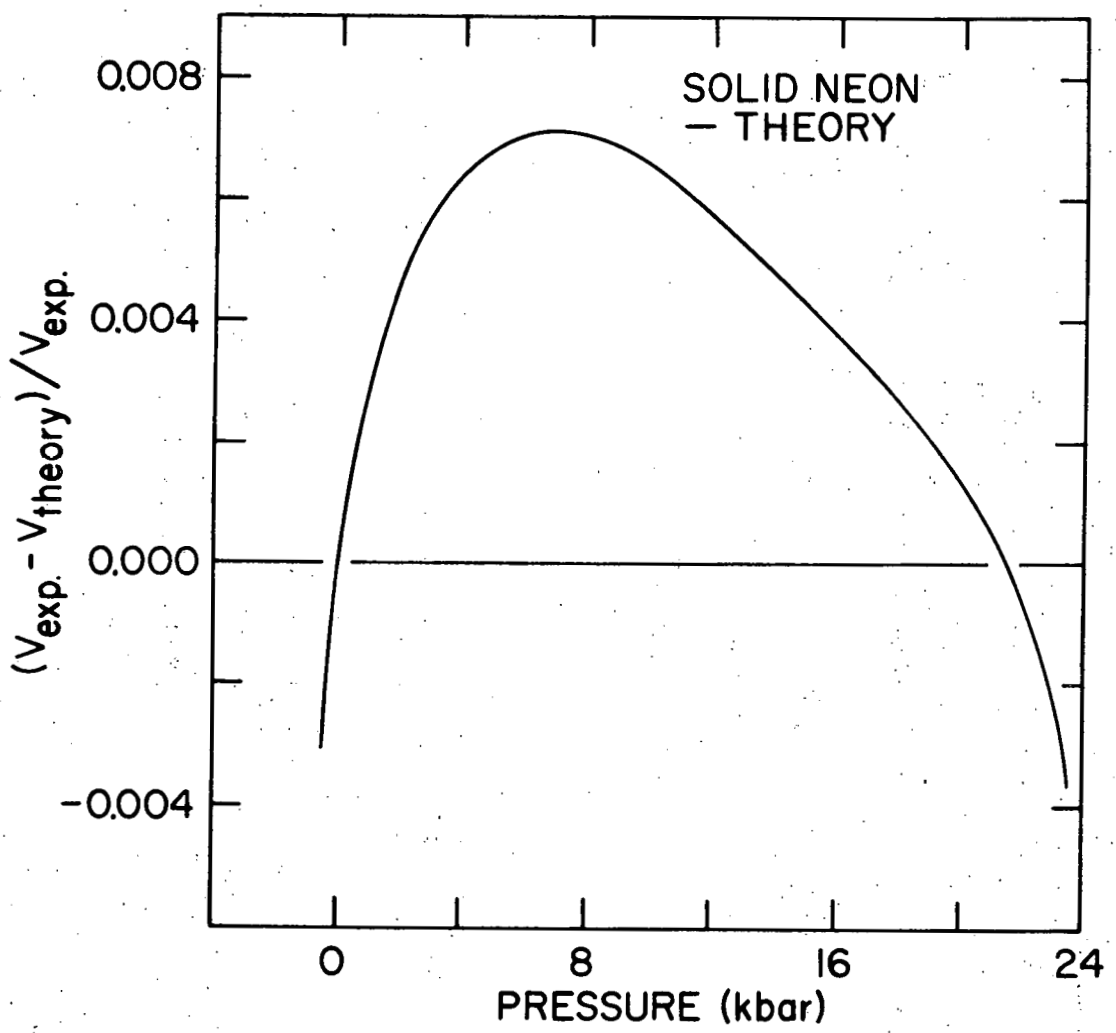

Figure 24. The difference between the theoretically calculated T=0 K isotherm of Hansen (18) and the present smoothed 4.2 K isotherm.

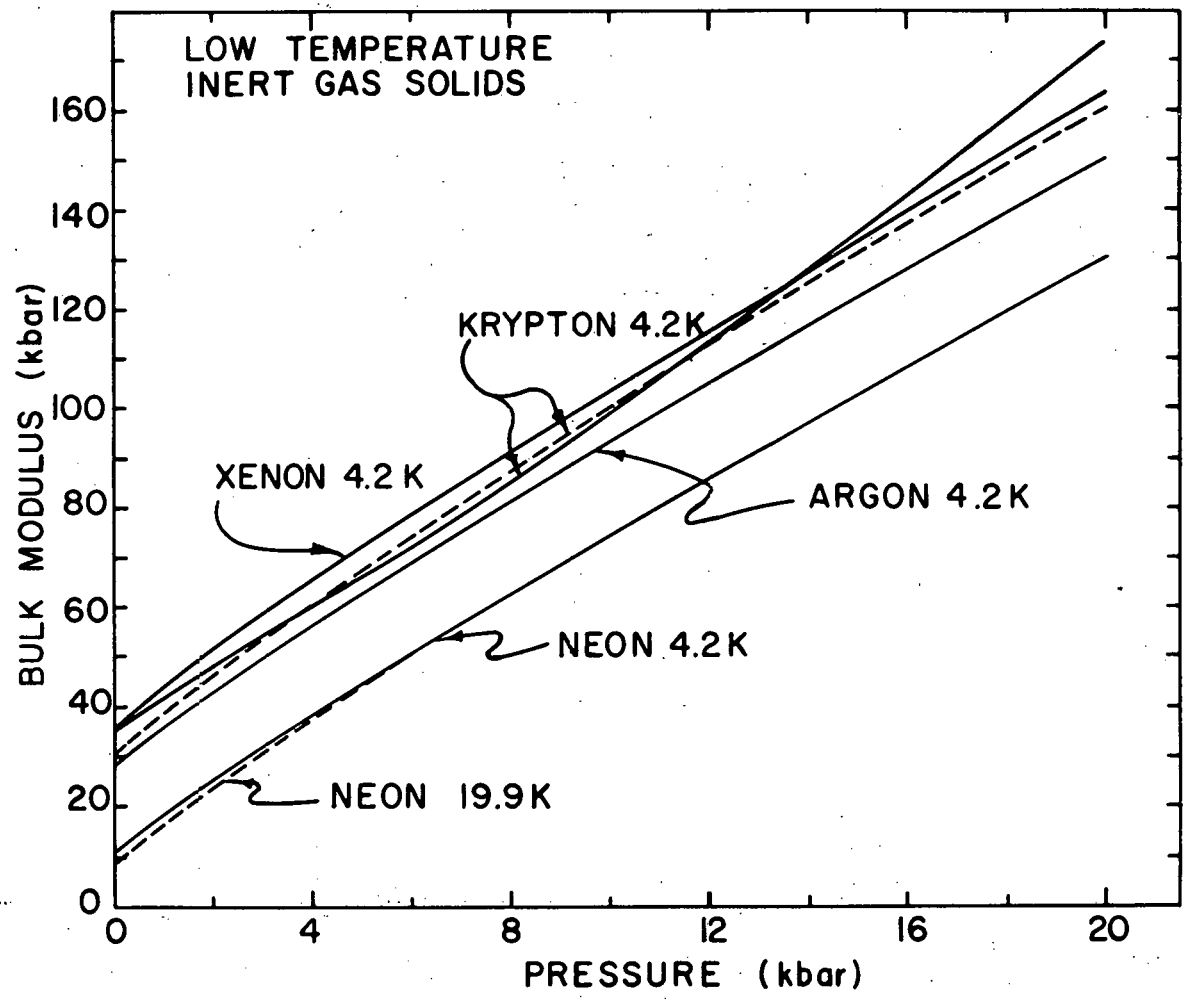

Figure 25. The isothermal bulk modulus, B_T, as a function of pressure for neon at 4.2 K and 19.9 K, and for argon, krypton, and xenon at 4.2 K. See the text for details with respect to the two 4.2 K curves for krypton.

anomalous since the bulk modulus does not increase smoothly with pressure. Both the second and third order relations (Equation IV-14) fitted the experimental data equally well, but the higher order equation was chosen since it gave better agreement with other experiments (Figures 17 and 18). The data appear to have been over-fitted, and the dashed curve represents the results of using the second order relation which represents the experimental data ($P \geq 1$ kbar) equally well, but which does not give good P=0 agreement. In particular, this relation gives $B_o(T=0) = 31.3$ kbar, in disagreement with the value of 34.5 kbar which is obtained from other data. The reason for the differences between krypton and the other solids is not understood.

It is interesting to observe that $\eta = dB_o/dP$ (Figure 25) appears to be the same for each of the solids above 6 kbar, if the dashed curve for krypton is assumed. In the low pressure region, less than 6 kbar, η for the various solids appears to increase with decreasing pressure.

Figure 25 suggests that a reduced equation of state may apply approximately to these solidified gases. In this case the internal energy can be represented by

$$U_o(V) = \epsilon f(V/V_o) \qquad (VI-2)$$

where ϵ is a constant and $f(V/V_o)$ contains the functional dependence on V/V_o. Then the bulk modulus can be written as

$$B_o = \left(\frac{\epsilon}{V_o}\right) \left(\frac{V}{V_o}\right) f''(V/V_o) \; . \qquad (VI-3)$$

This suggests that $B_o(\epsilon/V_o)^{-1}$ is the same function of the reduced volume

(V/V_o) for each of these solids. This postulate is tested in Figure 26 which gives $B_o(V_o/V)$ for argon, krypton, and xenon as a function of $B_o(V_o/V)$ for neon at 4.2 K (the second order coefficients were used in calculating these values for krypton). Equation VI-3 appears to be valid for these solids, except at low pressures ($V_o/V \leq 1.05$) where systematic deviations appear, especially for krypton.

Thermal Contributions to the Equation of State

The second term of Equation I-2, $P^*(T,V)$, contains the temperature-dependent contribution to the equation of state. This quantity, the thermal pressure, is the horizontal (constant volume) difference between the isotherms for 0 K and the temperature T (see Figures 9, 14, 19, and 23). The 0 K (4.2 K) isotherm must be extrapolated to negative pressures to obtain thermal pressures for volumes greater than the 0 K equilibrium volume. This is the reason for calculating negative pressures in Appendix D. The coefficients in Appendix B for the various isotherms represent smooth equations of state from which $P^*(T,V)$ can be calculated. Plots of $P^*(T,V)$ as a function of temperature are given in Figures 27-29 for argon, krypton, and xenon respectively for selected molar volumes. The isochores within each of these figures are parallel within experimental accuracy ($10^{-3}V$), as the solid lines show. Table 8 summarizes the quantities, $(\partial P^*/\partial T)_V$ and $B_T^* = -V(\partial P^*/\partial V)_T$ (Equation I-6) which can be calculated from these figures for each solid. Thermal effects are so small for neon that a similar analysis cannot be applied to it. A discussion of the thermal equation of state for solid neon is given elsewhere (7).

Equation I-3 suggests that the isothermal bulk modulus can be

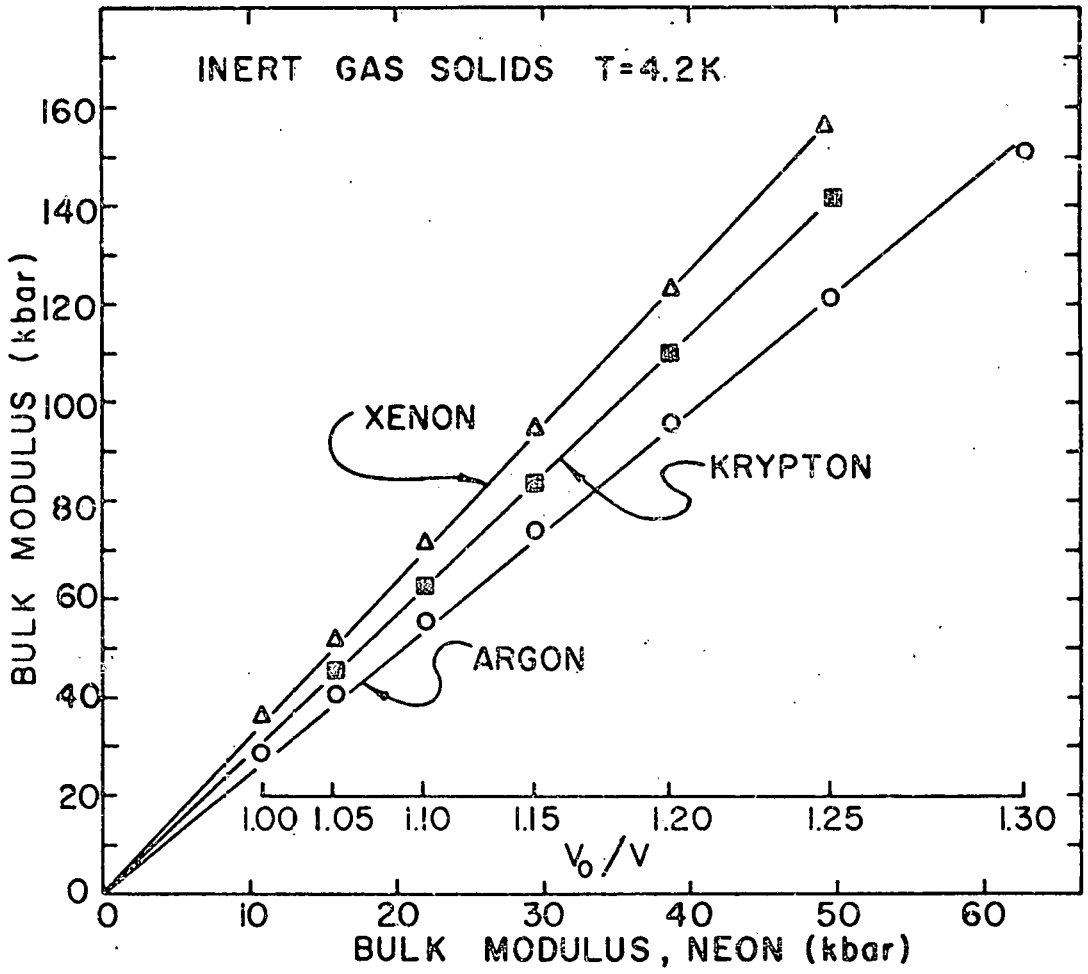

Figure 26. A comparison at common values of V_o/V of the 0 K bulk moduli for solid argon, krypton, and xenon in terms of the bulk moduli for solid neon.

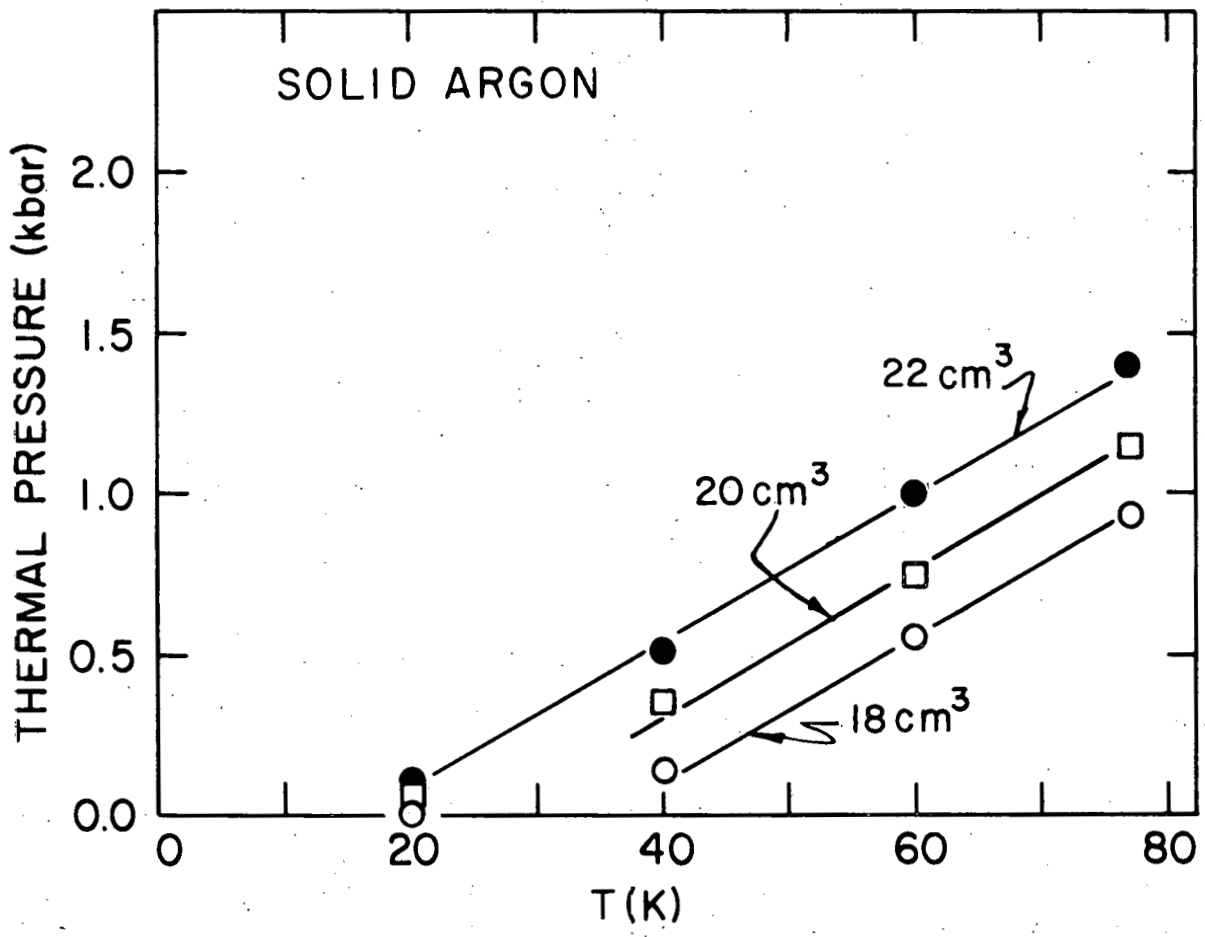

Figure 27. The thermal pressure, P^*, as a function of temperature for three selected molar volumes for solid argon.

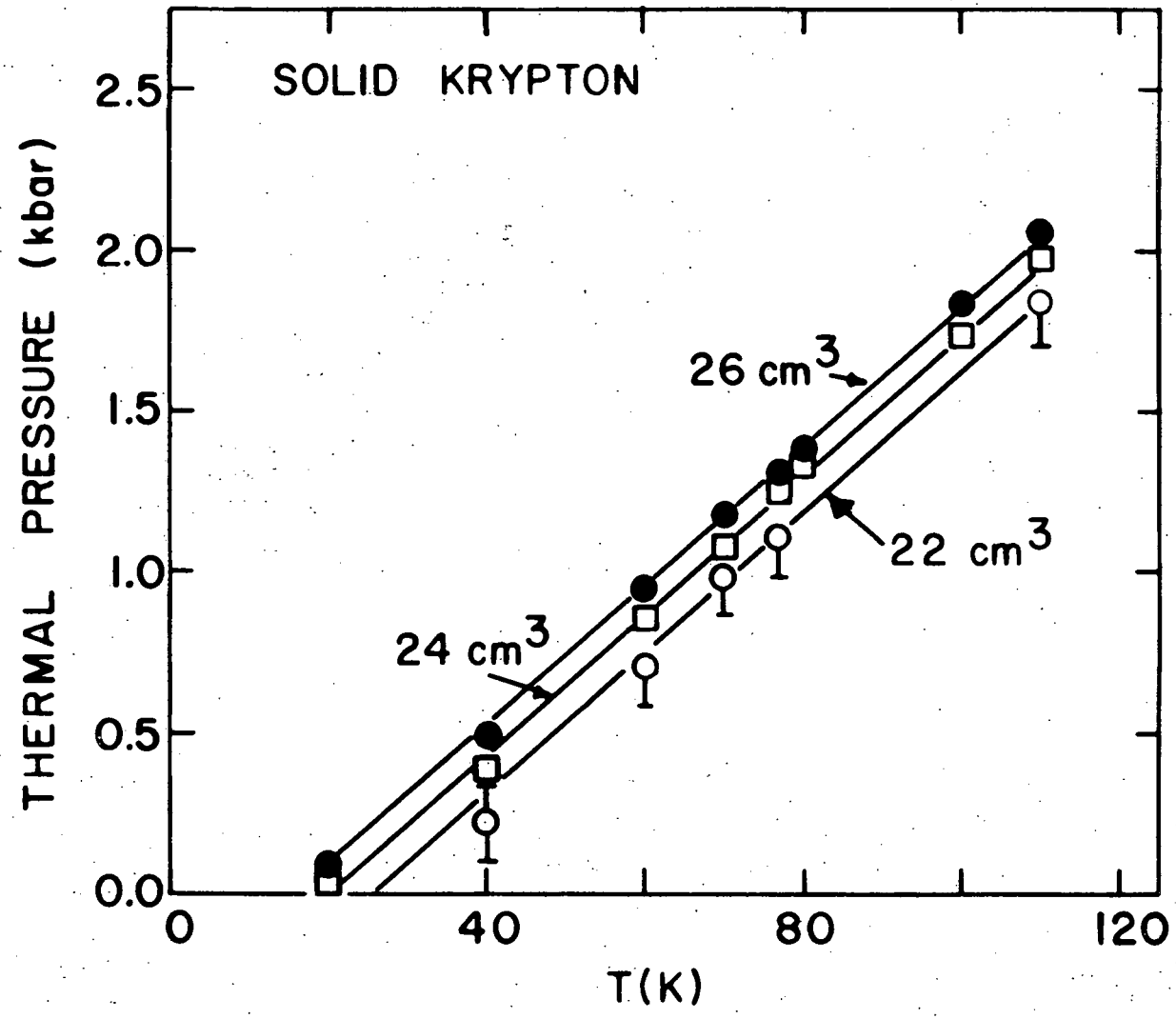

Figure 28. The thermal pressure, P^*, as a function of temperature for three selected molar volumes for solid krypton. The error bars correspond to $\pm 10^{-3}V$.

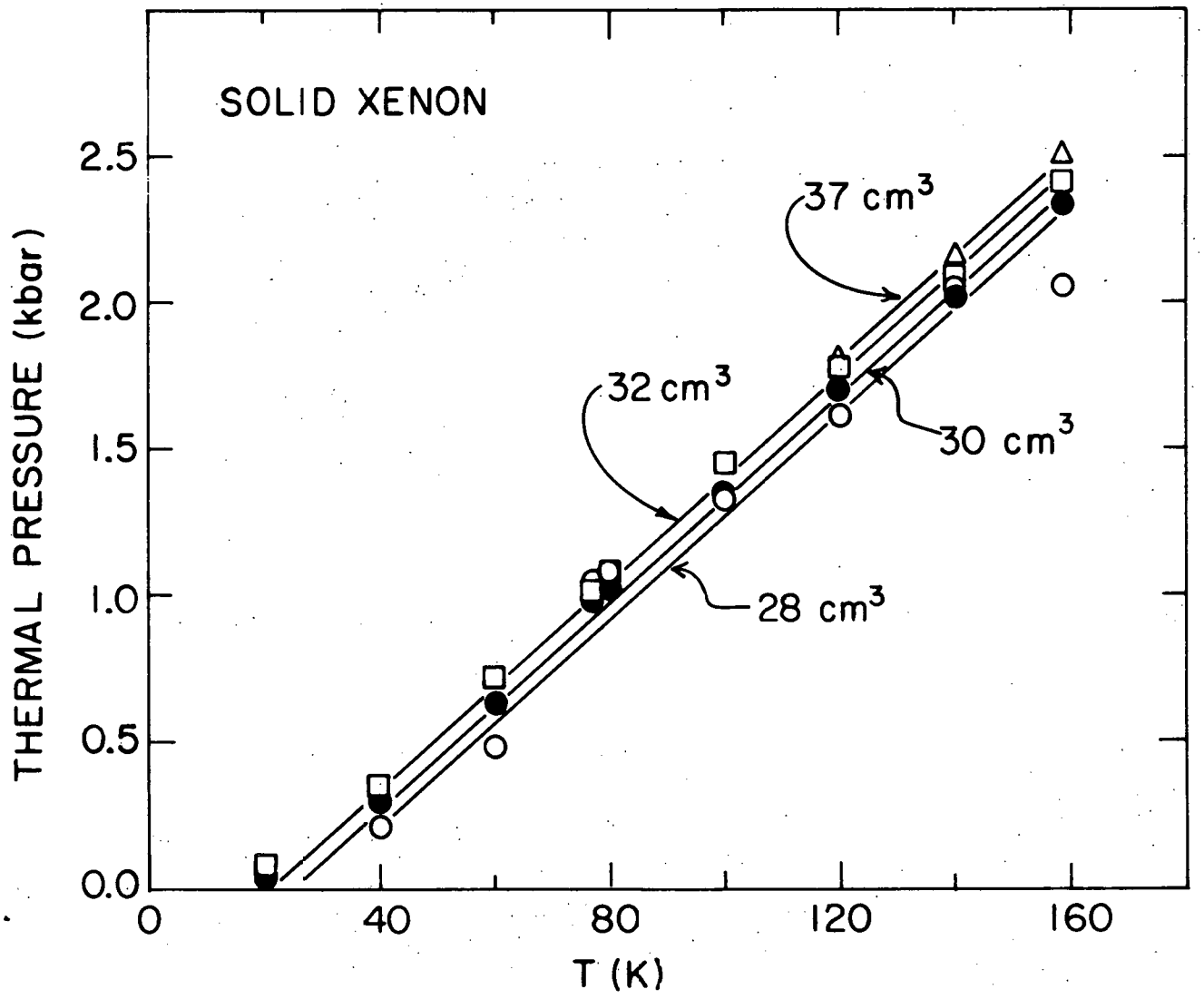

Figure 29. The thermal pressure, P^*, as a function of temperature for three selected molar volumes for solid xenon.

Table 8. A summary of results calculated from Figures 27, 28, and 29 for argon, krypton, and xenon, respectively. V_{Max} is the value of the molar volume at P=0 for the highest temperature.

Sample	V_{Max} (cm^3/mole)	$(\partial P^*/\partial T)_V$ (kbar/K)	$B_T^* = -V(\partial P^*/\partial V)_T$ (kbar)
argon	24.28	0.023	-2.7
krypton	29.69	0.022	-1.6
xenon	38.50	0.018	-0.8

considered as the sum of two terms, a temperature-independent 0 K term, $B_o(V)$, and a temperature-dependent term, $B_T^*(T,V)$. Figures 30-33 give plots of the bulk modulus as a function of temperature at constant volume for neon, argon, krypton, and xenon respectively, as calculated using the coefficients in Appendix B. Figures 13, 18, and 22 give similar calculated plots for argon, krypton, and xenon for larger molar volumes. The lines representing the isochores for a particular solid are drawn parallel, with a scatter in the data of roughly 1% in B_T for the larger molar volumes. These figures suggest that in all cases B_T decreases with increasing temperature, with only small effects (less than 3%) for neon and possibly xenon. Thus, the solid actually is becoming softer as the temperature is raised. This result was previously reported by Packard and Swenson (5)

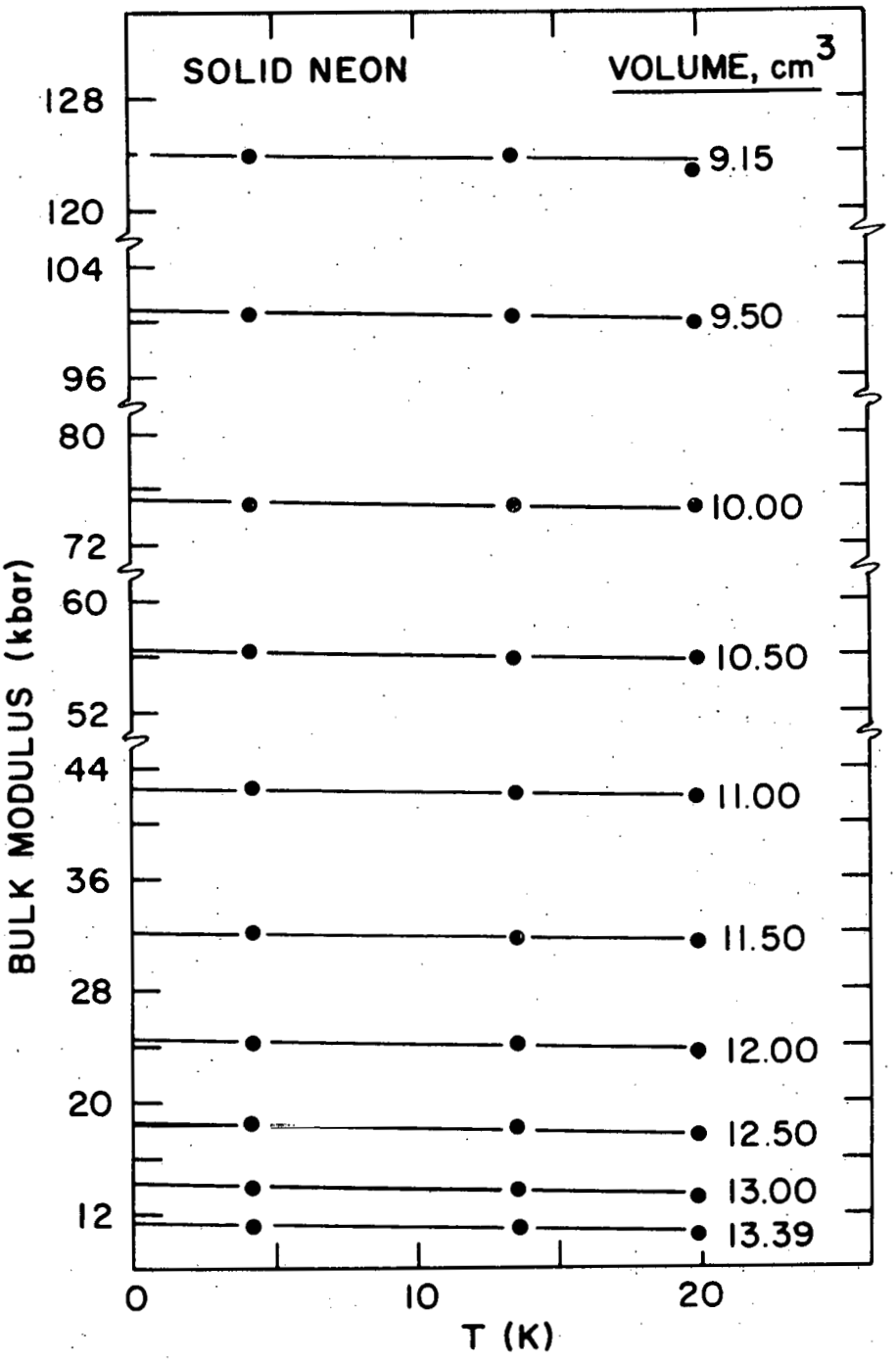

Figure 30. The temperature and volume dependence of B_T as calculated from the coefficients in Appendix B for solid neon for molar volumes less than $V_o = 13.39$ cm^3/mole.

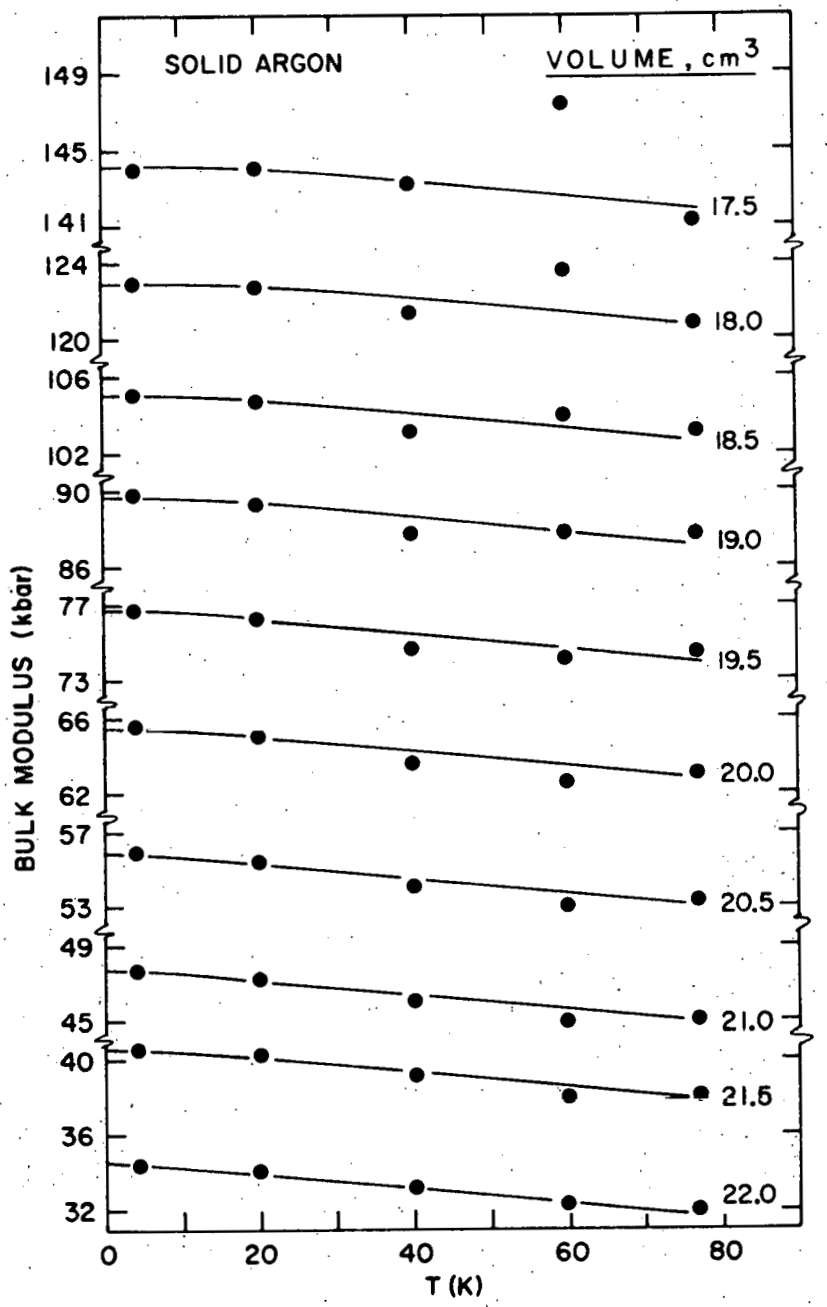

Figure 31. The temperature and volume dependence of B_T as calculated from the coefficients in Appendix B for solid argon. See Figure 13 for molar volumes greater than 22.00 cm^3/mole.

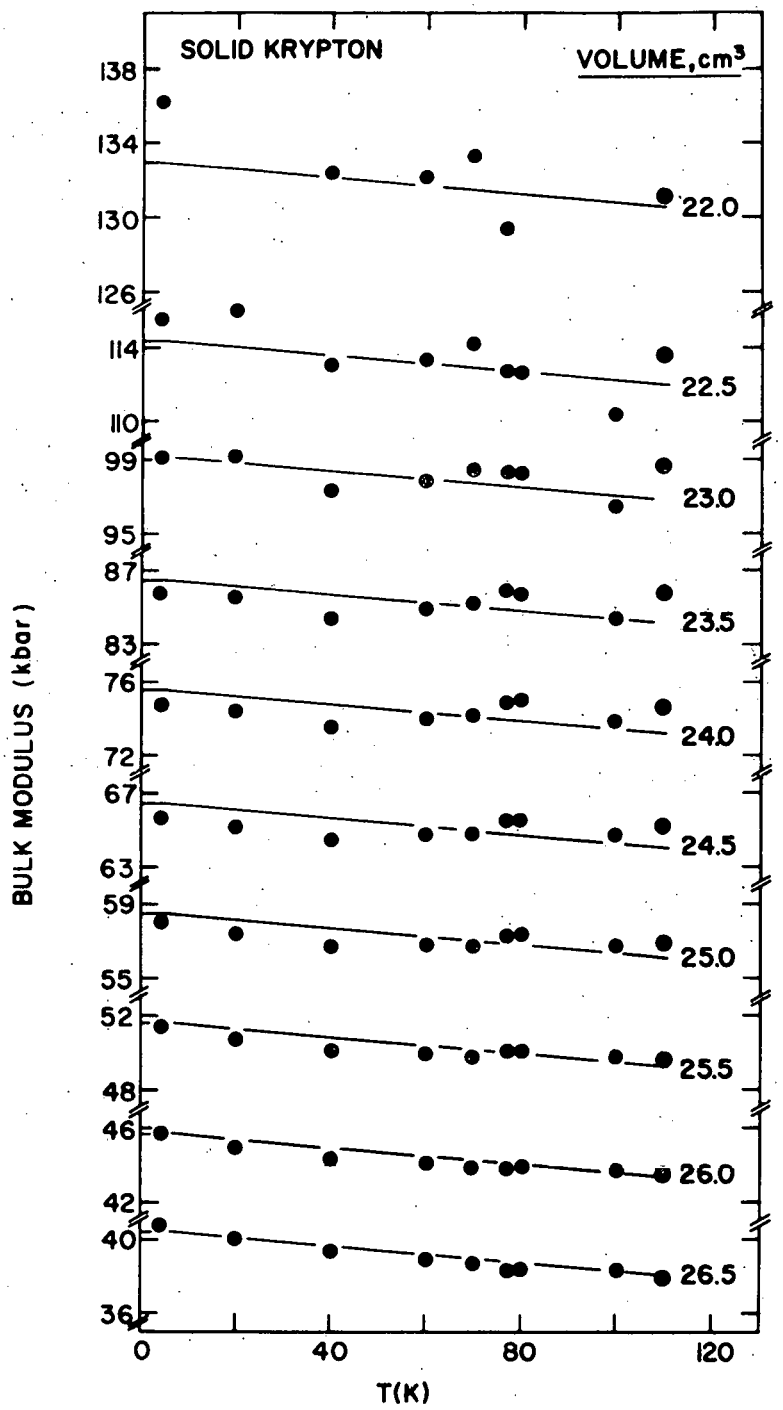

Figure 32. The temperature and volume dependence of B_T as calculated from the coefficients in Appendix B for solid krypton. See Figure 18 for molar volumes greater than 26.50 cm^3/mole.

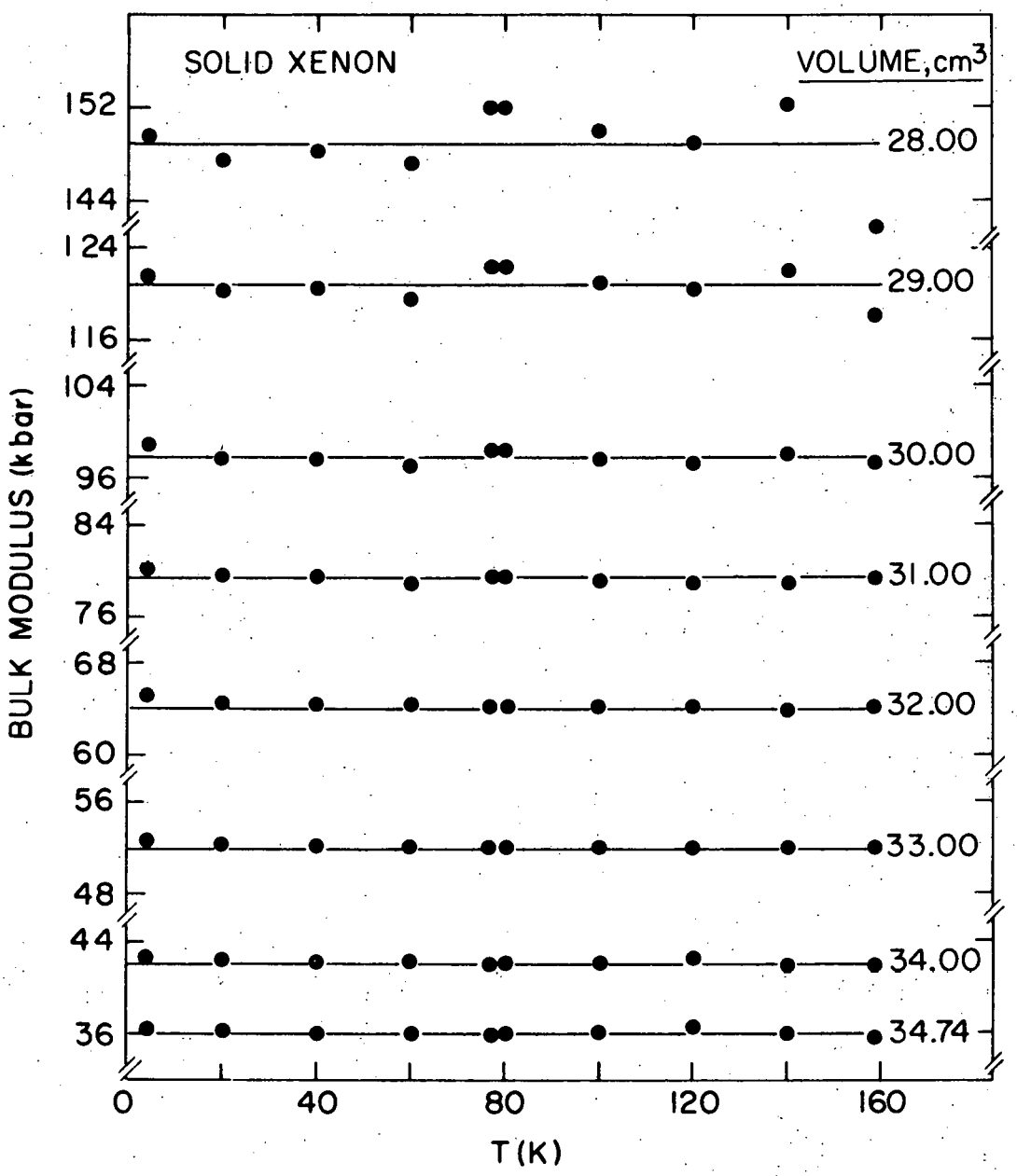

Figure 33. The temperature and volume dependence of B_T as calculated from the coefficients in Appendix B for solid xenon. See Figure 22 for molar volumes greater than 34.74 cm^3/mole.

for solid xenon and discussed in detail by Swenson (42).

Figures 27-29 and 30-33 give different representations of the equation of state and hence, are not independent. In particular, Figure 29 suggests that $P^*(T,V)$ for xenon is volume dependent and hence that a thermal contribution to the bulk modulus $B_T^* = -V(\partial P^*/\partial V)_T = -0.8$ kbar (Table 8) must exist. It is indeed small, and is not apparent in Figure 33.

The Grüneisen relation (42) can be written as

$$\gamma = \beta B_T \, V/C_V = \left(\frac{\partial P}{\partial T}\right)_V \left(\frac{V}{C_V}\right) \qquad \text{(VI-4)}$$

where β is the thermal expansion coefficient and C_V is the specific heat at constant volume. Values for $\gamma(T)$ at high temperature ($T > \Theta_D$) and low pressure as given by Tilford and Swenson (37) are compared with those calculated using $(\partial P/\partial T)_V$ (Table 8) from the present data and values for C_V (Table 9) from the literature (43,44,45). C_V has been measured directly for argon (43) and xenon (44), while corrected C_P data must be used for krypton (45). The agreement between the two values of γ is excellent, which suggests that the simple lattice dynamical model which leads to Equation VI-4 applies to these solids.

Swenson (42) has suggested that the same model should lead to a simple relation for B_T^* at high temperatures

$$B_T^* = -\left(\frac{9}{8}\right) (R \, \Theta_D \, \gamma^2/V) \, . \qquad \text{(VI-5)}$$

The calculated values for this quantity are compared with the experimental values (Table 8) in Table 9 for argon, krypton, and xenon. The agreement again is quite good, since the "experimental" values are good only to

Table 9. A comparison between values of the Grüneisen constant and between the thermal contributions to the bulk modulus as they are obtained from the present experiment and from other sources or relations.

Sample	C_V	γ_∞ [a]	γ	$\Theta_{D\infty}$ (K)	B_T^* (kbar) (Equation VI-5)	B_T^* (kbar) (Table 8)
argon	2.6R [b]	2.74	2.6	85 [d]	-2.5	-2.7
krypton	3.0R [d]	2.80	2.6	65 [d]	-1.6	-1.6
xenon	3.0R [c]	2.86	2.8	55 [e]	-1.1	-0.8

[a] Reference 37.

[b] Reference 43.

[c] Reference 44.

[d] Reference 45.

[e] Reference 46.

approximately $\pm$ 0.4 kbar.

Figure 34 is a plot of $B_T(T,V)$ vs. pressure for each of the solids, where T is chosen near the triple point for each solid. The 4.2 K neon isotherm is repeated from Figure 25 to give a sense of scale between this and the low temperature plot. It is remarkable that the pressure dependence of B_T is the same (within 5%) for argon, krypton, and xenon near their respective triple point temperatures. The coincidence of the curves for

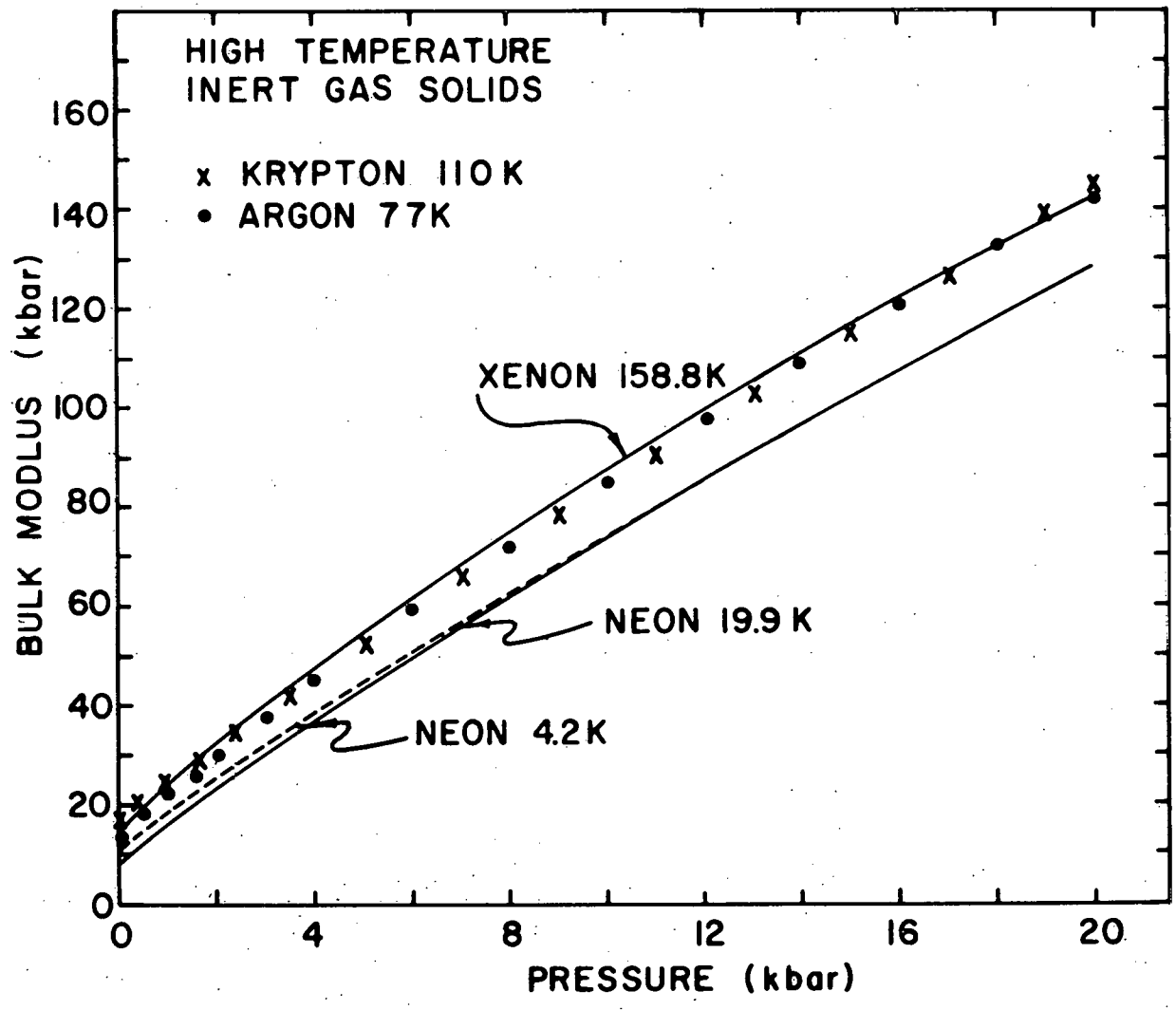

Figure 34. The isothermal bulk modulus, B_T, as a function of pressure for neon at 4.2 K and 19.9 K, and for argon, krypton, and xenon near their triple point temperatures.

the three heavier solids suggests a common classical reduced equation of state for these solids.

BIBLIOGRAPHY

1. G. K. Horton, Amer. J. Phys. 36, 93 (1968).

2. N. Bernardes and C. A. Swenson, Solids Under Pressure, edited by D. Warschauer and W. Paul (McGraw-Hill Book Company, Inc., New York, 1963), p. 101.

3. J. W. Stewart, J. Phys. Chem. Solids 1, 146 (1956).

4. J. W. Stewart, J. Phys. Chem. Solids 29, 641 (1968).

5. J. R. Packard and C. A. Swenson, J. Phys. Chem. Solids 24, 1405 (1963).

6. D. A. Benson, Ph.D. Thesis, Princeton University, 1968 (unpublished).

7. M. S. Anderson, R. O. Fugate, and C. A. Swenson (to be published).

8. D. N. Batchelder, D. L. Losee, and R. O. Simmons, Phys. Rev. 162, 767 (1967).

9. O. G. Peterson, D. N. Batchelder, and R. O. Simmons, Phys. Rev. 150, 703 (1966).

10. A. O. Urvas, D. L. Losee, and R. O. Simmons, J. Phys. Chem. Solids 28, 2269 (1967).

11. D. L. Losee and R. O. Simmons, Phys. Rev. 172, 944 (1968).

12. H. J. Coufal, R. Veith, P. Korpiun, and E. Lüscher, J. Appl. Phys. 41, 5082 (1970).

13. P. A. Bezuglyi, R. O. Plakhotin, and L. M. Tarasenko, Sov. Phys.-Solid State 12, 934 (1970).

14. R. Balzer, D. S. Kupperman, and R. O. Simmons, Phys. Rev. B4, 3636 (1971).

15. P. A. Bezuglyi, L. M. Tarasenko, and O. I. Baryshevskii, Sov. Phys.-Solid State 13, 2003 (1972).

16. G. J. Keeler and D. N. Batchelder, J. Phys. C3, 510 (1970).

17. W. S. Gornall and B. P. Stoicheff, Phys. Rev. B4, 4518 (1971).

18. J. P. Hansen, Phys. Rev. 172, 919 (1968).

19. J. A. Barker and A. Pompe, Australian J. Chem. 21, 1683 (1968).

20. M. V. Bobetic and J. A. Barker, Phys. Rev. B2, 4169 (1970).

21. J. A. Barker, R. A. Fisher, and R. O. Watts, Mol. Phys. 21, 657 (1971).

22. J. A. Barker, M. V. Bobetic, and M. L. Klein, Phys. Letters 34A, 415 (1971).

23. M. L. Klein, T. R. Koehler, and R. L. Gray (to be published).

24. R. I. Beecroft and C. A. Swenson, J. Phys. Chem. Solids 18, 329 (1961).

25. C. E. Monfort, M.S. Thesis, Iowa State University, 1964 (unpublished).

26. R. Q. Fugate and C. A. Swenson (to be published).

27. L. L. Sparks, R. L. Powell, and W. J. Hall, Natl. Bur. Stds. (U.S.) Report 9712 (1968).

28. C. E. Monfort and C. A. Swenson, J. Phys. Chem. Solids 26, 623 (1965).

29. J. R. Macdonald, Rev. Mod. Phys. 38, 669 (1966).

30. C. E. Monfort and C. A. Swenson, J. Phys. Chem. Solids 26, 291 (1965).

31. M. S. Anderson, E. J. Gutman, J. R. Packard, and C. A. Swenson, J. Phys. Chem. Solids 30, 1587 (1969).

32. F. Birch, J. Geophysical Research 57, 227 (1952).

33. O. L. Anderson, J. Phys. Chem. Solids 27, 547 (1966).

34. J. A. Barker, M. L. Klein, and M. V. Bobetic, Phys. Rev. B2, 4176 (1970).

35. R. A. Fisher and R. O. Watts (to be published).

36. P. Korpiun and H. J. Coufal, Phys. Stat. Sol. (a) 6, 187 (1971).

37. C. R. Tilford and C. A. Swenson, Phys. Rev. B5, 719 (1972).

38. V. G. Manzhelii, V. G. Gavrilko, and E. I. Voitovich, Sov. Phys.-Solid State 9, 1157 (1967).

39. V. G. Gavrilko and V. G. Manzhelii, Sov. Phys.-Solid State 6, 1734 (1965).

40. M. L. Klein and W. G. Hoover, Phys. Rev. B4, 537 (1971).

41. M. L. Klein and W. G. Hoover, Phys. Rev. B4, 539 (1971).

42. C. A. Swenson, J. Phys. Chem. Solids 29, 1337 (1968).

43. F. Haenssler, K. Gamper, and B. Serin, J. Low Temp. Phys. 3, 23 (1970).

44. K. Gamper, J. Low Temp. Phys. 6, 35 (1972).

45. R. H. Beaumont, H. Chihara, and J. A. Morrison, Proc. Phys. Soc. (London) 78, 1462 (1961).

46. H. Fenichel and B. Serin, Phys. Rev. 142, 490 (1966).

ACKNOWLEDGMENTS

The successful completion of this work has been the contribution of many individuals; the author especially wishes to express his gratitude to the following individuals:

Dr. C. A. Swenson for suggesting the problem and giving advice and encouragement throughout its completion;

David Hansen and Mel Colter for their help with the preliminary results;

The various individuals in the author's group who formed the daily environment and provided stimulating discussions;

The author's wife, Carol, for patient encouragement and self-sacrifice.

APPENDIX A

Unsmoothed Isotherms for Neon, Argon, Krypton, and Xenon

The following pages give the experimental data for each sample in terms of the molar volume (cm^3/mole), after correction for sample holder thermal expansion, pressure distortion, and any sample loss or dial gauge shifts. The data for the isotherms (vertical columns) are given from left to right in the order which the compression runs were made. The molar volumes listed are calculated from the experimental sample lengths using the conversion factors given in the following table for each sample. These are based on the actual, unadjusted, experimental sample lengths (Table 3). An entry of 0.0 indicates that data for that pressure were unreliable. An extra significant figure is included to eliminate a rounding error.

Table 10. The conversion factors (V(4.2 K, P=0)/L(4.2 K,P=0), Equation IV-16) used to convert experimental sample lengths into molar volumes (units, cm^3/mole-in.).

Sample	Sample Diameter		
	0.500 in.	0.354 in.	0.250 in.
neon	27.441	35.236	43.549
argon I	46.601	66.513	92.375
II	45.611	-	73.034
krypton	57.067	104.433	113.131
xenon	72.273	102.898	159.568

0.500 IN. DIAMETER NEON DATA.

PRESSURE KILOBAR	TEMPERATURE, KELVIN			
	4.200	19.900	13.500	4.200
0.25	0.0	13.390	13.192	0.0
0.50	12.864	13.096	12.941	12.883
0.75	12.668	12.855	12.727	12.679
1.00	12.494	12.638	12.542	12.504
1.50	12.189	12.293	12.228	12.200
2.00	11.934	12.015	11.962	11.942
3.00	11.521	11.568	11.538	11.523
4.00	11.193	11.223	11.201	11.193
5.00	10.919	10.943	10.926	10.921
6.00	10.692	10.713	10.695	10.698
7.00	10.501	10.511	10.502	10.505

0.354 IN. DIAMETER NEON DATA.

PRESSURE KILOBAR	TEMPERATURE, KELVIN			
	4.200	19.900	13.500	4.200
0.50	0.0	13.114	12.958	12.862
0.75	12.667	12.854	12.722	12.672
1.00	12.495	12.636	12.527	12.491
1.50	12.189	12.288	12.213	12.188
2.00	11.933	12.007	11.952	11.931
3.00	11.521	11.566	11.532	11.517
4.00	11.193	11.228	11.209	11.193
5.00	10.918	10.946	10.928	10.920
6.00	10.690	10.710	10.699	10.691
7.00	10.492	10.505	10.495	10.490
8.00	10.319	10.327	10.319	10.317
9.00	10.161	10.168	10.161	10.158
10.00	10.018	10.021	10.019	10.018
11.00	9.888	9.892	9.886	9.888
12.00	9.771	9.771	9.769	9.771
13.00	9.665	9.663	9.663	9.661
14.00	9.568	9.564	9.562	9.564

0.250 IN. DIAMETER NEON DATA.

PRESSURE KILOBAR	TEMPERATURE, KELVIN			
	4.200	12.700	19.600	4.200
1.00	12.455	12.494	12.599	12.455
2.00	11.886	11.895	11.945	11.886
3.00	11.462	11.471	11.496	11.466
4.00	11.136	11.145	11.162	11.132
5.00	10.869	10.871	10.895	10.869
6.00	10.631	10.636	10.660	10.640
7.00	10.431	10.437	10.450	10.437
8.00	10.258	10.263	10.269	10.265
9.00	10.099	10.101	10.110	10.103
10.00	9.960	9.960	9.964	9.962
11.00	9.831	9.831	9.836	9.833
12.00	9.709	9.709	9.713	9.711
13.00	9.600	9.600	9.604	9.604
14.00	9.497	9.493	9.502	9.497
15.00	9.404	9.399	9.404	9.404
16.00	9.317	9.312	9.314	9.319
17.00	9.238	9.229	9.233	9.238
18.00	9.162	9.153	9.155	9.162
19.00	9.089	9.080	9.080	9.089
20.00	9.022	9.013	9.013	9.022

0.500 IN. DIAMETER ARGON DATA. SAMPLE I

PRESSURE KILOBAR	TEMPERATURE, KELVIN				
	18.900	59.700	67.900	77.700	40.200
0.25	0.0	23.384	23.629	24.020	22.808
0.50	22.259	23.084	23.287	23.618	22.592
0.75	22.096	22.828	23.005	23.289	22.385
1.00	21.937	22.605	22.756	23.010	22.194
1.50	21.639	22.200	22.328	22.526	21.861
2.00	21.369	21.860	21.958	22.128	21.559
3.00	20.894	21.277	21.361	21.494	21.040
4.00	20.494	20.810	20.880	20.989	20.608
5.00	20.150	20.415	20.471	20.569	20.240
6.00	19.852	20.079	20.125	20.216	19.920
7.00	19.587	19.789	19.831	19.908	19.643

0.500 IN. DIAMETER ARGON DATA. SAMPLE II

PRESSURE KILOBAR	TEMPERATURE, KELVIN			
	19.600	4.200	60.500	77.000
0.25	0.0	0.0	23.356	23.908
0.50	22.246	0.0	23.073	23.557
0.75	22.084	22.011	22.814	23.245
1.00	21.924	21.865	22.591	22.977
1.50	21.638	21.588	22.199	22.522
2.00	21.369	21.326	21.851	22.135
3.00	20.894	20.869	21.272	21.501
4.00	20.492	20.478	20.799	21.002
5.00	20.151	20.142	20.406	20.575
6.00	19.854	19.844	20.064	20.206
7.00	19.572	19.575	19.756	19.889

0.354 IN. DIAMETER ARGON DATA.

PRESSURE KILOBAR	TEMPERATURE, KELVIN				
	20.000	4.200	59.400	76.700	40.000
0.50	0.0	0.0	23.049	23.532	22.573
0.75	22.068	0.0	22.800	23.229	22.378
1.00	21.916	21.843	22.575	22.960	22.195
1.50	21.631	21.571	22.177	22.503	21.857
2.00	21.366	21.316	21.835	22.119	21.556
3.00	20.895	20.872	21.258	21.491	21.046
4.00	20.505	20.478	20.798	20.991	20.622
5.00	20.157	20.131	20.408	20.549	20.248
6.00	19.843	19.827	20.064	20.191	19.917
7.00	19.563	19.553	19.773	19.874	19.626
8.00	19.318	19.301	19.489	19.586	19.369
9.00	19.094	19.074	19.235	19.325	19.135
10.00	18.883	18.870	19.008	19.095	18.920
11.00	18.695	18.682	18.803	18.885	18.723
12.00	18.515	18.505	18.606	18.687	18.529
13.00	18.346	18.340	18.425	18.502	18.358
14.00	18.182	18.182	18.254	18.328	18.195

0.250 IN. DIAMETER ARGON DATA. SAMPLE I

PRESSURE KILOBAR	TEMPERATURE, KELVIN				
	20.000	4.200	40.100	77.200	60.000
1.00	0.0	0.0	0.0	22.485	0.0
1.50	21.135	0.0	21.389	22.022	21.676
2.00	20.868	20.831	21.091	21.627	21.317
3.00	20.401	20.373	20.581	20.992	20.754
4.00	20.007	19.979	20.152	20.483	20.293
5.00	19.656	19.635	19.779	20.052	19.899
6.00	19.352	19.338	19.450	19.690	19.556
7.00	19.079	19.063	19.150	19.368	19.249
8.00	18.827	18.808	18.891	19.077	18.975
9.00	18.589	18.578	18.652	18.808	18.733
10.00	18.378	18.366	18.427	18.576	18.505
11.00	18.179	18.165	18.217	18.363	18.291
12.00	17.988	17.983	18.027	18.157	18.093
13.00	17.816	17.812	17.850	17.970	17.905
14.00	17.653	17.650	17.717	17.796	17.737
15.00	17.503	17.499	17.533	17.635	17.574
16.00	17.363	17.358	17.388	17.481	17.426
17.00	17.231	17.231	17.252	17.342	17.284
18.00	17.111	17.111	17.121	17.206	17.153
19.00	16.982	16.989	17.000	17.080	17.023
20.00	16.865	16.878	16.873	16.954	16.901

0.250 IN. DIAMETER ARGON DATA. SAMPLE II

PRESSURE KILOBAR	TEMPERATURE, KELVIN				
	19.700	4.200	40.000	77.200	60.000
1.00	0.0	0.0	21.959	22.747	22.323
1.50	21.378	0.0	21.623	22.253	21.897
2.00	21.116	21.073	21.326	21.860	21.542
3.00	20.639	20.623	20.815	21.221	20.973
4.00	20.238	20.225	20.377	20.714	20.510
5.00	19.888	19.877	20.005	20.297	20.132
6.00	19.586	19.578	19.684	19.935	19.799
7.00	19.308	19.304	19.389	19.618	19.500
8.00	19.060	19.057	19.120	19.329	19.232
9.00	18.821	18.819	18.882	19.069	18.989
10.00	18.613	18.607	18.664	18.834	18.760
11.00	18.419	18.408	18.456	18.623	18.553
12.00	18.236	18.226	18.266	18.419	18.356
13.00	18.063	18.062	18.088	18.233	18.174
14.00	17.898	17.905	17.925	18.060	18.003
15.00	17.750	17.756	17.774	17.902	17.847
16.00	17.611	17.614	17.633	17.760	17.701
17.00	17.481	17.483	17.500	17.615	17.559
18.00	17.362	17.356	17.372	17.480	17.424
19.00	17.242	17.240	17.248	17.356	17.300
20.00	17.134	17.134	17.119	17.238	17.180

0.5 IN. DIAMETER KRYPTON DATA.

PRESSURE KILOBAR	TEMPERATURE, KELVIN				
	77.000	99.900	40.500	4.200	20.300
0.25	28.419	0.0	0.0	0.0	0.0
0.50	28.104	0.0	0.0	0.0	0.0
0.75	27.837	0.0	0.0	0.0	0.0
1.00	27.591	28.116	26.904	26.534	26.615
1.50	27.146	27.600	26.555	26.243	26.303
2.00	26.756	27.156	26.230	25.966	26.009
3.00	26.099	26.428	25.665	25.449	25.485
4.00	25.566	25.828	25.186	25.007	25.035
5.00	25.101	25.329	24.767	24.617	24.636
6.00	24.701	24.899	24.410	24.277	24.297
7.00	24.358	24.525	24.099	23.977	23.997

0.5 IN. DIAMETER KRYPTON DATA.

PRESSURE KILOBAR	TEMPERATURE, KELVIN		
	60.100	77.200	100.100
0.25	0.0	28.392	29.089
0.50	27.698	28.101	28.723
0.75	27.468	27.833	28.399
1.00	27.245	27.583	28.109
1.50	26.852	27.143	27.601
2.00	26.499	26.761	27.155
3.00	25.900	26.099	26.425
4.00	25.387	25.557	25.830
5.00	24.950	25.090	25.330
6.00	24.569	24.692	24.897
7.00	24.242	24.353	24.531

0.354 IN. DIAMETER KRYPTON DATA.

PRESSURE KILOBAR	TEMPERATURE, KELVIN				
	76.700	68.200	23.100	4.200	43.300
0.75	27.701	27.529	0.0	0.0	27.006
1.00	27.450	27.289	26.505	26.400	26.818
1.50	27.012	26.876	26.199	26.097	26.474
2.00	26.632	26.510	25.899	25.816	26.150
3.00	25.995	25.890	25.372	25.316	25.591
4.00	25.453	25.368	24.918	24.871	25.106
5.00	24.983	24.919	24.522	24.479	24.668
6.00	24.580	24.517	24.162	24.119	24.292
7.00	24.209	24.151	23.838	23.795	23.942
8.00	23.881	23.828	23.540	23.508	23.645
9.00	23.580	23.536	23.274	23.247	23.368
10.00	23.324	23.265	23.029	23.007	23.107
11.00	23.068	23.019	22.799	22.787	22.867
12.00	22.844	22.795	22.595	22.584	22.653
13.00	22.630	22.587	22.412	22.401	22.454
14.00	22.431	22.388	22.245	22.234	22.272

0.354 IN. DIAMETER KRYPTON DATA.

PRESSURE KILOBAR	TEMPERATURE, KELVIN				
	60.400	79.700	81.200	100.700	110.300
0.50	0.0	28.009	28.108	0.0	28.887
0.75	27.340	27.737	27.826	28.301	28.522
1.00	27.122	27.487	27.571	27.993	28.204
1.50	26.745	27.059	27.132	27.493	27.656
2.00	26.410	26.673	26.746	27.065	27.191
3.00	25.796	26.031	26.099	26.350	26.443
4.00	25.284	25.488	25.540	25.745	25.838
5.00	24.836	25.003	25.056	25.233	25.311
6.00	24.438	24.596	24.638	24.784	24.858
7.00	24.082	24.215	24.262	24.399	24.450
8.00	23.767	23.891	23.928	24.054	24.095
9.00	23.473	23.589	23.626	23.747	23.774
10.00	23.207	23.318	23.351	23.460	23.486
11.00	22.973	23.083	23.101	23.204	23.229
12.00	22.747	22.854	22.870	22.970	22.991
13.00	22.540	22.635	22.656	22.746	22.767
14.00	22.341	22.436	22.457	22.538	22.558

0.250 IN. DIAMETER KRYPTON DATA.

PRESSURE KILOBAR	TEMPERATURE, KELVIN				
	77.000	68.500	38.100	4.200	60.300
2.00	26.690	26.532	26.096	25.825	26.407
3.00	26.016	25.891	25.528	25.319	25.801
4.00	25.454	25.352	25.046	24.871	25.278
5.00	24.983	24.898	24.620	24.478	24.830
6.00	24.574	24.494	24.255	24.125	24.438
7.00	24.210	24.125	23.926	23.807	24.080
8.00	23.879	23.812	23.630	23.517	23.772
9.00	23.573	23.522	23.340	23.267	23.477
10.00	23.295	23.248	23.078	23.015	23.209
11.00	23.051	23.004	22.844	22.793	22.959
12.00	22.828	22.787	22.627	22.585	22.736
13.00	22.617	22.580	22.427	22.387	22.531
14.00	22.417	22.387	22.234	22.205	22.342
15.00	22.240	22.200	22.065	22.039	22.160
16.00	22.064	22.028	21.901	21.873	21.994
17.00	21.903	21.868	21.753	21.725	21.829
18.00	21.750	21.719	21.598	21.587	21.679
19.00	21.600	21.571	21.461	21.455	21.531
20.00	21.469	21.438	21.329	21.323	21.399

0.250 IN. DIAMETER KRYPTON DATA.

PRESSURE KILOBAR	TEMPERATURE, KELVIN		
	77.000	110.000	77.000
1.00	27.523	0.0	27.508
1.50	27.057	0.0	27.049
2.00	26.656	27.219	26.655
3.00	25.999	26.461	25.992
4.00	25.454	25.849	25.447
5.00	24.985	25.313	24.980
6.00	24.570	24.856	24.573
7.00	24.210	24.450	24.210
8.00	23.880	24.095	23.882
9.00	23.577	23.785	23.586
10.00	23.310	23.494	23.314
11.00	23.070	23.225	23.067
12.00	22.829	22.995	22.825
13.00	22.617	22.772	22.615
14.00	22.419	22.565	22.416
15.00	22.238	22.376	22.238
16.00	22.064	22.186	22.059
17.00	21.898	22.019	21.903
18.00	21.742	21.853	21.747
19.00	21.593	21.702	21.592
20.00	21.454	21.559	21.458

0.500 IN. DIAMETER XENON DATA.

PRESSURE KILOBAR	TEMPERATURE, KELVIN				
	158.600	100.000	77.000	80.000	60.000
0.25	37.620	35.842	0.0	0.0	0.0
0.50	37.072	35.496	34.967	35.011	0.0
0.75	36.600	35.183	34.704	34.745	34.362
1.00	36.184	34.891	34.460	34.492	34.137
1.50	35.481	34.378	34.010	34.029	33.725
2.00	34.885	33.924	33.598	33.617	33.338
3.00	33.927	33.154	32.875	32.891	32.644
4.00	33.151	32.504	32.270	32.263	32.060
5.00	32.498	31.943	31.734	31.734	31.549
6.00	31.924	31.459	31.276	31.268	31.110
7.00	31.430	31.026	30.858	30.842	30.707

0.500 IN. DIAMETER XENON DATA.

PRESSURE KILOBAR	TEMPERATURE, KELVIN				
	20.000	4.200	40.100	80.000	76.800
0.50	0.0	0.0	0.0	34.986	34.970
0.75	0.0	0.0	34.007	34.720	34.710
1.00	0.0	0.0	33.804	34.473	34.463
1.50	33.211	33.116	33.423	34.013	34.016
2.00	32.872	32.799	33.062	33.595	33.598
3.00	32.273	32.222	32.422	32.869	32.875
4.00	31.740	31.699	31.867	32.251	32.263
5.00	31.278	31.246	31.379	31.715	31.734
6.00	30.874	30.846	30.958	31.248	31.276
7.00	30.499	30.465	30.561	30.829	30.851

0.500 IN. DIAMETER XENON DATA.

PRESSURE KILOBAR	TEMPERATURE, KELVIN				
	119.900	140.000	158.800	99.900	76.900
0.25	36.305	36.885	37.572	0.0	0.0
0.50	35.924	36.430	37.035	35.468	34.952
0.75	35.569	36.035	36.573	35.150	34.702
1.00	35.259	35.676	36.162	34.872	34.456
1.50	34.714	35.052	35.467	34.371	34.009
2.00	34.219	34.526	34.879	33.924	33.598
3.00	33.382	33.637	33.921	33.149	32.869
4.00	32.694	32.899	33.152	32.505	32.264
5.00	32.105	32.280	32.497	31.943	31.732
6.00	31.596	31.737	31.930	31.454	31.276
7.00	31.132	31.265	31.443	31.015	30.851

0.500 IN. DIAMETER XENON DATA.

PRESSURE KILOBAR	TEMPERATURE, KELVIN		
	120.000	76.900	140.100
0.25	36.314	0.0	36.869
0.50	35.934	34.958	36.419
0.75	35.614	34.701	36.026
1.00	35.275	34.457	35.674
1.50	34.726	34.010	35.056
2.00	34.229	33.598	34.530
3.00	33.401	32.862	33.645
4.00	32.704	32.257	32.913
5.00	32.124	31.727	32.292
6.00	31.610	31.269	31.750
7.00	31.161	30.861	31.267

0.354 IN. DIAMETER XENON DATA.

PRESSURE KILOBAR	TEMPERATURE, KELVIN				
	99.600	59.900	19.500	4.200	40.000
0.50	35.852	0.0	0.0	0.0	0.0
0.75	35.538	34.749	0.0	0.0	0.0
1.00	35.246	34.525	33.926	0.0	34.220
1.50	34.724	34.095	33.563	33.528	33.826
2.00	34.262	33.701	33.224	33.182	33.461
3.00	33.487	33.019	32.612	32.580	32.807
4.00	32.830	32.413	32.067	32.048	32.224
5.00	32.259	31.895	31.588	31.567	31.720
6.00	31.760	31.412	31.148	31.140	31.273
7.00	31.297	30.998	30.755	30.745	30.864
8.00	30.892	30.611	30.403	30.393	30.497
9.00	30.521	30.264	30.072	30.067	30.155
10.00	30.179	29.948	29.772	29.766	29.845
11.00	29.868	29.653	29.484	29.497	29.559
12.00	29.584	29.383	29.227	29.251	29.297
13.00	29.320	29.135	28.997	29.009	29.051
14.00	29.071	28.900	28.768	28.786	28.826

0.354 IN. DIAMETER XENON DATA.

PRESSURE KILOBAR	TEMPERATURE, KELVIN				
	80.100	76.900	99.800	139.900	158.800
0.50	35.441	0.0	35.858	36.791	37.345
0.75	35.159	35.115	35.544	36.406	36.893
1.00	34.900	34.855	35.256	36.047	36.486
1.50	34.416	34.381	34.733	35.409	35.784
2.00	33.996	33.964	34.269	34.881	35.211
3.00	33.275	33.230	33.483	33.999	34.252
4.00	32.631	32.586	32.817	33.253	33.490
5.00	32.073	32.047	32.246	32.618	32.814
6.00	31.593	31.559	31.745	32.070	32.240
7.00	31.161	31.127	31.288	31.594	31.726
8.00	30.760	30.735	30.880	31.156	31.291
9.00	30.399	30.378	30.510	30.759	30.893
10.00	30.073	30.051	30.174	30.402	30.530
11.00	29.767	29.748	29.863	30.072	30.194
12.00	29.485	29.478	29.577	29.777	29.886
13.00	29.229	29.220	29.320	29.498	29.607
14.00	28.991	28.977	29.078	29.235	29.337

0.354 IN. DIAMETER XENON DATA.

PRESSURE KILOBAR	TEMPERATURE, KELVIN	
	120.100	139.700
0.50	36.307	0.0
0.75	35.955	36.364
1.00	35.634	36.009
1.50	35.054	35.397
2.00	34.567	34.861
3.00	33.724	33.967
4.00	33.025	33.240
5.00	32.432	32.596
6.00	31.910	32.060
7.00	31.441	31.572
8.00	31.022	31.141
9.00	30.645	30.751
10.00	30.296	30.392
11.00	29.974	30.067
12.00	29.688	29.766
13.00	29.408	29.493
14.00	29.160	29.233

0.250 IN. DIAMETER XENON DATA.

PRESSURE KILOBAR	TEMPERATURE, KELVIN				
	76.700	80.000	40.000	4.200	20.100
1.00	34.247	34.262	33.530	0.0	0.0
1.50	33.747	33.804	33.172	0.0	32.943
2.00	33.329	33.389	32.830	32.531	32.607
3.00	32.613	32.666	32.183	31.944	32.007
4.00	31.997	32.047	31.611	31.419	31.469
5.00	31.463	31.498	31.113	30.953	30.993
6.00	30.977	31.012	30.677	30.533	30.557
7.00	30.542	30.576	30.270	30.143	30.163
8.00	30.160	30.187	29.903	29.792	29.795
9.00	29.796	29.826	29.573	29.469	29.477
10.00	29.466	29.488	29.244	29.153	29.161
11.00	29.168	29.182	28.950	28.879	28.879
12.00	28.884	28.898	28.682	28.611	28.614
13.00	28.625	28.635	28.440	28.376	28.373
14.00	28.365	28.371	28.183	28.132	28.140
15.00	28.134	28.137	27.969	27.909	27.913
16.00	27.920	27.926	27.765	27.704	27.706
17.00	27.719	27.719	27.567	27.514	27.506
18.00	27.524	27.519	27.387	27.342	27.326
19.00	27.341	27.323	27.211	27.163	27.155
20.00	27.170	27.152	27.047	27.015	26.986

0.250 IN. DIAMETER XENON DATA.

PRESSURE KILOBAR	TEMPERATURE, KELVIN				
	60.100	76.600	119.800	76.900	158.800
1.00	33.914	34.168	0.0	34.231	35.865
1.50	33.499	33.706	34.404	33.747	35.185
2.00	33.119	33.301	33.926	33.317	34.596
3.00	32.421	32.597	33.103	32.613	33.625
4.00	31.812	31.985	32.396	31.991	32.842
5.00	31.304	31.447	31.818	31.447	32.198
6.00	30.838	30.974	31.309	30.982	31.630
7.00	30.403	30.538	30.846	30.542	31.122
8.00	30.024	30.144	30.428	30.149	30.663
9.00	29.669	29.780	30.048	29.788	30.268
10.00	29.342	29.442	29.702	29.474	29.882
11.00	29.064	29.144	29.388	29.172	29.544
12.00	28.780	28.860	29.088	28.884	29.230
13.00	28.533	28.601	28.813	28.617	28.949
14.00	28.269	28.336	28.555	28.365	28.679
15.00	28.042	28.107	28.304	28.134	28.429
16.00	27.832	27.888	28.079	27.904	28.194
17.00	27.625	27.684	27.857	27.700	27.971
18.00	27.428	27.489	27.652	27.500	27.763
19.00	27.253	27.301	27.451	27.317	27.553
20.00	27.077	27.138	27.277	27.146	27.374

0.250 IN. DIAMETER XENON DATA.

PRESSURE KILOBAR	TEMPERATURE, KELVIN				
	140.100	99.800	77.000	119.800	140.000
1.00	35.482	34.693	34.237	34.973	35.472
1.50	34.844	34.168	33.750	34.416	34.850
2.00	34.310	33.706	33.332	33.923	34.310
3.00	33.414	32.915	32.616	33.097	33.405
4.00	32.673	32.255	31.997	32.424	32.660
5.00	32.035	31.692	31.460	31.840	32.035
6.00	31.479	31.191	30.977	31.315	31.479
7.00	30.998	30.744	30.542	30.860	30.998
8.00	30.559	30.321	30.147	30.444	30.556
9.00	30.184	29.954	29.792	30.067	30.168
10.00	29.822	29.616	29.461	29.697	29.801
11.00	29.484	29.310	29.166	29.383	29.475
12.00	29.175	29.010	28.876	29.083	29.168
13.00	28.893	28.743	28.628	28.817	28.893
14.00	28.635	28.467	28.368	28.550	28.627
15.00	28.392	28.228	28.134	28.307	28.376
16.00	28.156	28.006	27.915	28.063	28.140
17.00	27.929	27.797	27.703	27.861	27.932
18.00	27.722	27.599	27.524	27.650	27.727
19.00	27.518	27.403	27.328	27.462	27.527
20.00	27.344	27.232	27.157	27.275	27.352

APPENDIX B

Polynomial Coefficients for the Smooth Representations for Neon, Argon Krypton, and Xenon

The following pages list for each solid, the coefficients A_n for the Lennard-Jones representation, $P(T,V) = \sum_{n=0}^{N} A_n V^{-(2n+3)}$, of the full-range (all pressure) experimental data for each isotherm, the root mean square deviation (RMSD) (units, cm^3/mole) of the data from the values calculated, and the resulting extrapolated values of the P=0 molar volume, V_o (units, cm^3/mole), and bulk modulus, B_o (units, kbar). The polynomials in each case are valid for pressures from 0 to 20 kbar, with the exception of krypton at 20 K, 80 K, and 100 K where P=0 to 13 kbar. The coefficients give pressures in kbar when molar volumes are expressed in cm^3.

Two adjustments have been made to the experimental data of Appendix A in obtaining the smoothed isotherms which are described by the following fit coefficients. First, isobaric plots were made to reduce the data to a common temperature where the experimental isotherm temperature differed slightly for the different diameter samples. Second, the reference lengths of the samples (L_{o4}, Table 3) were adjusted in certain cases to compensate for evident systematic differences between data for different samples which appeared as the computer fitting was being carried out. Thus, the actual data (before adjustment to a common temperature) which were used to obtain these fit coefficients are not in all cases identical with those in Appendix A, but differ from them by an additive amount which was determined empirically and which is given in the table below.

Table II. Corrections to be added to the data of Appendix A (units, cm^3/mole) to obtain the experimental data which were used to determine the fit coefficients (see Chapter V for details).

Sample	Sample Diameter		
	0.500 in.	0.354 in.	0.250 in.
neon	0	0	+0.057
argon I	0	0	+0.253
II	0	-	+0.449
krypton	-0.136	0	0
xenon	+0.348	0	+0.629

SOLID NEON

TEMPERATURE	FIT CONSTANTS	ROOT MEAN SQUARE DEVIATION (DELTA V)
	V0= 13.394 B0= 10.98	
4.2 K	A0= -1.3681582822D 04 A1= 2.5434212278D 06 A2= -1.5963727949D 07	0.006
	V0= 13.490 B0= 10.27	
13.5 K	A0= -1.2909749129D 04 A1= 2.4042981212D 06 A2= -9.9761975798D 06	0.005
	V0= 13.759 B0= 8.27	
19.9 K	A0= -9.0508931642D 03 A1= 1.2851474396D 06 A2= 1.0045658055D 08 A3= -3.6630535727D 09	0.005

SOLID ARGON

TEMPERATURE	FIT CONSTANTS	ROOT MEAN SQUARE DEVIATION (DELTA V)
	V0= 22.557 B0= 28.64	
4.2 K	A0= -1.81891336830 05 A1= 1.01479636770 08 A2= -4.54403804000 09	0.010
	V0= 22.641 B0= 27.55	
20.0 K	A0= -1.74683875320 05 A1= 9.71257066320 07 A2= -3.88364013390 09	0.009
	V0= 23.035 B0= 23.54	
40.0 K	A0= -1.51020554600 05 A1= 8.39278540160 07 A2= -2.01425648390 09	0.011
	V0= 23.627 B0= 18.59	
60.0 K	A0= -1.17592122090 05 A1= 6.28685979870 07 A2= 1.54993883160 09	0.020
	V0= 24.284 B0= 14.07	
77.0 K	A0= -5.70175165240 04 A1= -1.19660918890 06 A2= 2.58506678660 10 A3= -3.13516780830 12	0.012

SOLID KRYPTON

TEMPERATURE	FIT CONSTANTS	ROOT MEAN SQUARE DEVIATION (DELTA V)
	V0= 27.098 B0= 35.56	
4.2 K	A0= -6.8439320181D 05	0.006
	A1= 8.6752776605D 08	
	A2= -3.5775072628D 11	
	A3= 6.5903997058D 13	
	V0= 27.205 B0= 33.94	
20.0 K	A0= -6.4201717292D 05	0.005
	A1= 8.1175750895D 08	
	A2= -3.3372215387D 11	
	A3= 6.2618794898D 13	
	V0= 27.570 B0= 30.43	
40.0 K	A0= -5.3711217972D 05	0.006
	A1= 6.5389145734D 08	
	A2= -2.4727903591D 11	
	A3= 4.6047799031D 13	
	V0= 28.047 B0= 26.50	
60.0 K	A0= -4.3222801828D 05	0.010
	A1= 5.0165580514D 08	
	A2= -1.6772022299D 11	
	A3= 3.1907230126D 13	
	V0= 28.324 B0= 24.44	
70.0 K	A0= -3.9360995677D 05	0.008
	A1= 4.5369798166D 08	
	A2= -1.4671426116D 11	
	A3= 2.8930465936D 13	

SOLID KRYPTON

TEMPERATURE	FIT CONSTANTS	ROOT MEAN SQUARE DEVIATION (DELTA V)
	V0= 28.561 B0= 21.78	
77.0 K	A0= -2.5370239405D 05	0.016
	A1= 2.0695086244D 08	
	V0= 28.655 B0= 21.33	
80.0 K	A0= -2.5092124139D 05	0.020
	A1= 2.0603895654D 08	
	V0= 29.283 B0= 18.29	
100.0 K	A0= -2.2962091904D 05	0.020
	A1= 1.9689729338D 08	
	V0= 29.686 B0= 15.98	
110.0 K	A0= -1.9408073803D 05	0.012
	A1= 1.5782231134D 08	
	A2= 1.1648719705D 10	

SOLID XENON

TEMPERATURE	FIT CONSTANTS	ROOT MEAN SQUARE DEVIATION (DELTA V)
	V0= 34.740 B0= 36.28	
4.2 K	A0= -8.2853470194D 05 A1= 1.0820192021D 09 A2= -9.9080172851D 10	0.020
	V0= 34.829 B0= 35.51	
20.0 K	A0= -8.2285919073D 05 A1= 1.0865304917D 09 A2= -1.0717645513D 11	0.021
	V0= 35.136 B0= 33.04	
40.0 K	A0= -7.6800008564D 05 A1= 1.0116001880D 09 A2= -7.8349457994D 10	0.023
	V0= 35.556 B0= 30.23	
60.0 K	A0= -7.1993405509D 05 A1= 9.6133456942D 08 A2= -6.4676675454D 10	0.022
	V0= 35.974 B0= 27.28	
77.0 K	A0= -6.3497341018D 05 A1= 8.2173652342D 08	0.025
	V0= 36.017 B0= 27.06	
80.0 K	A0= -6.3223213540D 05 A1= 8.2015072985D 08	0.030

SOLID XENON

TEMPERATURE	FIT CONSTANTS	ROOT MEAN SQUARE DEVIATION (DELTA V)
	V0= 36.525 B0= 24.55	
100.0 K	A0= -5.98088671070 05 A1= 7.57884509800 08	0.029
	V0= 37.007 B0= 22.50	
120.0 K	A0= -5.70041777140 05 A1= 7.80675783610 08	0.020
	V0= 37.653 B0= 19.23	
140.0 K	A0= -4.82391194460 05 A1= 6.40088126180 08 A2= 6.21421177010 10	0.024
	V0= 38.502 B0= 14.76	
158.8 K	A0= -1.57208146400 05 A1= -3.05690899430 08 A2= 1.01712368080 12 A3= -3.23926839000 14	0.022

APPENDIX C

Deviation Plots for Neon, Argon, Krypton, and Xenon

The following pages present plots as a function of pressure of the difference between the experimental volume data for each solid (Appendix A, after adjustment of the sample lengths as in Appendix B) and the calculated volumes which are obtained from the coefficients of Appendix B.

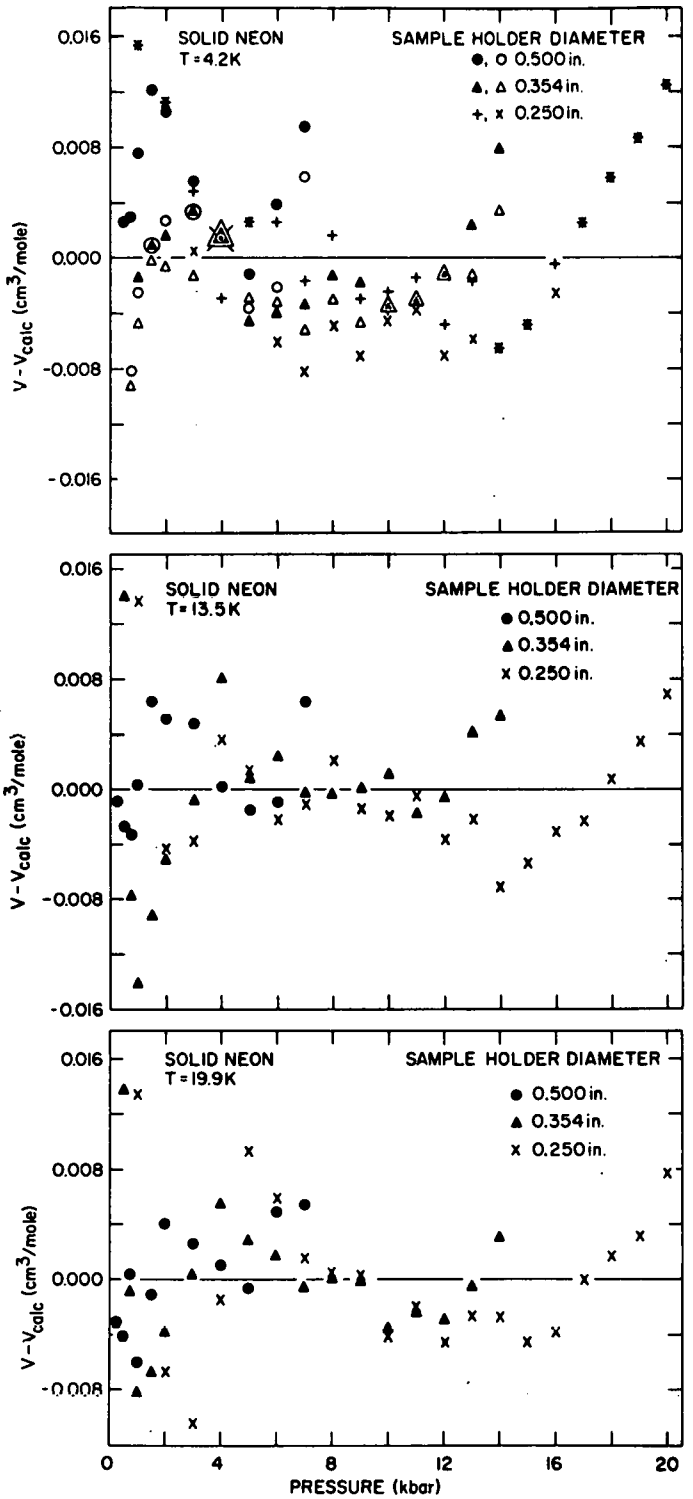
SOLID NEON
T=4.2K
SAMPLE HOLDER DIAMETER
●, ○ 0.500in.
▲, △ 0.354in.
+, x 0.250in.
SOLID NEON
T=13.5K
SAMPLE HOLDER DIAMETER
● 0.500in.
▲ 0.354in.
x 0.250in.
SOLID NEON
T=19.9K
SAMPLE HOLDER DIAMETER
● 0.500in.
▲ 0.354in.
x 0.250in.
V-Vcalc (cm3/mole)
0.016
0.008
0.000
-0.008
-0.016
0
4
8
12
16
20
PRESSURE (kbar)

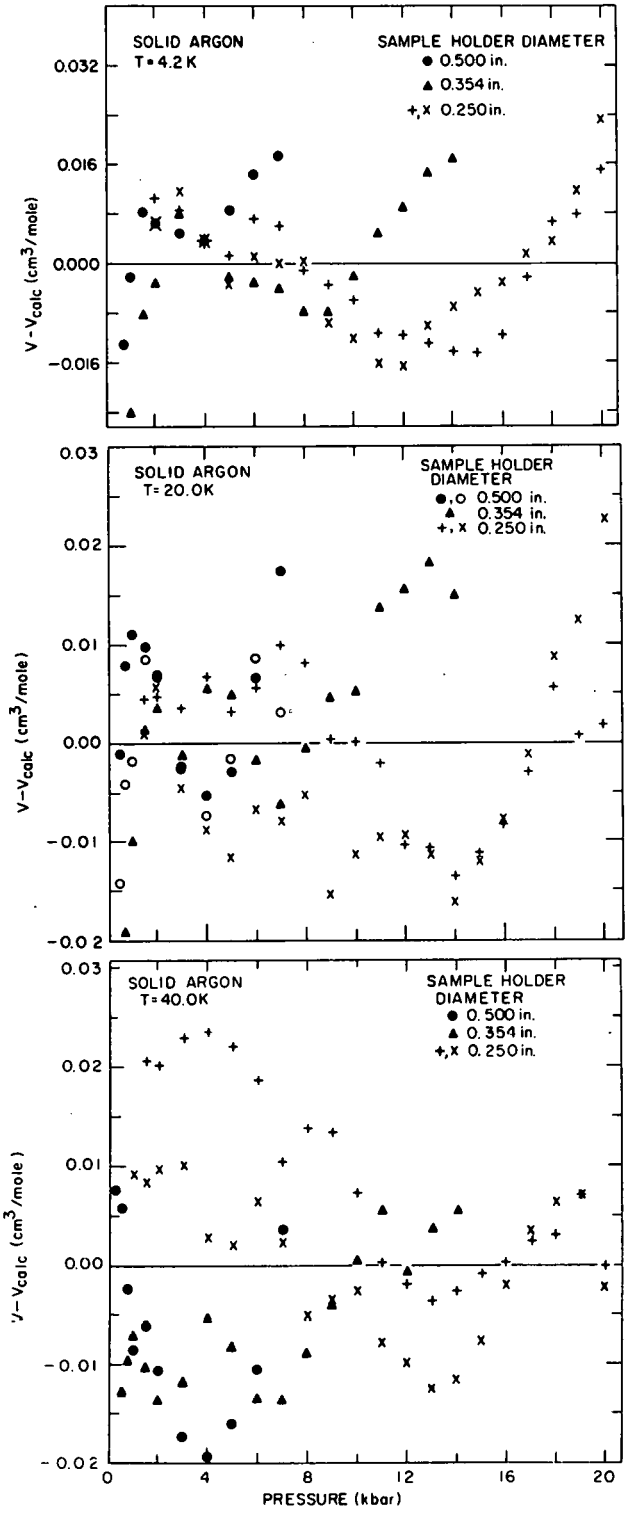
SOLID ARGON
T = 4.2 K
SAMPLE HOLDER DIAMETER
● 0.500 in.
▲ 0.354 in.
+,x 0.250 in.
0.032
0.016
0.000
−0.016
V − Vcalc (cm³/mole)
SOLID ARGON
T = 20.0K
SAMPLE HOLDER DIAMETER
●,o 0.500 in.
▲ 0.354 in.
+,x 0.250 in.
0.03
0.02
0.01
0.00
−0.01
−0.02
V − Vcalc (cm³/mole)
SOLID ARGON
T = 40.0K
SAMPLE HOLDER DIAMETER
● 0.500 in.
▲ 0.354 in.
+,x 0.250 in.
0.03
0.02
0.01
0.00
−0.01
−0.02
V − Vcalc (cm³/mole)
0
4
8
12
16
20
PRESSURE (kbar)

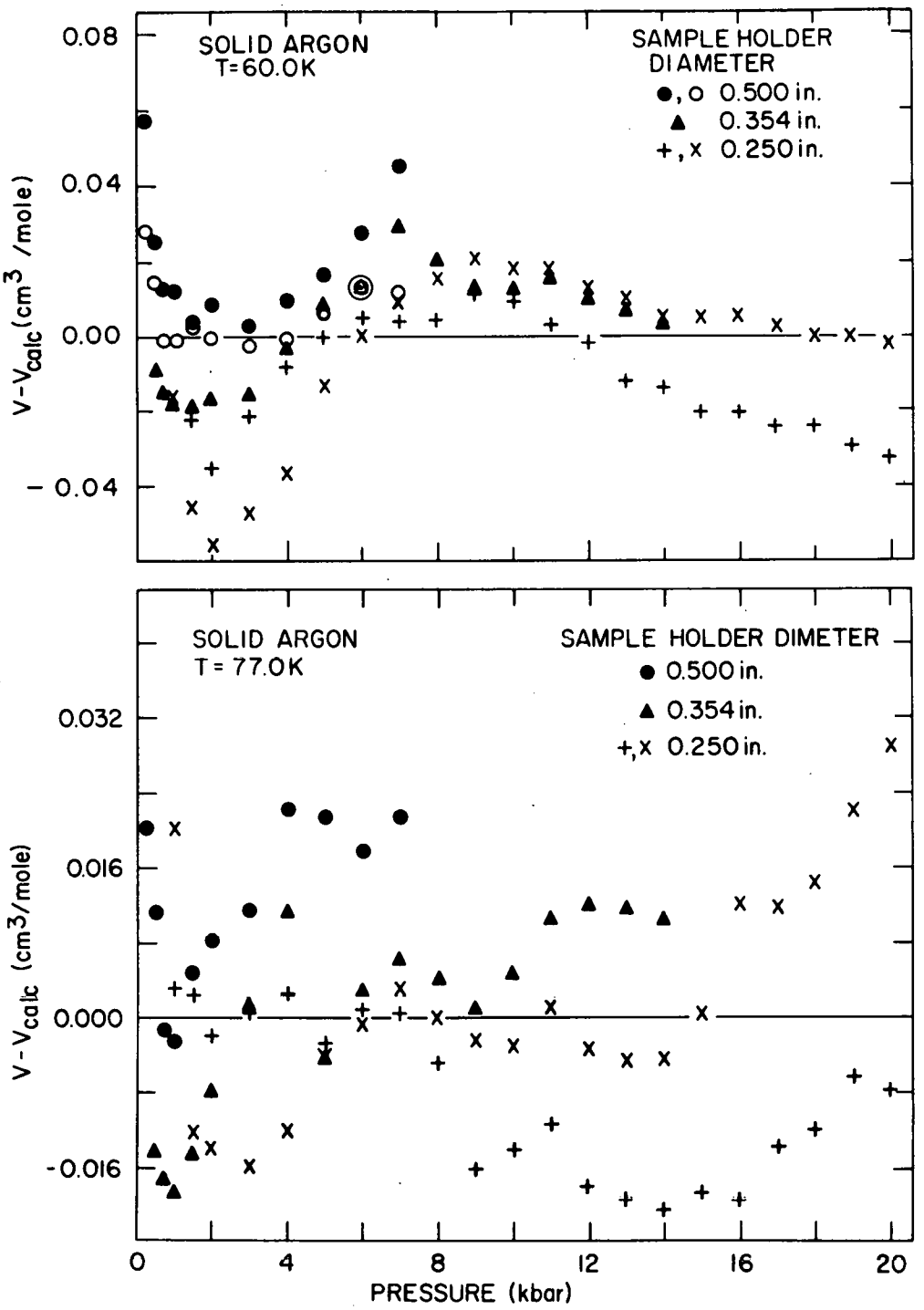
SOLID ARGON
T=60.0K
SAMPLE HOLDER
DIAMETER
●, o 0.500 in.
▲ 0.354 in.
+, x 0.250 in.
0.08
0.04
0.00
− 0.04
V-Vcalc (cm3 /mole)
SOLID ARGON
T = 77.0K
SAMPLE HOLDER DIMETER
● 0.500 in.
▲ 0.354 in.
+, x 0.250 in.
0.032
0.016
0.000
-0.016
V - Vcalc (cm3/mole)
0
4
8
12
16
20
PRESSURE (kbar)

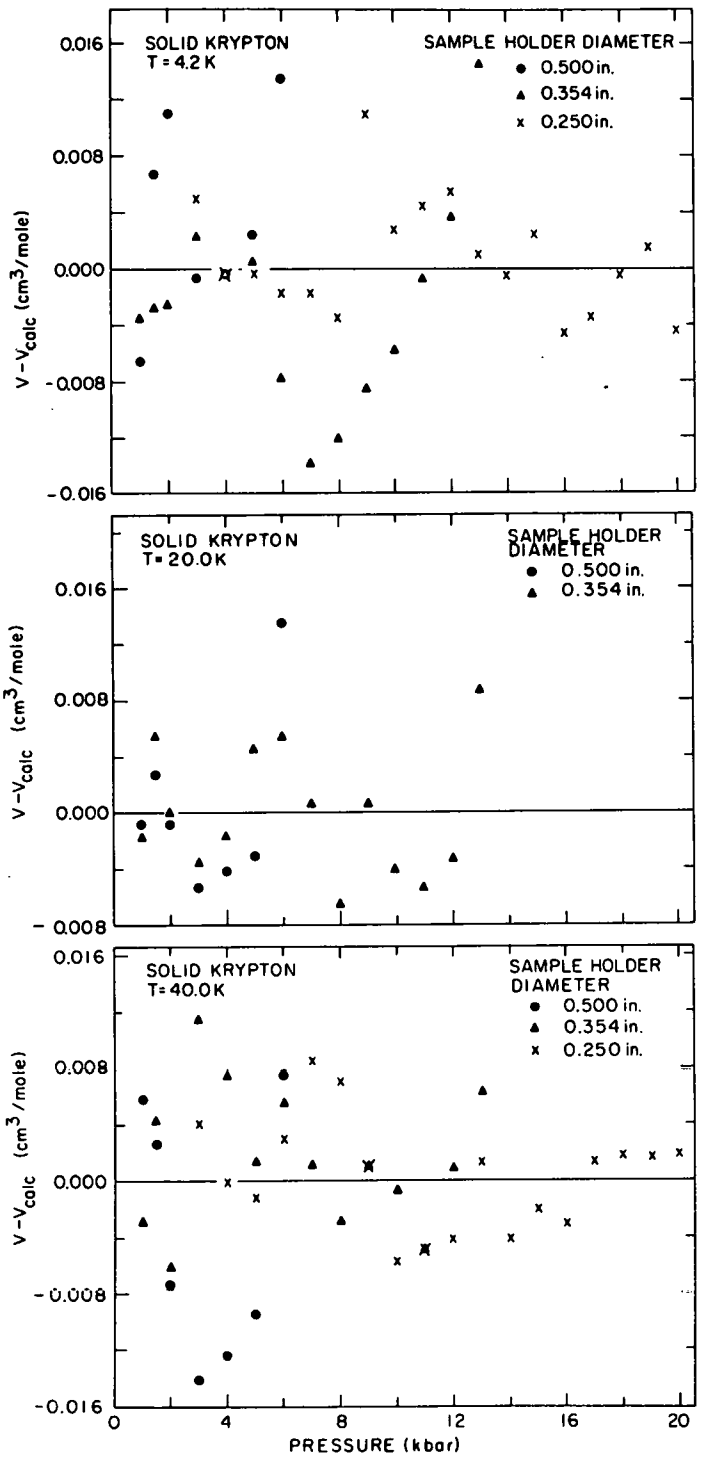
SOLID KRYPTON
T = 4.2 K
SAMPLE HOLDER DIAMETER
0.500 in.
0.354 in.
0.250 in.
SOLID KRYPTON
T = 20.0 K
SAMPLE HOLDER DIAMETER
0.500 in.
0.354 in.
SOLID KRYPTON
T = 40.0 K
SAMPLE HOLDER DIAMETER
0.500 in.
0.354 in.
0.250 in.
V - Vcalc (cm3/mole)
0.016
0.008
0.000
-0.008
-0.016
0
4
8
12
16
20
PRESSURE (kbar)

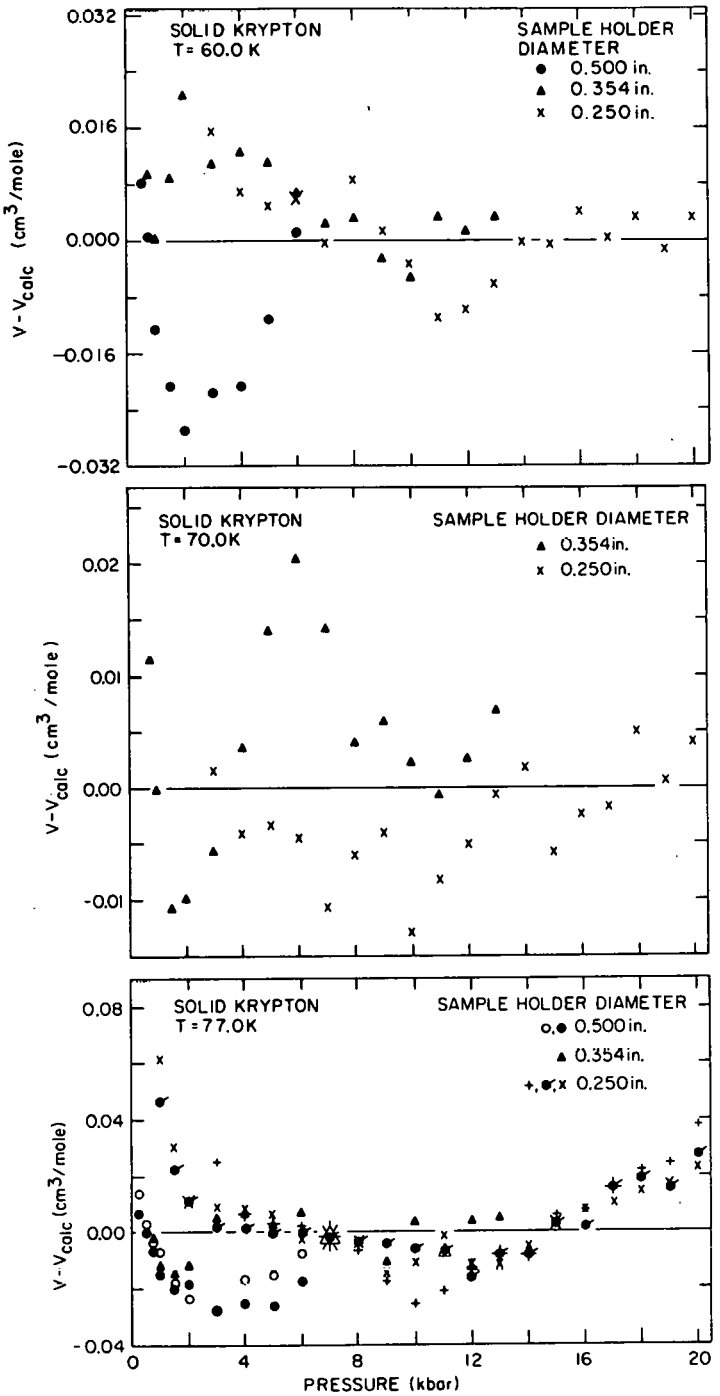
SOLID KRYPTON
T= 60.0 K
SAMPLE HOLDER DIAMETER
● 0.500 in.
▲ 0.354 in.
x 0.250 in.
V - Vcalc (cm3/mole)
0.032
0.016
0.000
-0.016
-0.032
SOLID KRYPTON
T= 70.0K
SAMPLE HOLDER DIAMETER
▲ 0.354in.
x 0.250in.
V-Vcalc (cm3/mole)
0.02
0.01
0.00
-0.01
SOLID KRYPTON
T = 77.0K
SAMPLE HOLDER DIAMETER
o,● 0.500in.
▲ 0.354in.
+,●,x 0.250in.
V - Vcalc (cm3/mole)
0.08
0.04
0.00
-0.04
0
4
8
12
16
20
PRESSURE (kbar)

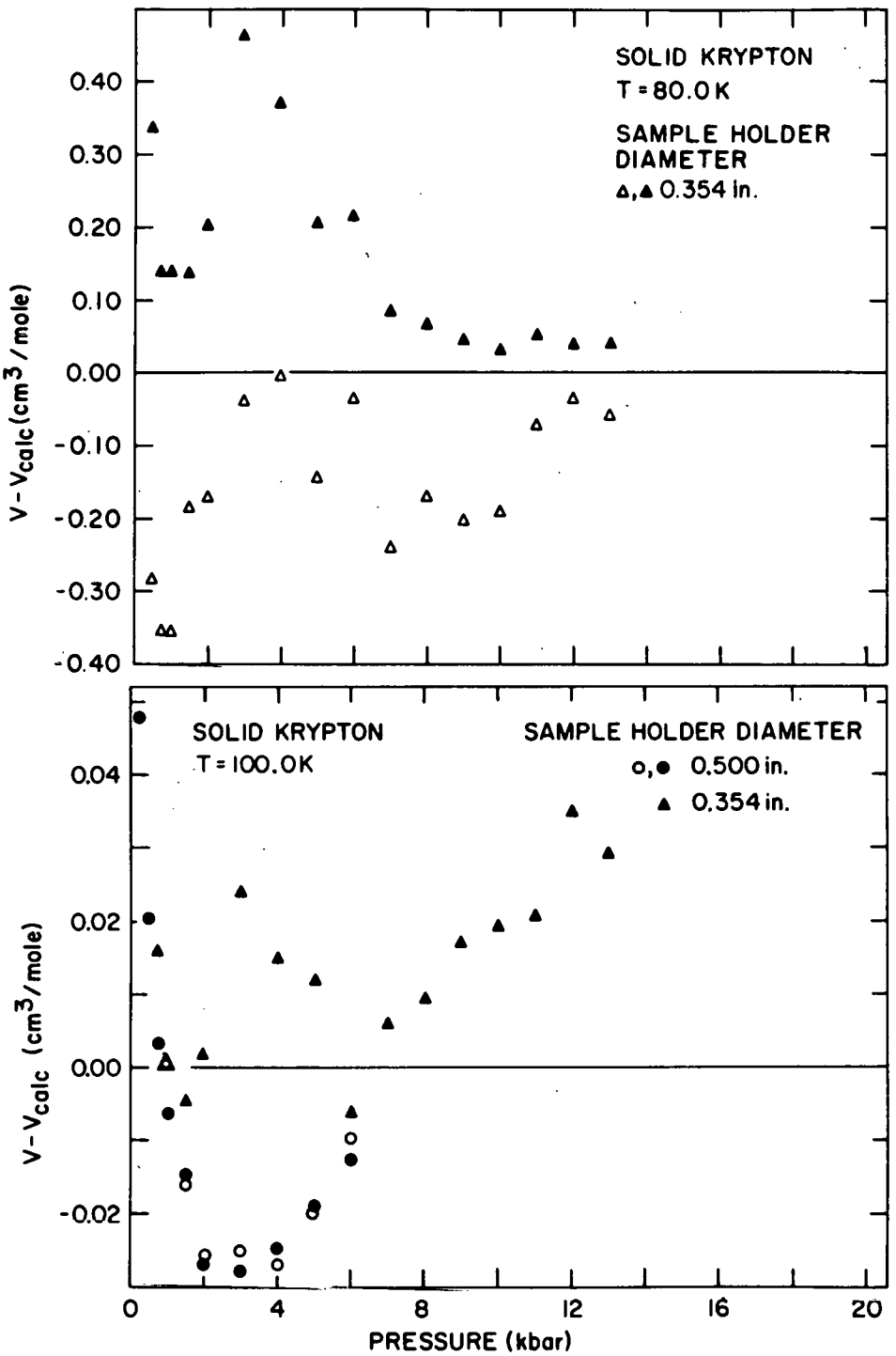
SOLID KRYPTON
T = 80.0 K
SAMPLE HOLDER DIAMETER
Δ,▲ 0.354 in.
0.40
0.30
0.20
0.10
0.00
-0.10
-0.20
-0.30
-0.40
V - Vcalc (cm3 / mole)
SOLID KRYPTON
T = 100.0 K
SAMPLE HOLDER DIAMETER
o,● 0.500 in.
▲ 0.354 in.
0.04
0.02
0.00
-0.02
V - Vcalc (cm3/mole)
0
4
8
12
16
20
PRESSURE (kbar)

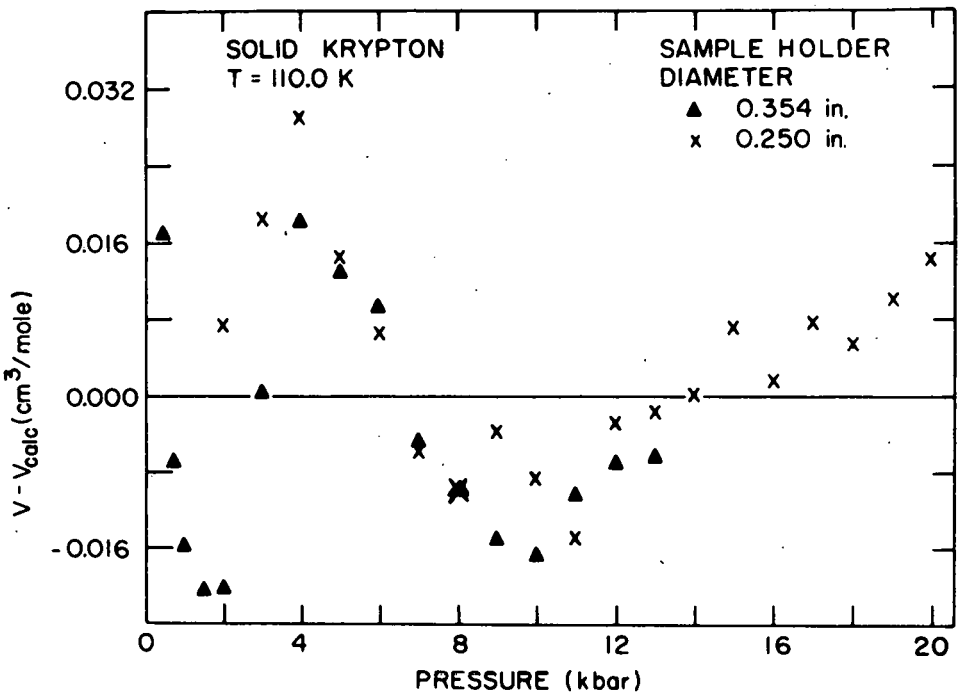
SOLID KRYPTON
T = 110.0 K
SAMPLE HOLDER
DIAMETER
▲ 0.354 in.
x 0.250 in.
0.032
0.016
0.000
-0.016
V - Vcalc (cm3/mole)
0
4
8
12
16
20
PRESSURE (kbar)

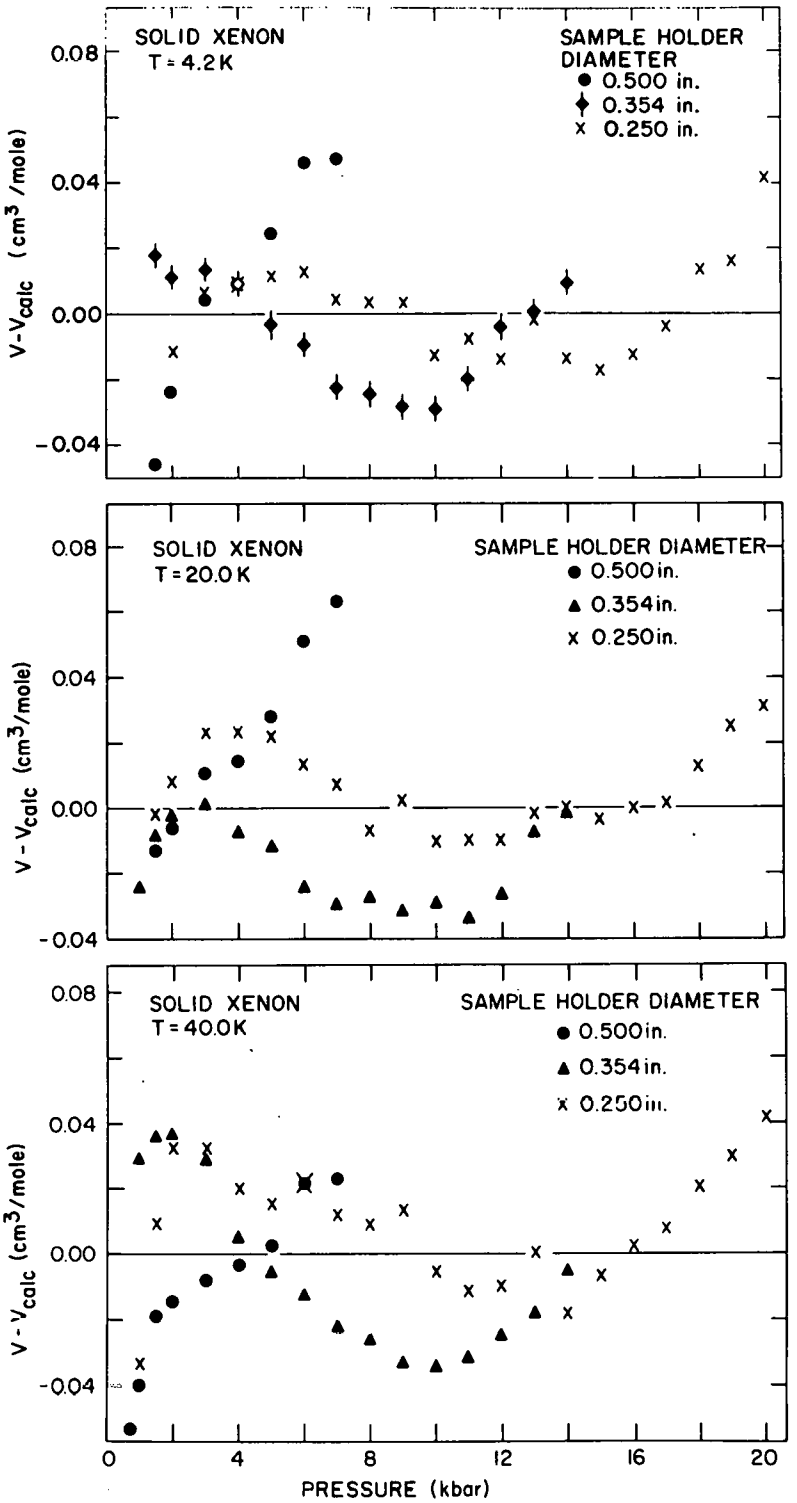
SOLID XENON
T = 4.2 K
SAMPLE HOLDER DIAMETER
● 0.500 in.
♦ 0.354 in.
x 0.250 in.
V - Vcalc (cm3 /mole)
0.08
0.04
0.00
-0.04
SOLID XENON
T = 20.0 K
SAMPLE HOLDER DIAMETER
● 0.500 in.
▲ 0.354 in.
x 0.250 in.
V - Vcalc (cm3/mole)
SOLID XENON
T = 40.0 K
SAMPLE HOLDER DIAMETER
● 0.500 in.
▲ 0.354 in.
x 0.250 in.
0
4
8
12
16
20
PRESSURE (kbar)

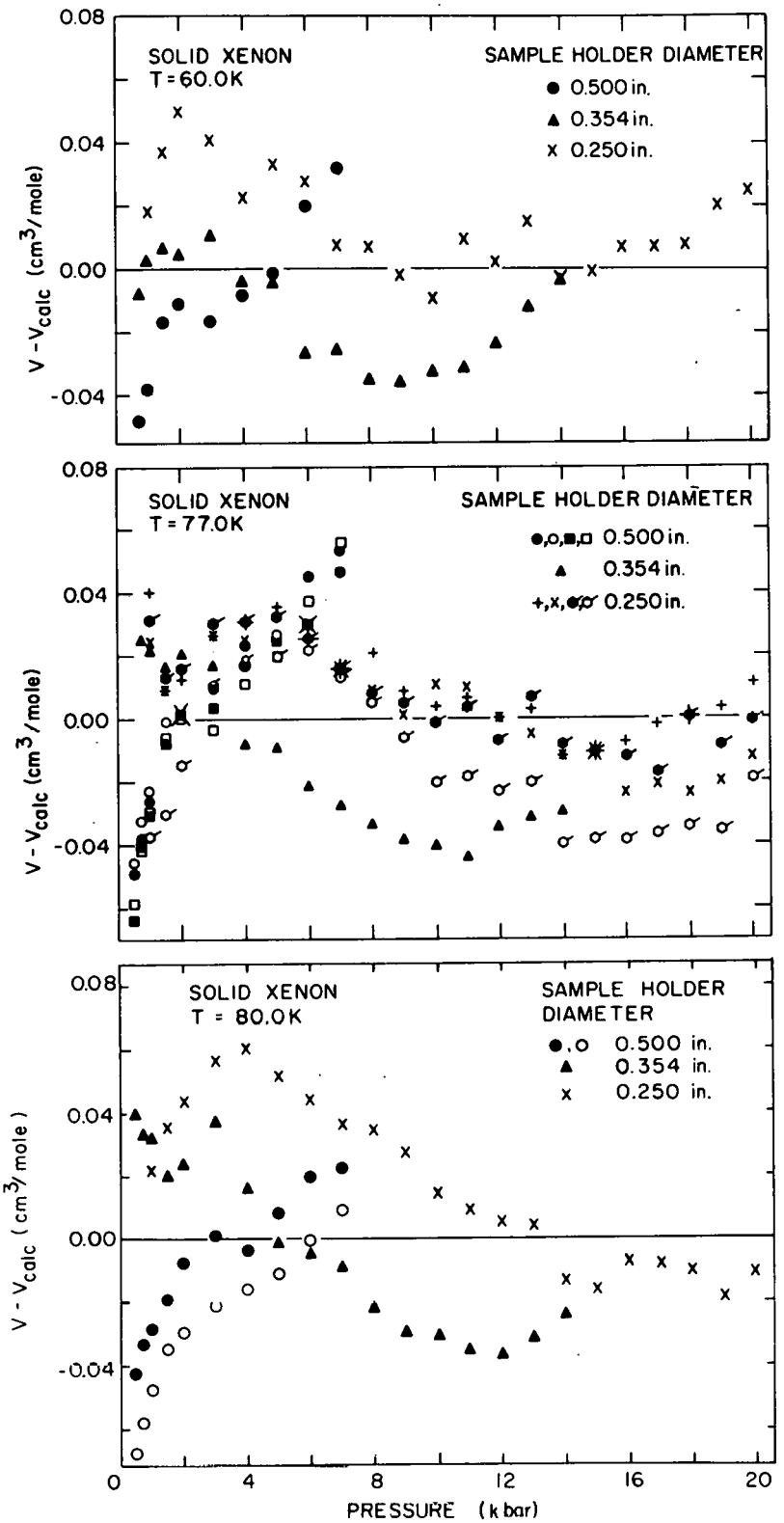
SOLID XENON
T=60.0K
SAMPLE HOLDER DIAMETER
● 0.500 in.
▲ 0.354 in.
x 0.250 in.
SOLID XENON
T=77.0K
SAMPLE HOLDER DIAMETER
●,○,■,□ 0.500 in.
▲ 0.354 in.
+,x,◐,◑ 0.250 in.
SOLID XENON
T = 80.0K
SAMPLE HOLDER DIAMETER
●,○ 0.500 in.
▲ 0.354 in.
x 0.250 in.
V - Vcalc (cm3/mole)
0.08
0.04
0.00
-0.04
0
4
8
12
16
20
PRESSURE (k bar)

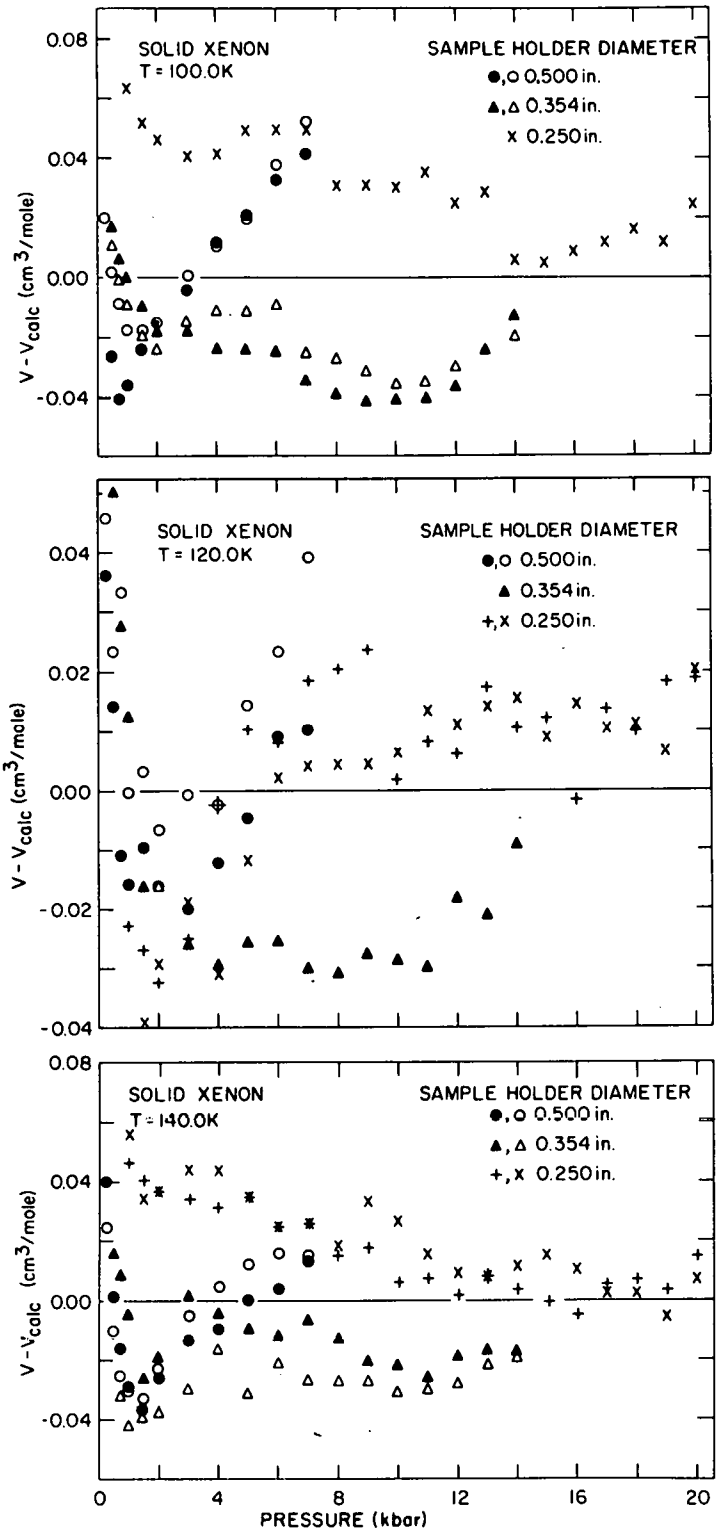
SOLID XENON
T = 100.0K
SAMPLE HOLDER DIAMETER
●,○ 0.500 in.
▲,△ 0.354 in.
x 0.250 in.
SOLID XENON
T = 120.0K
SAMPLE HOLDER DIAMETER
●,○ 0.500 in.
▲ 0.354 in.
+,x 0.250 in.
SOLID XENON
T = 140.0K
SAMPLE HOLDER DIAMETER
●,○ 0.500 in.
▲,△ 0.354 in.
+,x 0.250 in.
V - Vcalc (cm3/mole)
PRESSURE (kbar)
0.08
0.04
0.00
-0.04
0.02
-0.02
0
4
8
12
16
20

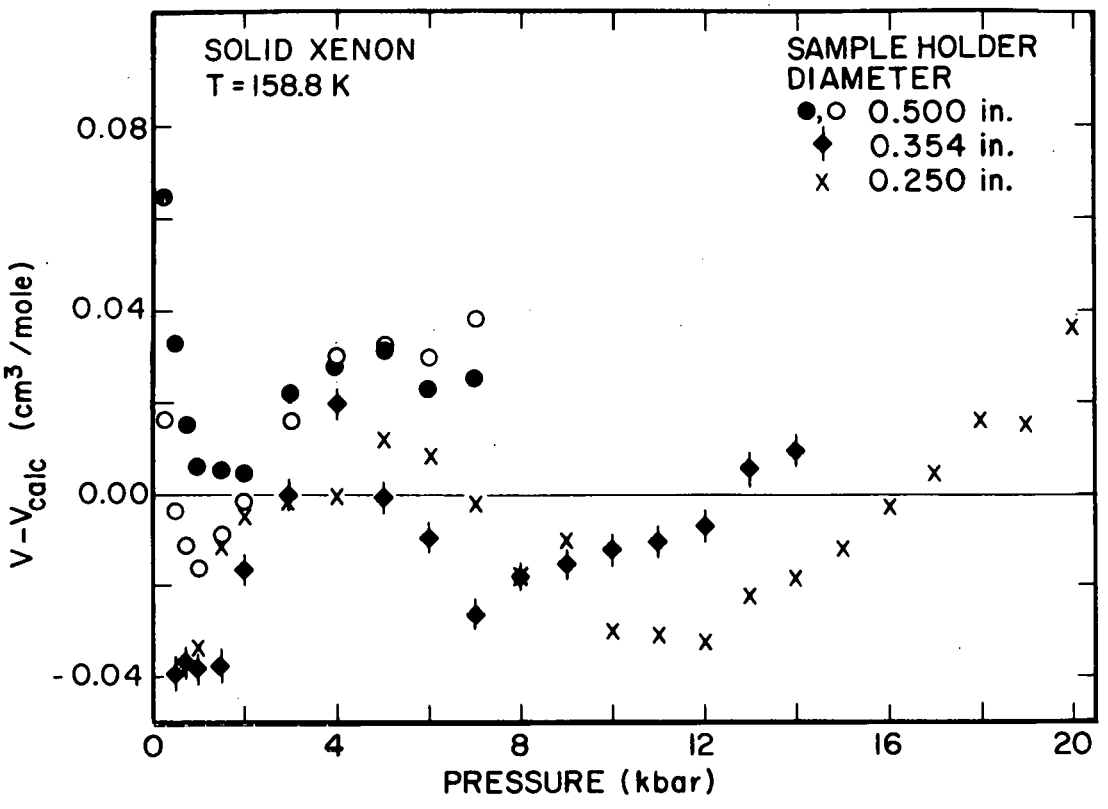
SOLID XENON
T = 158.8 K
SAMPLE HOLDER DIAMETER
●,○ 0.500 in.
♦ 0.354 in.
x 0.250 in.
0.08
0.04
0.00
-0.04
V-V_calc (cm³/mole)
0
4
8
12
16
20
PRESSURE (kbar)

APPENDIX D

4.2 K Equations of State for the Rare Gas Solids

The following pages present smoothed 4.2 K values of the pressure, $P_o(V)$, and the bulk modulus, $B_o(V)$, as calculated for selected molar volumes using the coefficients in Appendix B.

SOLID NEON

MOLAR VOLUME (CM3)	PO (V) (KBAR)	BO (V) (KBAR)
13.76	-0.266	8.83
13.50	-0.084	10.31
13.39	-0.000	10.97
13.00	0.368	13.79
12.50	0.995	18.31
12.00	1.858	24.24
11.50	3.049	32.04
11.00	4.694	42.39
10.50	6.975	56.24
10.00	10.156	74.95
9.50	14.627	100.48
9.06	20.082	130.83

SOLID ARGON

MOLAR VOLUME (CM3)	PO (V) (KBAR)	BO (V) (KBAR)
24.28	-1.595	15.61
24.00	-1.404	17.31
23.63	-1.116	19.78
23.50	-1.004	20.71
23.00	-0.517	24.64
22.64	-0.104	27.85
22.56	-0.000	28.64
22.00	0.787	34.46
21.50	1.648	40.56
21.00	2.684	47.66
20.50	3.930	55.90
20.00	5.426	65.50
19.50	7.223	76.70
19.00	9.381	89.78
18.50	11.975	105.08
18.00	15.094	123.00
17.50	18.849	144.04
17.36	20.032	150.57

SOLID KRYPTON

MOLAR VOLUME (CM3)	PO (V) (KBAR)	BO (V) (KBAR)
29.69	-2.459	19.53
29.28	-2.176	21.53
29.00	-1.963	23.00
28.66	-1.676	24.93
28.56	-1.592	25.48
28.50	-1.538	25.84
28.32	-1.371	26.93
28.05	-1.105	28.65
28.00	-1.053	28.98
27.57	-0.582	31.95
27.21	-0.145	34.67
27.10	0.000	35.56
27.00	0.131	36.36
26.00	1.673	45.71
25.00	3.696	57.96
24.00	6.388	74.74
23.00	10.054	98.99
22.00	15.224	136.18
21.32	20.061	173.85

SOLID XENON

MOLAR VOLUME (CM3)	PO (V) (KBAR)	BO (V) (KBAR)
38.50	-2.517	14.87
38.00	-2.310	16.92
37.65	-2.146	18.47
37.50	-2.071	19.17
37.00	-1.797	21.64
36.53	-1.504	24.19
36.00	-1.128	27.35
35.56	-0.774	30.22
35.14	-0.398	33.21
35.00	-0.263	34.25
34.83	-0.093	35.57
34.74	-0.000	36.28
34.00	0.848	42.63
33.00	2.268	52.80
32.00	4.078	65.19
31.00	6.381	80.33
30.00	9.311	98.87
29.00	13.037	121.64
28.00	17.784	149.72
27.59	20.090	163.07